Design of Voiceband Echo Cancellers

by

Mahdi Yahya Zaidan

A Thesis Presented to the

FACULTY OF THE COLLEGE OF GRADUATE STUDIES

KING FAHD UNIVERSITY OF PETROLEUM & MINERALS

DHAHRAN, SAUDI ARABIA

In Partial Fulfillment of the
Requirements for the Degree of

MASTER OF SCIENCE

In

ELECTRICAL ENGINEERING

January, 1990

DESIGN OF VOICEBAND ECHO CANCELLERS

BY

MAHDI YAHYA ZAIDAN

A Thesis Presented to the

FACULTY OF THE COLLEGE OF GRADUATE STUDIES

KING FAHD UNIVERSITY OF PETROLEUM & MINERALS

DHAHRAN, SAUDI ARABIA

In Partial Fulfillment of the
Requirements for the Degree of

MASTER OF SCIENCE

In

ELECTRICAL ENGINEERING

JANUARY, 1990

KING FAHD UNIVERSITY OF PETROLEUM AND MINERALS
DHAHRAN, SAUDI ARABIA

COLLEGE OF GRADUATE STUDIES

This thesis, written by ***MAHDI YAHYA ZAIDAN*** under the direction of his Thesis Advisor and approved by his Thesis Committee, has been presented to and accepted by the Dean of the College of Graduate Studies, in partial fulfillment of the requirements for the degree of ***MASTER OF SCIENCE*** in ***ELECTRICAL ENGINEERING.***

THESIS COMMITEE

Dr. M. S. El-Hennawey (Chairman)

Dr. M. Atiquzzaman (Member)

Dr. M. Bettayeb (Member)

Department Chairman

Dean, College of Graduate Studies

Date: 16th January, 1990

To My Beloved Parents, Sisters, Brother

and to Those Who Shared Their Care and Concern

ACKNOWLEDGEMENT

First of all, I thank " *ALLAH* " for all the knowledge and science *HE* has given to mankind including myself. Thanks are also to our Prophet *MOHAMMED, PEACE BE UPON HIM*, who encourages us as Moslems to seek science wherever it can be found.

Acknowledgement is due to *King Fahd University of Petroleum and Minerals* for support of this research and to *King Abdulaziz City of Science and Technology* for partial support of this research.

I would like to express my deep appreciation to my thesis advisor, *Dr. Mohamed S. El-Hennawey*, for his patient guidance and his generous support and encouragement. I would also like to express my gratefulness to the other committee members, *Dr. Mohammed Atiquzzaman* and *Dr. Maamar Bettayeb*, for their valuable suggestions, helpful remarks and their kind co-operation.

Thanks to *Mr. Les Brown* and *Mr. Ian Melhewish* of ESE-Limited, Canada for providing us a real-life channel which is used in the simulation.

Special thanks are to *Mr. Mohammed Redwan*, *Mr. Jamal Hamdan*, *Mr. Hatim AL-Banna*, *Mr. Adel Abdul Hadi*, *Mr. Husain Masoudi*, *Mr. Siyad Ma*, *Mr. Mohammed Banat* and *Mr. Mohammed Ameerjan* for their assistance in producing this work in a nice form, and to all my *Brothers*, *Friends* and many others for the memorable days we shared together.

خلاصة الرسالة

عنوان البحث : تصميم وحدات إلغاء الصدى في شبكات الهاتف

اسم الطالب : مهدي يحيى زيدان

التخصص : هندسة كهربائية

تاريخ الدرجة : جمادى الآخرة ١٤١٠هـ / يناير ١٩٩٠م

لقد أمكن بث البيانات من وإلى نقطتي الاتصال آنياً عبر خطوط الهاتف التحويلية بسرعات عالية باستخدام مايسمى بـ (لاغي الصدى) والذي يتكون من مُرشح مُوائم وظيفتهُ إلغاء الصدى الذي ينتج عن تباين المعاوقة في شبكات الهاتف .

وتعتبر مجانبة التردد للموجات التي تستخدم في الاتصالات البعيدة أهم المشكلات التي تحول دون فعالية أداء لاغيات الصدى . مما استدعى استخدام لاغيات صدى تُساق بالبيانات ذاتها . تتكون هذه اللاغيات من تركيب تقاطعي مزدوج متبوع بدوّار وحلقة طور مغلقة حيث تتم مواءمة مشتركة بين معاملات اللاغي وحلقة الطور المغلقة وهذا مايعرف بـ «التوائم المشترك» .

لقد تم في هذه الرسالة تصميم لاغي صدى يُساق بالبيانات ذاتها ويعمل ضمن حزمة ترددات صوت الإنسان ، كما تم اختباره بالمحاكاة تحت تأثير عوامل سلبية مختلفة ، مع التركيز على مشكلة مجانبة التردد للموجات أنفة الذكر . وقد قمنا خلال المحاكاة بالتحقق من فعالية أداء طريقة التوائم المشترك المذكورة أعلاه حيث أظهرت النتائج والتحليلات أن هذه الطريقه تتطلب عدداً هائلاً من العمليات الحسابية بالإضافة إلى تأثر أداء لاغي الصدى كلياً في حالات التغير الطوري المفاجئ .

وقد اقترح في هذه الرسالة استخدام طريقة جديدة تسمى « التوائم المتتابع » للتغلب على مشكلة مجانبة التردد للموجات . ولقد أظهرت نتائج الاختبار بالمحاكاة فعالية أداء هذه الطريقة بالنسبة إلى عدد العمليات الحسابية المطلوب أو بالنسبة إلى حدوث تغير طوري مفاجئ .

إضافة إلى ذلك فقد اقترح اسلوب جديد لتقدير انحراف الطور أثناء إرسال البيانات ، وذلك بالاستفادة من فكرة مايسمى بـ « خوارزمية الإشارة العددية » . مما يساهم في تبسيط بناء النظام ومن ثم يقلل تكاليف انتاجه .

درجة الماجستير في العلوم

جامعة الملك فهد للبترول والمعادن

الظهران ، المملكة العربية السعودية

جمادى الآخره ١٤١٠هـ - يناير ١٩٩٠م

ABSTRACT

Title : **DESIGN OF VOICEBAND ECHO CANCELLERS**

By : **Mahdi Yahya Zaidan**

Major Field : **Electrical Engineering**

Date : **January 1990**

High-speed full-duplex data transmission over the general switched telephone network has been achieved with the use of echo cancellers. Echo cancellers are adaptive filters used to cancel the echo which is generated in the telephone network due to impedance mismatches.

Frequency offset is considered to be a major problem affecting the performance of echo cancellers. The existing solution of this problem is to use a data-driven echo canceller having a cross-coupled structure which is followed by a rotator and a phase-locked loop (PLL). A joint adaptation for the canceller taps and the PLL is performed.

In this thesis, a voiceband data-driven echo canceller is designed. It is tested through simulation under various impairments with the emphasis on the frequency offset. The existing solution of frequency offset effect is also investigated through the simulation. Results of simulation show that the computation complexity and the degradation due to the phase hit are two main drawbacks of this solution.

A new technique for frequency offset compensation called **'sequential adaptation'** is proposed and tested here through simulation. The proposed technique is seen to be effective in terms of computation complexity and overcoming the phase hit effect. Moreover, **a new approach** to phase estimation during data mode is proposed. This approach utilizes the idea of the sign algorithm and contributes in the direction of reducing the complexity of the system.

MASTER OF SCIENCE DEGREE

KING FAHD UNIVERSITY OF PETROLEUM AND MINERALS
DHAHRAN, SAUDI ARABIA

January 1990

CONTENTS

LIST OF TABLES

Table

LIST OF FIGURES

Figure

LIST OF NOTATIONS

A	complex symbol
T	symbol time duration (seconds)
T′	sampling time (seconds)
*	convolution process
n	time index with respect to T
k	time index with respect to T′
E	expectation operator
ε	mean-squared value
Δ	gradient vector
φ	taps error vector
α	canceller stepsize
$(\,)^*$	conjugate of ( )
$(\,)^T$	transpose of ( )
$\hat{(\,)}$	estimate of ( )
γ	instantaneous angle error
θ	angle due frquency offset

CHAPTER 1

INTRODUCTION

1.1 OVERVIEW

In recent years, data communication has found increasing application for many purposes, such as data transfer, data collection, data storage and remote processing [1]. Computer and data networks have been developed for these applications. Until now, the existing telephone network has permenantly been used as the transmission medium to provide either leased lines service for point-to-point connections or dial-up service for switched connections. Long-distance circuits in this network exhibit a number of impairments, such as linear distortion, phase jitter, frequency offset and echo (for dial lines). Therefore, rather sophisticated terminal equipment (voiceband modems) have been already designed and developed rapidly to achieve data transmission at the highest possible rate.

1.2 HALF AND FULL-DUPLEX DATA TRANSMISSION OVER THE TELEPHONE NETWORK

In the half-duplex mode of operation, one direction of data transmission (either receiving or transmitting) is hold at a time. Many applications require the simultaneous data transmission in opposite directions at a time (full-duplex operation). This mode of operation has a number of advantages such as [1]:

(a) Elimination of modem turn-around time.

(b) The possibility of interactive protocols.

(c) The opportunity to derive full profit from the short setup time of connections in data networks.

Conventionally, full-duplex operation can be achieved by two ways:

(a) The application of four-wire circuits (leased line service) where each two wire is reserved for each direction of transmission.

(b) Signal separation by frequency division multiplexing over the dialed line.

Although a quite high data transmission rate can be achieved using the four wire circuits, it is very expensive compared to the cost of dial line (two-wire circuit). The four-wire circuits may be justified in case of heavy data traffic.

In the case of frequency division multiplexing, the channel bandwidth is divided equally for the two signals. Therefore, it is not feasible at data rates greater than 2400 bps owing to the limit of the 3 kHz telephone line bandwidth. This stems from Shannon's channel capacity theorem. The theorem states that the maximum transmission rate of reliable information can not exceed the

the maximum transmission rate of reliable information can not exceed the channel capacity [2].

It would be, then, attractive to enhance the already existing dial lines' connection, for economical purposes. However, to achieve high rates of transmission, the two directions of transmission should share the same frequency band. This has already been achieved by echo cancellers which are capable of separating transmit and receive signals to a very high degree of accuracy, while utilizing the full band for both signals

Nowadays, with the clever use of echo cancellers, full-duplex service on two-wire circuits (dial lines) , is allowed with full bandwidth available for both directions of transmission. This approach has been seen to be promising since it is more elegant and economical .

1.3 PROBLEM IDENTIFICATION AND MOTIVATION OF THE RESEARCH

Echo in telephone network is generated due to impedance mismatch at the hybrid coupler. The hybrid coupler does the job of transfering from two-wire to four-wire circuits and vice versa. This echo signal interfers with the far incoming signal during full duplex transmission.

Echo canceller removes the generated echo by synthesizing a replica of this echo and subtracting it from the incoming received signal. It has been shown,

[3], [4], [5], that echo cancellers are promising solution for full duplex, data transmission. In particular, when the channel is linear and time-invariant.

However, one of the major problems encountered in the echo cancellation is the presence of frequency offset that may be introduced if a carrier system exists [6], [7]. In this case, the estimated echo has a positive or a negative frequency offset over the incoming echo. Although, the amount of frequency offset can be very small (around 1 Hz in U.S.A.), it degrades substantially the performance of the standard echo cancellers [7].

Several techniques have been proposed to overcome the frequency offset problem. The Phase Lock Loop (PLL) has been seen to be a good solution [6], [8]. Moreover, some modifications have been introduced to the basic structure of the echo canceller to make it capable of compensation for frequency offset using 'cross-coupled structures' [8]. The problem with the already existing technique is the computation complexity, besides its degraded performance if there is no frequency offset.

Another serious problem associated with echo cancellers is the effect of the phase hit that may be introduced to the incoming echo due to the irregularities in telephone switching equipment. By phase hit, we mean a step change of 45, 90 or 180 degrees. This has been found to degrade the convergence of the canceller. One more problem is associated with the timing. While the echo canceller should be synchronized with the timing of the near end transmitter, the receiver should be synchronized with the transmitter at the far end. This means

that two A/D converters are needed, which adds complexity to the system.

The work done in this thesis is mainly concerned with the three problems mentioned above. It is aimed to optimize the existing technique for echo cancellation in presence of frequency offset, in the sense of computation complexity. Moreover, we propose a new approach for phase estimation in data mode that may be a good solution for the timing problem mentioned above, with reduced complexity, suitable for data mode.

1.4 SCOPE OF THE THESIS

To begin with, all the work of this thesis has been performed on a simulated system. The system design almost matches the practical requirements and the CCITT* specifications. The FORTRAN language on the IBM 3090 was used in the simulation.

In this thesis a detailed study and investigation of the echo cancellation has been carried out. Effects of various impairments (e.g. noise, phase hit, and frequency offset) are investigated.

A new technique for frequency offset compensation called **'sequential adaptation'** is proposed and evaluated. The proposed technique is expected to

---

* CCITT stands for the International Telegraphs and Telephone Consultative Committee.

be effective in terms of computation complexity. It has also a good performance specially, if the introduced frequency offset is within 0.5 Hz.

Finally, a **new approach** to estimate the phase difference between the incoming echo and the estimated echo, is developed. This new approach is used in data mode. It utilizes the idea of the sign algorithm [9] in determining the error direction.

1.5 THESIS ORGANIZATION

In Chapter 2, the echo phenomena in telephone network; causes and types, are discussed. Conventional methods of echo control are described. At the end of the chapter, a mathematical model of the echo signal in data transmission is given.

A detailed literature survey of echo canceller's structures and types is given in Chapter 3. Advantages and disadvantages of each type are also stated and analysed. The adaptation technique, the LMS algorithm, used in echo cancellers is reviewed with all necessary derivations. Finally, some problems incountered in echo cancellation are presented with the emphasis on the frequency offset problem, in which we are interested in this thesis.

The system design is presented and shown in Chapter 4. Various blocks from which the system is built are explained, with the necessary mathematical derivations.

Then in Chapter 5, all results of the investigation made on the echo cancellation problems are presented and analysed. Effects of noise and frequency offset on the performance of the echo canceller are shown. Performance of the existing technique for frequency offset compensation is also evaluated. The Chapter terminates with an overview of the problems associated with the existing technique.

The new proposed technique **(sequential adaptation)** for frequency offset compensation is given and justified in Chapter 6. Qualitative and quantitative comparison between the existing technique and the new proposed one is also discussed. Moreover, the **new approach** to phase estimation mentioned in Section 1.4 is presented and verified at the end of this chapter.

Finally, conclusions and suggestions for further work are given in the last chapter (Chapter 7). The developed Fortran program simulating the system design and the new proposed techniques for frequency offset and phase estimation is given in the appendix.

CHAPTER 2

ECHO PHENOMENA

Most of the conversations take place in presence of echos. We hear echos of our voice waves when they are reflected by walls or neighboring objects. These echos are really noticable and annoying if the time delay between the speech and them exceeds a few tens of milliseconds [10].

Echos are also generated in telephone networks. Whenever a signal encounters a mismatch in impedance at any point of the circuit, a portion of it gets reflected. In this chapter, we shall have a look at a typical telephone network. This will help in understanding the sources of echo in telephone networks. Then, conventional methods of echo control are described. Moreover, the full-duplex data transmission over telephone network is discussed.

2.1 TYPICAL TELEPHONE NETWORK

A typical long distance telephone network is shown in Fig. 2.1. Every telephone set in a given local area is connected to its central office by a two-wire

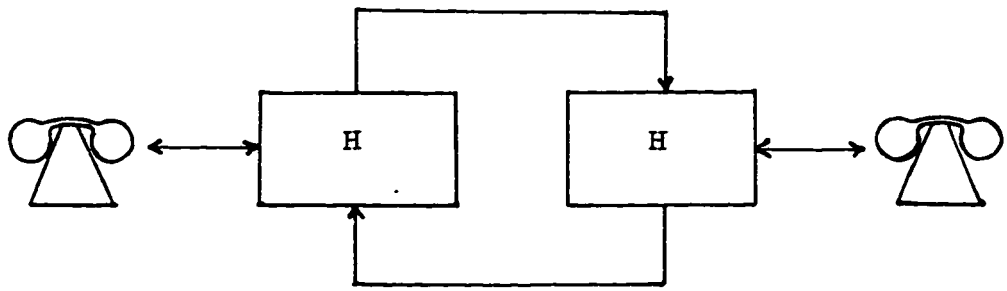

(a) Simplified telephone connection.

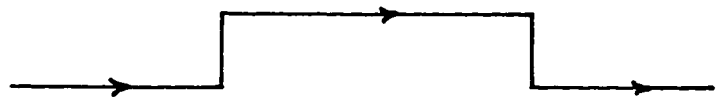

(b) Talker Speech path

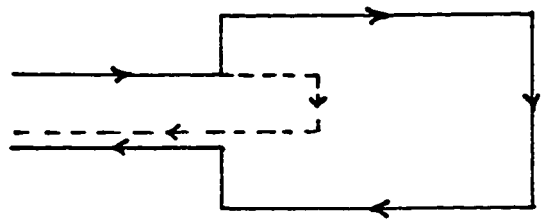

(c) Talker echo

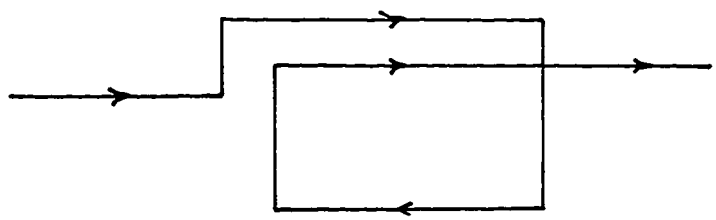

(d) Listener echo

Figure 2.1 A typical long-distance telephone network.

line (called the customer's loop or local loop) which serves for communication in both direction. This results in considerable saving of wires as well as of local switching equipment [10].

Two-wire circuits are quite satisfactory for local telephone calls which are set up by simply connecting the two customers' loops at the same central office. However, for circuits longer than about 55 km, a separate path is necessary for each direction of transmission because of two main reasons. First, long circuits require amplifications, and amplifiers are one way devices. Second, for reasons of economy, most long-distance calls are multiplexed, and multiplexing requires that signals in the two directions be sent over different frequency slots. Hence, we should have a way of connecting or converting from two-wire to four-wire and vice versa. A device that accomplishes this task is called a hybrid or, sometimes, is called a hybrid transformer. One such device is needed at each end, as shown in Fig. 2.1. The details of the hybrid are shown in Fig. 2.2. Basically, it is a bridge circuit. Ideally, the two transformers are identical and the balancing impedance is exactly equal to the impedance of the two-wires circuit at all frequencies. If so, then any signal originating on the "in" side of the four-wire circuit gets coupled to the two-wire circuit, but produces no response in the "out" side of the four-wire circuit. A signal originating in the two-wire circuit couples to both paths of the four-wire circuit. However, it has no effect on the "in" side because the amplifiers in that circuit point in the opposite direction [10].

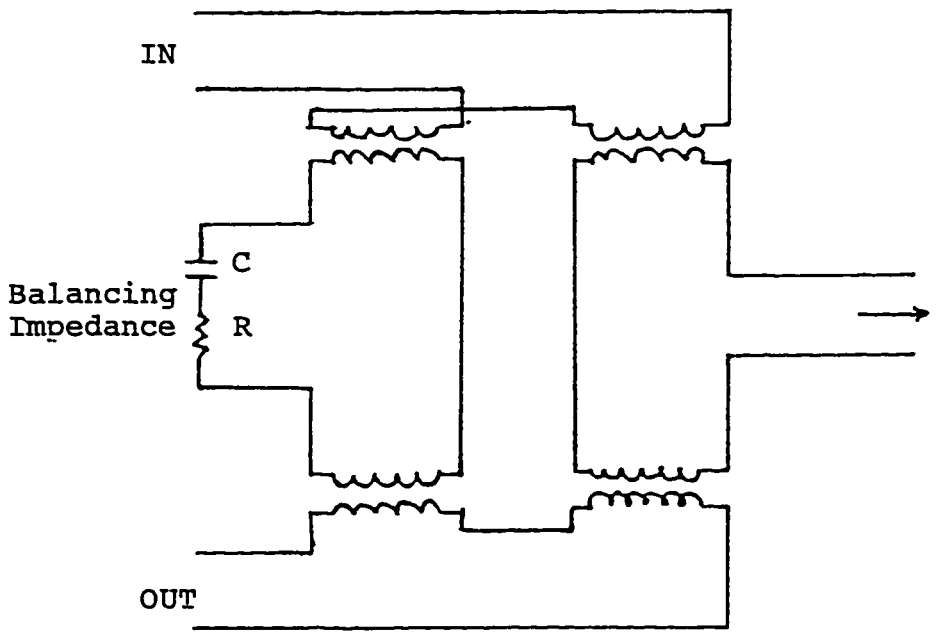

Figure 2.2 Details of a hybrid circuit.

If the bridge is not perfectly balanced, i.e. the balancing impedance is slightly different from the line impedance, the "in" side is coupled to the "out" side of the hybrid, thus giving rise of echo. The only way to prevent such an echo is to make the balancing impedance exactly identical to the impedance of the two-wire circuit within the frequency band of interest. However, the number of existing local loops of a wide variety of line impedance is so large that one can not design individual hybrid for each line.

As it does not appear to be economically feasible to replace the local network by a four-wire network, the best that can be done is to select a compromise balancing impedance to approximate a wide range of lines. Obviously, the amount of echo will now depend on the difference of the compromise impedance and the actual impedance of the particular line the hybrid is connected to. Typically a 600- Ω resistor with a 2-μF capacitor connected in series form such an impedance. In the U.S., such an impedance gives an average attenuation from the input to the output of the hybrid of about 11 dB discounting physical hybrid losses, with a standard deviation of 3 dB [10]. In Saudi Arabia the 2-μF capacitor is omitted [11].

2.2 ECHO : CAUSES AND TYPES

As already seen in Section 2.1, impedance mismatches at the hybrid couplers are the main sources of echoes. Other sources are impedance mismatches in station equipment and irregularities in local loops and other

components of the telephone circuit [12]. Figure 2.1(b) shows the talker speech path. Some energy leaks directly through the first hybrid encountered by the talker signal. This signal is called the "near echo". Similarly, some energy leaks through the hybrid at the other end of the four-wire circuit and is looped back to the talker. This signal is called the "far echo", Fig 2.1(c). These two echo components have different characteristics as seen in Fig 2.3. The near-end echo is characterized by a short time delay, usually less than 20 ms. It has a large amplitude, which in some cases can be up to 10 dB below the transmitted signal. However, the far-end echo has a much lower level, but a longer time delay. This time delay varies according to the transmission distance from a few milliseconds to hundreds of milliseconds. One other type of echo, called listener echo, is shown in Fig. 2.1(d). As can be seen in the figure, the listener echo is actually the talker signal after reflecting back again to the listener. This listener echo signal is very weak and can be neglected.

2.3 CONVENTIONAL METHODS OF ECHO CONTROL IN VOICE COMMUNICATION

The importance of dealing with echos in telephone network has been recognized since the very early days of long-distance telephony [13]. Depending on the length of the circuit we have three main procedures for echo control in voice communication.

1) On short circuits, a certain loss, say L dB, is inserted in each direction of

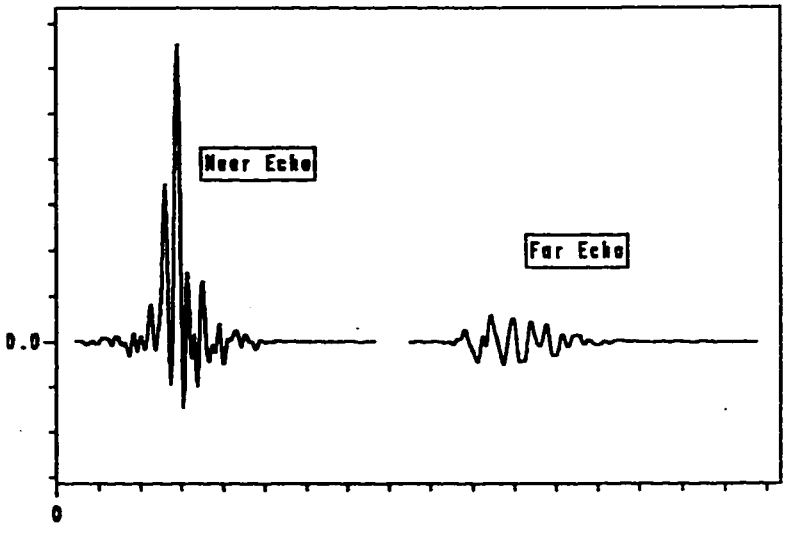

Figure 2.3 Typical echo impulse response.

transmission at the four-wire portions. This attenuates the signal by L dB, while at the same time attenuating the echo by 2L dB. Thus the signal to far echo ratio is improved by L dB.

2) For circuits exceeding about 3200 km in length, the last procedure can not be used because it results in unacceptably low levels at the receiver. For such circuits a device called echo suppressor is used. A simplified echo suppressor logic is shown in Fig. 2.4 for the right hand portion of Fig. 2.1. Basically it consists of a voice-operated switch whose action is controlled by the speech of the users. These echo suppressors have been used successfully for over 50 years on circuits with round-trip delay up to about 100 ms [10].

3) For very long circuits (satellite links) where the delay can be up to 600 ms, new devices called echo cancelers are used. These devices are basically adaptive tapped-delay line filter. They are capable of synthesizing a replica of the echo signal. This replica is then subtracted from the incoming echo signal.

2.4 FULL-DUPLEX DATA TRANSMISSION OVER TELEPHONE NETWORKS

Although echo cancellers were first proposed in 1966, [14], [15], to replace echo suppressors in telephone network for better intelligibility of speech, nowadays they are finding increasing application in data communication systems, especially in full-duplex high data rate transmission. The first study to

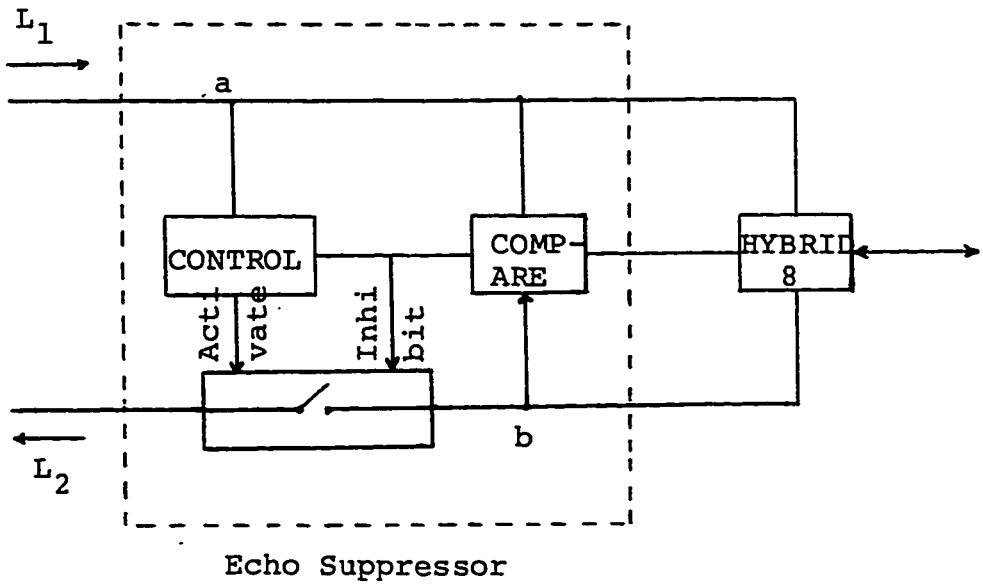

Figure 2.4 Simplified echo suppressor logic.

evaluate the feasibility of using the echo canceller for use in voice-band full-duplex data transmission on two-wire circuits appeared in 1973 by Koll and Weinstein [3]. Since that day, several structures, more appropriate to data signals, have been studied by exploiting some properties of the data: their binary nature and their bandwidth.

Figure 2.5 shows how the telephone network is used for data transmission. The two telephone sets shown in Fig. 2.1 are replaced by two modems; each modem has its own transmitter and receiver. As mentioned earlier in Section 1.2, to achieve higher rates for full-duplex data transmission the two directions must share the full frequency band of the telephone channel. The interference due to the generated echo is aimed to be cancelled by the echo cancelller. Notice that the near echo loops back from the hybrids at the modem location and the local central office, and the far echo loops back to the modem from the corresponding hybrids at the far end. The purpose of the echo canceller is to synthesize a replica or an estimate of the real line echo which is then subtracted from the incoming signal, as shown in Fig. 2.6. Figure 2.7 shows a typical dialed connection using cancellers for full-duplex data transmission. Here we have two cancellers, one at each end of the circuit. The canceller in side A synthesizes a replica of both the near and the far echo due to the signal transmitted from transmitter A, while the canceller in side B. synthesizes a replica of both the near and the far echo due to the signal transmitted from transmitter B.

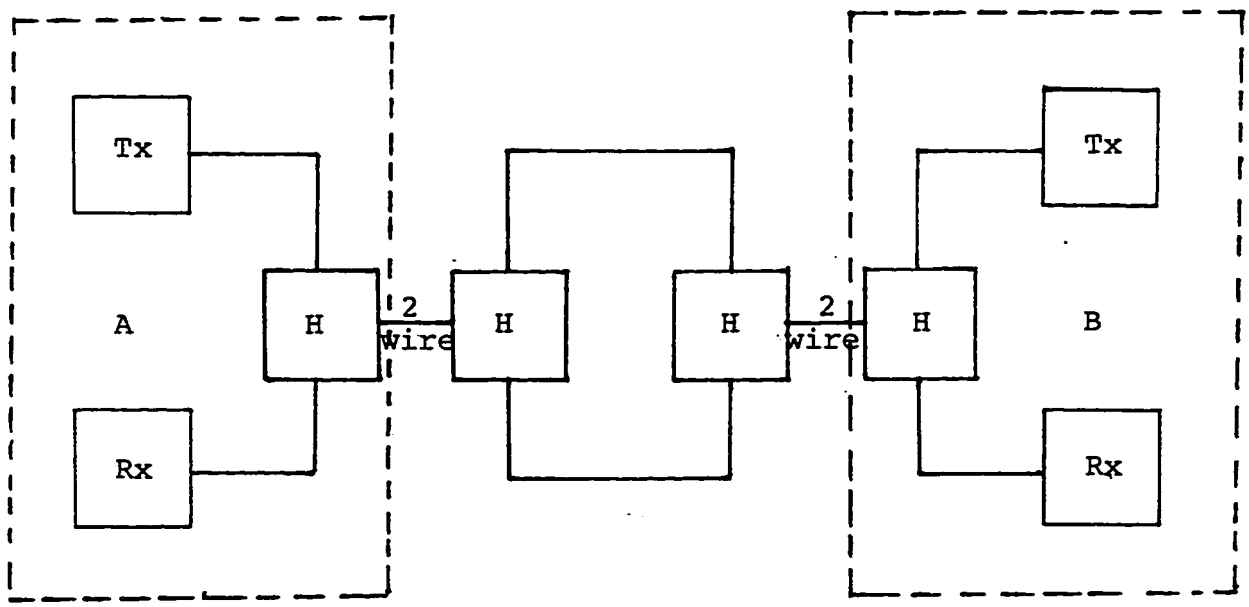

Figure 2.5 Typical dialed connection for data transmission

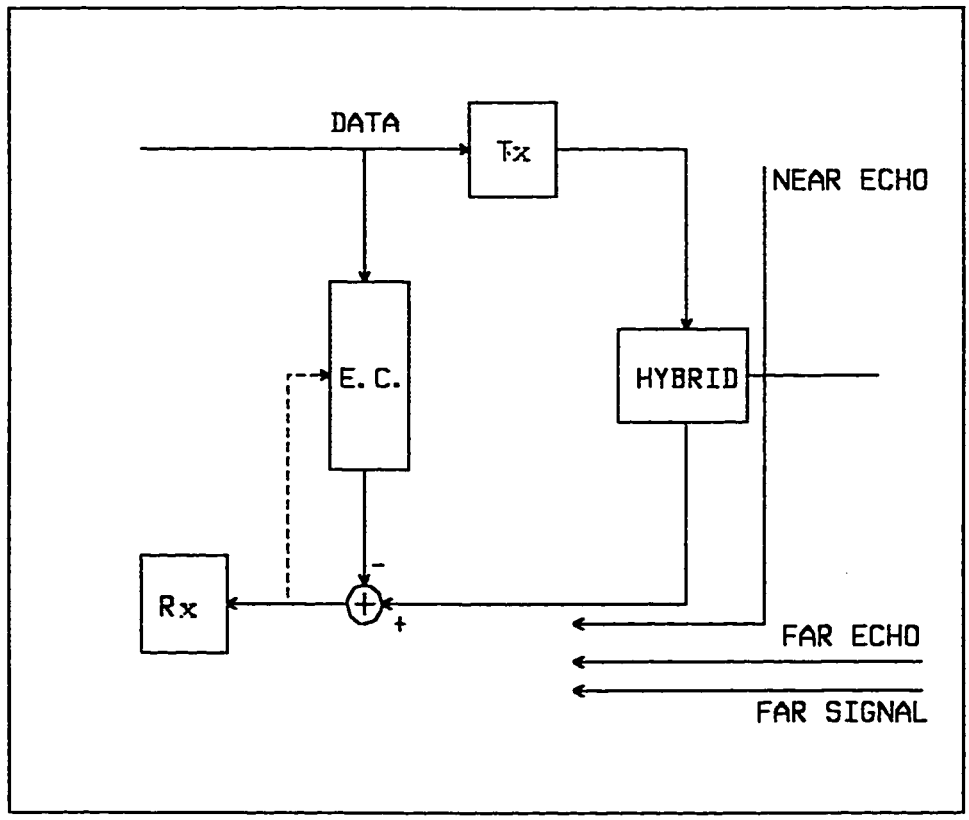

Figure 2.6 Use of echo canceller at station location.

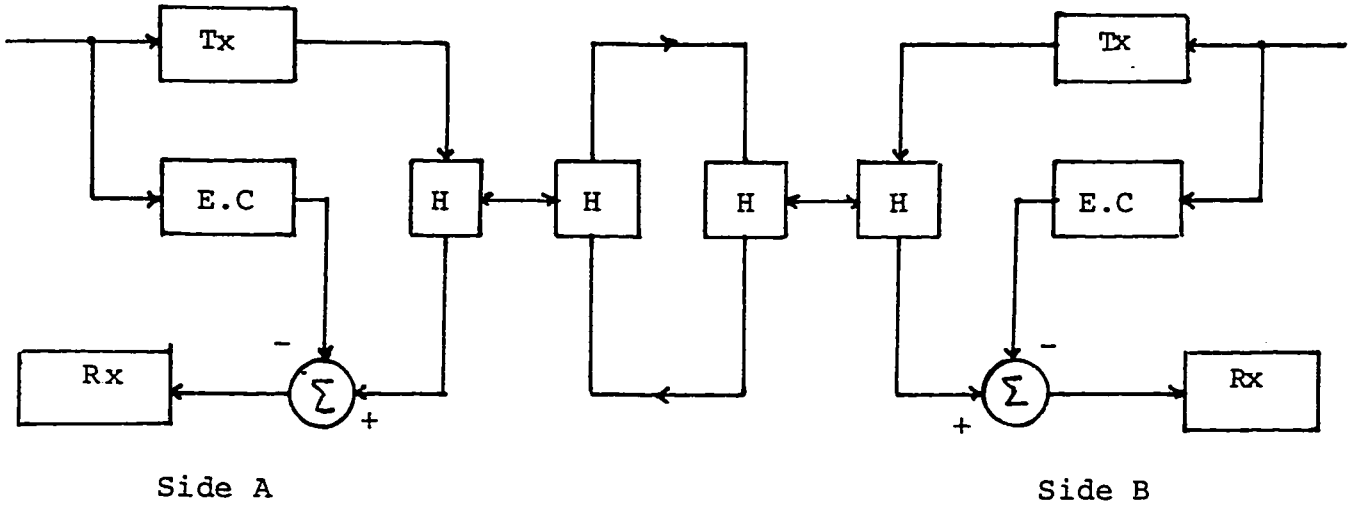

Figure 2.7 Typical dialed connection for full duplex data transmission.

2.5 ECHO SIGNAL MODELING IN DATA TRANSMISSION

A two-dimensional (in-phase and quadrature) modulated signal is generally represented by the expression

$$s(t) = \mathrm{Re}\ \{ \sum_n A_n g(t-nT) e^{jw_c t} \} \tag{2.1}$$

where $A_n = a_n + jb_n$ is the discrete-valued multilevel complex symbol to be transmitted, g(t) is the baseband pulse shape, 1/T is the symbol rate and $w_c/2\pi$ is the carrier frequency. After passing through the echo channel with impulse response $h_e(t)$, the received echo signal, which we desire to cancel, is

$$r_e(t) = \mathrm{Re}\ \{ \sum_n A_n h(t-nT) e^{jw_c t} \} \tag{2.2}$$

where h(t) is defined as

$$h(t) = g(t) * h_e(t) \tag{2.3}$$

in which '*' denotes the convolution operation.

Thus, the echo signal $r_e(t)$ can be obtained by feeding the symbols A_n to a bandpass filter with impulse response h(t). In this case, it is assumed the echo channel is linear and therefor completely described by its impulse response.

2.6 SUMMARY

Echo signal is generated in telephone network due impedance mismatches at the hybrid couplers. For full duplex data transmission, echo cancellers have

been seen to be a good solution for the echo problem. Echo canceller were first proposed to replace the echo suppressor in voice communication. However, they are heavily used in full-duplex. For this reason, various structures have been developed for this application. These structures are presented and analysed in the next chapter.

CHAPTER 3

ECHO CANCELLERS

It has been mentioned earlier in the previous chapter that various structures, more appropriate for data transmission, have been proposed since 1973 [5,6,8,16]. Each structure has its own advantages and disadvantages. A detailed literature survey of these structures is give in this chapter. Also, we will be exposed to some problems encountered in echo cancellation.

3.1 BASIC STRUCTURE

The most general echo canceller structure is shown in Fig. 3.1. Basically it is an adaptive tapped-delay-line filter. The tabs of the filter, which are used to store the past values of the input sequence, are spaced by time T s., where T is equal to the symbol interval in the conventional structure. The adjustable coefficient set $c_m(n)$, with $1 \le m \le M$, defines the various weightings applied to the delay-line taps at time index n in order to replicate the line echo $r_e(n)$, where M is the length of the filter.

If u(n) is the input sequence to the canceller, then the output is given by

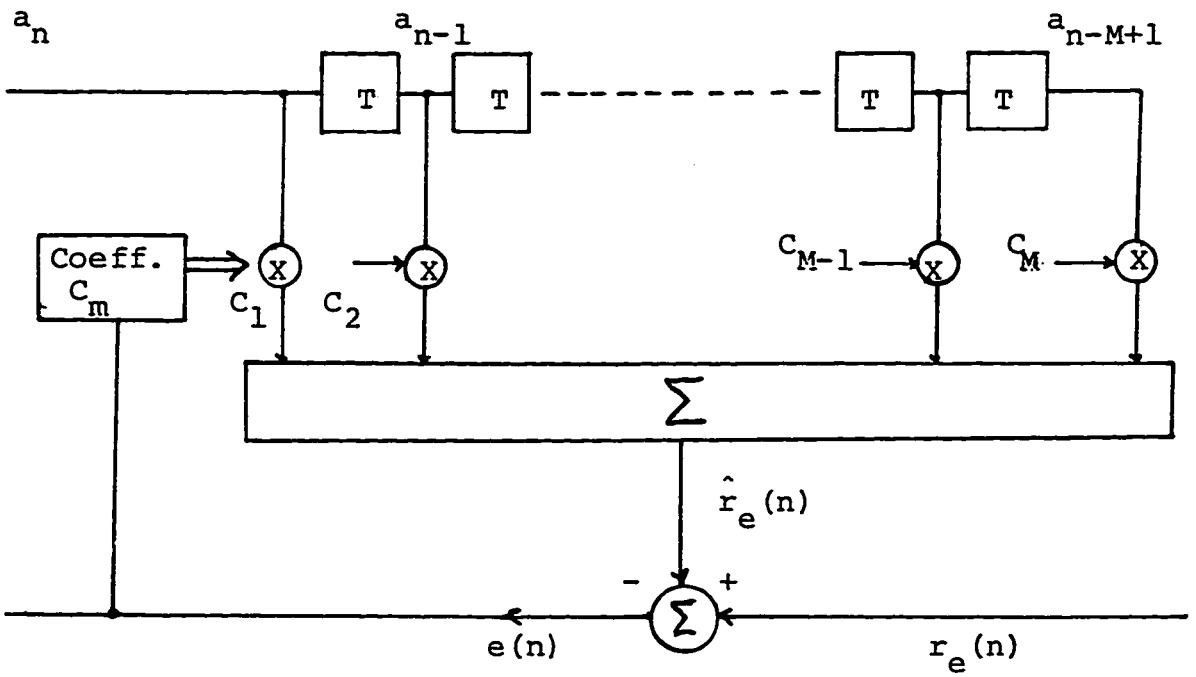

Figure 3.1 Basic structure of an Echo Canceller.

$$\hat{r}_e(n) = \sum_{m=1}^{M} c_m(n)\, u(n-m+1) \tag{3.1}$$

Which can be rewritten as

$$\hat{r}_e(n) = \sum_{m=1}^{M} u(n)\, c_m(n-m+1) \tag{3.2}$$

Notice that Eq. (3.2) is very similar to Eq. (2.2). If we assume that there is no transmitted signal from the far end, then the error after the subtractor (Fig. 3.1) is

$$e(n) = r_e(n) - \hat{r}_e(n) \tag{3.3}$$

The coefficients are updated under the control of the error signal e(n) according to an adaptation criterion which is usually the least-mean-squared (LMS) algorithm (presented in details in Sect. 3.2.1) until they converge to the impulse response of the echo channel h(t).

Assuming that the signal is transmitted at a power level of 0 dBm, then the received near echo signal will be at -10 dBm due to the 10 dB attenuation of the hybrid. However, the far signal is received typically at about -30 dBm. With the echo being considered as noise, then, the signal-to-noise ratio (S/N) will be -20 dB, which is very low for proper receiving and correct decision for the far transmitted signal. The S/N should be at least from 20 to 30 dB at the receiver. Therefor, the echo canceller must provide enhancement of at least 40 to 50 dB.

The measure that is used to know how well the canceller performs is the Echo-Return-Loss Enhancement (ERLE) [7]. It is defined as

$$\text{ERLE} = -10 \log \left[\frac{E[e^2]}{E[r_e^2]} \right] \tag{3.4}$$

where $r_e(n)$ and $e(n)$ are as defined in Eqs. (2.2) and (3.3) respectively. " E " represents the expectaion operator. The ERLE measures the degree to which the echo has been attenuated, and it is maximized by minimizing the mean-squared error, $E[e^2]$.

The number of tabs M of the delay line is governed by the echo time delay range to be covered. The echo canceller structure of Fig. 3.1 is not quite appropriate for long delayed far end echos due to the huge number of echo canceller coefficients implied. Moreover, the near echo and the far echo have different characteristics. The near echo has a large amplitude. The hybrid introduces mainly linear distortion. This is not true for far end echo. The far echo has relatively lower amplitude and propagates through a channel which is generally dispersive, time varying and sometimes non-linear. Hence, it is found to be more convenient to break the canceller into two parts, a "near canceller" and a "far canceller" as shown in Fig. 3.2. More detailed discussion about the far echo effects will be presented later.

The echo canceller shown in Fig. 3.2 consists of two distinct sections dealing respectively, with the near end and far end echoes. They are separated by a bulk delay. This bulk delay depends on the transmission distance and must be adjusted to each connection. It can be determined by sounding the echo channel with an appropriately designed pulse. Then, a provided timing circuitry

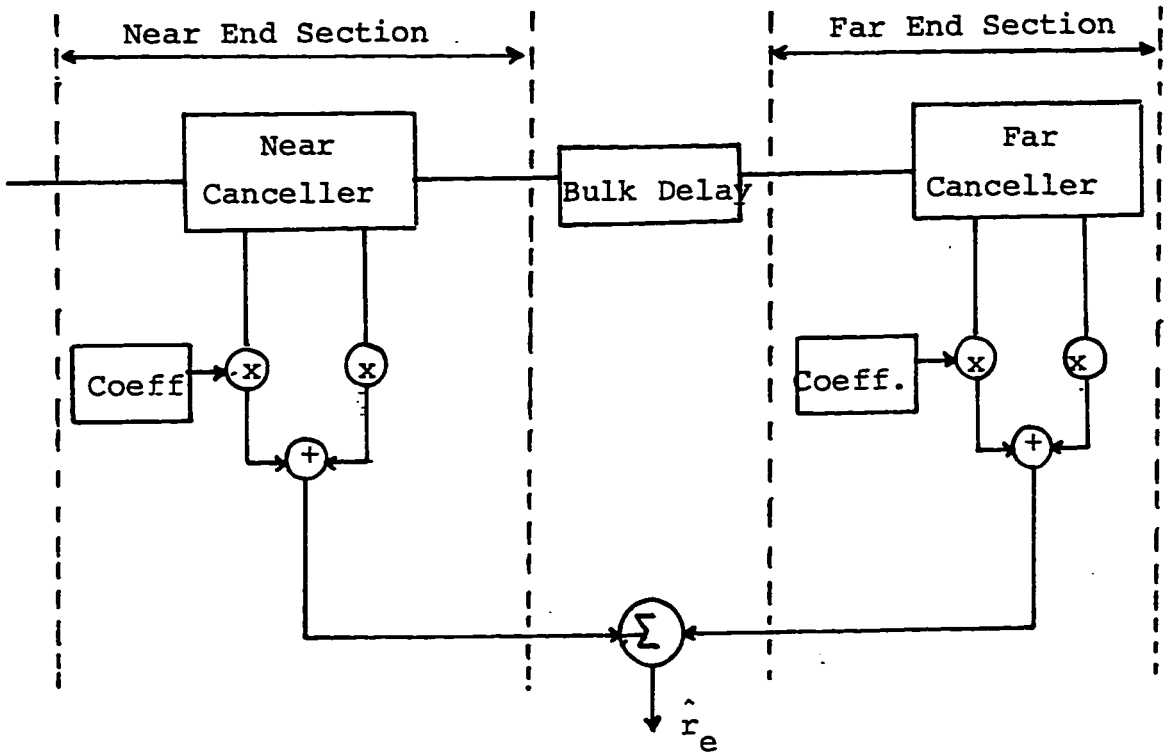

Figure 3.2 Echo canceller with a bulk delay.

measures the propagation time of the sounding pulse and set the canceller with the correct bulk delay [12]. More details about modem training sequence to determine the bulk delay ican be found in [17]. With this improvement the number of active echo canceller tabs M is greatly reduced.

Due to the involvement of a more dispersive channel, the far canceller requires a large memory span than the near canceller. However, under worst-case conditions of hybrid leakage and signal levels, the near canceller has to provide a much larger attenuation than the far canceller. In both cases, these attenuations generally have to be achieved under "double-talking" (full-duplex transmission) conditions. In the case of the far canceller, this should be achieved in the presence of time-varying and nonlinear echo-channel impairments [7].

3.2 ADAPTATION MECHANISMS

In the preceding section, we saw that the echo signal is closely modeled by the output of an echo canceller. This canceller represents the echo channel. The echo channel is seen to depend greatly on the particular switching connection which has a wide variability from one call to another, even between the same end points. Accordingly, the echo canceller coefficients should be determined for each call in advance, prior to the start of data transmission. Similar to the automatic equalization procedure [18], a training sequence is assigned to the echo canceller and is transmitted through the channel at the

same time. When this sequence returns as an echo, it is used by the canceller to adjust the coefficients according to a certain adaptation mechanism. In this section, the gradient algorithm is discussed since it is the commonly used in echo cancellation due to its simplicity.

3.2.1 The Gradient Approach [19]

The gradient approach is reviewed with reference to Fig. 3.1. Let u(n) be the input sequence to the filter and $c_m(n)$, i = 1,2,...,M be the filter coefficients at time index n. The output $\hat{r}_e(t)$ of the filter at time index n is

$$\hat{r}_e(n) = \sum_{m=1}^{M} c_m(n)u(n-m+1) \tag{3.5}$$

The error signal e(n) is produced by comparing the output $\hat{r}_e(n)$ with the desired response $r_e(n)$

$$e(n) = r_e(n) - \hat{r}_e(n) \tag{3.6}$$

Let the mean-squared value of the error signal be denoted by

$$\varepsilon(n) = E[e^2(n)] \tag{3.7}$$

where E is the expectation operator. This mean-squared value is a real and positive quantity, representing the average power of e(n) when it is developed across a 1 ohm. Substituting Eq. (3.6) in (3.7), we get

$$\varepsilon(n) = \mathcal{E}[r_e^2(n)] - 2\mathcal{E}[r_e(n)\hat{r}_e(n)] + \mathcal{E}[\hat{r}_e^2(n)] \tag{3.8}$$

Next, substituting Eq. (3.5) in (3.8), and then interchanging the orders of summation and expectation in the two terms, we get

$$\varepsilon(n) = \mathcal{E}[r_e^2(n)] - 2\sum_{m=1}^{M} c_m(n)\,\mathcal{E}[r_e(n)u(n-m+1)]$$

$$+ \sum_{m=1}^{M}\sum_{j=1}^{M} c_m(n)c_j(n)\,\mathcal{E}[u(n-m+1)u(n-j+1)] \tag{3.9}$$

Assuming that the input signal u(n) and the desired response $r_e(n)$ are jointly stationary, the three terms on the right-hand side of Eq. (3.9) may be interpreted as follows:

1. The expectation $\mathcal{E}[r_e^2(n)]$ is equal to the mean-squared value of the desired response $r_e(n)$:

$$P_d = \mathcal{E}[r_e^2(n)] \tag{3.10}$$

2. The expectation $\mathcal{E}[r_e(n)u(n-m+1)]$ is equal to the cross-correlation function of the desired response $r_e(n)$ and the input signal u(n) for a lag of m-1:

$$p(m-1) = \mathcal{E}[r_e(n)u(n-m+1)], \qquad m = 1,2,...,M \tag{3.11}$$

3. Finally, the expectation $\mathcal{E}[u(n-m+1)u(n-j+1)]$ is equal to the autocorrelation function of the input signal u(n) for a lag of j-m:

$$r(j-m) = E[u(n-m+1)u(n-j+1)] \tag{3.12}$$

Thus, substituting Eqs. (3.10),(3.11), and (3.12) in (3.9), we find that the expression for the mean squared error may be written in the form

$$\varepsilon(n) = P_d - 2\sum_{m=1}^{M} c_m(n)p(m-1) + \sum_{m=1}^{M}\sum_{j=1}^{M} c_m(n)c_j(n)r(j-m) \tag{3.13}$$

Equation (3.13) states that the mean squared error $\varepsilon(n)$ is precisely a second-order function of the filter coefficients. Thus, we may visualize the dependence of $\varepsilon(n)$ on the filter coefficients as a bowl-shaped surface with a unique minimum. We refer to this surface as the error performance surface of the adaptive filter. The adaptive process has the task of continually seeking the bottom or minimum point of this surface, where the filter coefficients assume their optimum values.

The mean squared error $\varepsilon(n)$ attains its minimum value when its derivatives with respect to the tap coefficients c(m), for m = 1,2,...,M, are simultaneously zero. Differentiating Eq. (3.13) with respect to c(m), we get

$$\frac{\partial \varepsilon}{\partial c_m(n)} = -2p(m-1) + 2\sum_{j=1}^{M} c_j(n)r(j-m) \tag{3.14}$$

Setting this result to zero, we obtain the optimum values of the tap coefficients. Let these values be denoted by $c_{m_o}(n)$, for m = 1,2,...,M. They are given by the solution of the set of equations

$$\sum_{j=1}^{M} c_{j_o}(n)r(j-m) = p(m-1), \quad m = 1,2,...,M \tag{3.15}$$

Then, the minimum mean squared error resulting when the tapped-delay-line filter assumes its optimum conditions is

$$\varepsilon_{min}(n) = P_d - 2\sum_{m=1}^{M} c_{m_o}(n)p(m-1) + \sum_{m=1}^{M}\sum_{j=1}^{M} c_{m_o}(n)c_{j_o}(n)r(j-m) \tag{3.16}$$

By substituting Eq. (3.15) in (3.16), the expression of the minmum mean squared error may be simplified as follows:

$$\varepsilon_{min}(n) = P_d - \sum_{m=1}^{M} c_{m_o}(n)p(m-1) \tag{3.17}$$

We refer to a tapped-delay-line filter whose impulse response is defined by the Eq. (3.15) as optimum in the mean-squared sense. The adaptive process has the task of seeking this MMSE.

3.2.2 The Method of Steepest Descent

We would like to develop a recursive procedure whereby appropriate corrections are applied to these filter coefficients in such a way that we continually move closer to the minimum point of the error performance surface after each iteration. According to the method of steepest descent we proceed as follows:

1. We begin with a set of initial values for the filter coefficients, which could be zeros.

2. Using theses initial values, we compute the **gradient vector,** whose individual elements equal the first derivatives of the mean squared error $\varepsilon(n)$ with respect to the filter coefficients.

3. We compute the next values of the filter coefficients by making a change in the initial or present values in a direction opposite to that of the gradient vector (i.e; in the direction of the steepest descent of the error performance surface).

4. We go back to step (2) and repeat the procedure.

Let $\Delta(n)$ denote the M-by-1 gradient vector at time n, where M equals the number of the filter coefficients. The mth element of $\Delta(n)$, by definition, equals the first derivative of the mean squared error $\varepsilon(n)$ with respect to the filter coefficient $c_m(n)$, Eq. (3.14). The expression in Eq. (3.14) can be shown to be the following

$$\frac{\partial \varepsilon}{\partial c_m(n)} = -2\,E\,[e(n)u(n-m+1)], \qquad m = 1,2,...M \tag{3.18}$$

Equation (3.18) states that, except for the scaling factor 2, the mth element of the gradient vector $\Delta(n)$, is the negative of the cross-correlation between the error signal e(n) and the signal $u(n-m+1)$ at the mth tap input. We may rewrite Eq. (3.18) in matrix form as follows:

$$\Delta(n) = \begin{bmatrix} \partial\varepsilon(n)/\partial c_1(n) \\ \partial\varepsilon(n)/\partial c_2(n) \\ \cdot \\ \cdot \\ \cdot \\ \partial\varepsilon(n)/\partial c_M(n) \end{bmatrix}$$

$$= \begin{bmatrix} -2\,E\,[e(n)u(n)] \\ -2\,E\,[e(n)u(n-1)] \\ \cdot \\ \cdot \\ \cdot \\ -2E\,[e(n)u(n-M+1)] \end{bmatrix} \tag{3.19}$$

Taking out the common factor -2, the expectation operator, and the error signal e(n), Eq. (3.19) becomes

$$\Delta(n) = -2\,E\,[e(n)\mathbf{u}(n)] \tag{3.20}$$

where $\mathbf{u}(n)$ is the M-by-1 tap-input vector whose elements consist of the M tap inputs of the filter:

$$\mathbf{u}(n) = \begin{bmatrix} u(n) \\ u(n-1) \\ \cdot \\ \cdot \\ \cdot \\ u(n-M+1) \end{bmatrix} \tag{3.21}$$

We are now ready to formulate the steepest-descent algorithm for updating

the filter coefficients. Define the M-by-1 coefficient vector of the filter at time n as

$$\mathbf{c}(n) = \begin{bmatrix} c_1(n) \\ c_2(n) \\ \cdot \\ \cdot \\ \cdot \\ c_M(n) \end{bmatrix} \tag{3.22}$$

Then, according to the steepest-descent algorithm, the update value of the coefficient vector at time n + 1 is defined by

$$\mathbf{c}(n+1) = \mathbf{c}(n) + \tfrac{1}{2}\alpha[-\Delta(n)] \tag{3.23}$$

where α is a positive scalar and $\Delta(n)$ is the gradient vector at time n. Substituting Eq. (3.20) in (3.23), we get

$$\mathbf{c}(n+1) = \mathbf{c}(n) + \alpha E[e(n)\mathbf{u}(n)] \tag{3.24}$$

where the error signal e(n) equals

$$e(n) = r_e(n) - \mathbf{u}^T(n)\mathbf{c}(n) \tag{3.25}$$

where $\mathbf{u}^T(n)$ is the transpose of the tap-input vector.

The combination of Eqs. (3.24) and (3.25) defines the steepest-descent algorithm. The algorithm is initiated with an arbitrary guess c(0). It is customary to set all the tap-coefficients of the filter initially equal to zero. The

significant feature of the steepest-descent algorithm is that the gradient vector (and therefore the correction) may be conveniently computed without knowledge of the error performance surface.

3.2.3 The Least-Mean-Square (LMS) Algorithm

The main limitation of the steepest-descent algorithm is that it requires the exact measurements of the gradient vector at each iteration. This is not possible in reality. Hence, we derive estimates of the gradient vector from the available data. This is the task of the least-mean-squared (LMS) algorithm which uses instantaneous estimates of the gradient vector, based on sample values of the tap-input vector $\mathbf{u}(n)$ and the error signal $e(n)$. In particular, from Eq. (3.20) we deduce the following instantaneous estimate of the gradient vector:

$$\hat{\Delta}(n) = -2e(n)\mathbf{u}(n) \tag{3.26}$$

This is an unbiased estimate, because its expected values is exactly the same as the actual gradient vector of Eq. (3.2). The formulation of the least-mean-squared (LMS) algorithm is

$$\begin{aligned}\mathbf{c}(n+1) &= \mathbf{c}(n) + \tfrac{1}{2}\alpha[-\hat{\Delta}(n)] \\ &= \mathbf{c}(n) + \alpha e(n)\mathbf{u}(n)\end{aligned} \tag{3.27}$$

where α is the step-size parameter and the error signal $e(n)$ is defined by Eq. (3.25), reproduced here for convenience:

$$e(n) = r_e(n) - \mathbf{u}^T(n)\mathbf{c}(n) \tag{3.28}$$

Equations (3.27) and (3.28) completely describe the LMS algorithm. As with the steepest-descent algorithm, it is customary to initiate the LMS algorithm by setting all the coefficients of the filter equal to zero. The attractive feature of this algorithm is its relative simplicity; it does not require measurements of the pertinent correlation functions, nor does it require matrix inversion.

To assure convergence of both the steepest-descent and the LMS algorithms the step-size α should satisfy

$$0 < \alpha < \frac{2}{\lambda_{max}} \tag{3.29}$$

where λ_{max} is the largest eigenvalue of the correlation matrix $\mathbf{R} = E[\mathbf{u}(n)\mathbf{u}^T(n)]$.

3.3 CLASSIFICATIONS OF ECHO CANCELLERS

Based on their input, echo cancellers can mainly be classified into two types: voice-type canceller, which takes its input from the output of the transmitter, and a data-type canceller, which gets its input directly from the data symbols at the input of the transmitter. We shall briefly discuss each type individually and then give some comparison between the two.

3.3.1 Voice-Type Cancellers

The voice-type canceller was first proposed by Koll and Weinstein in 1973 [3] in the very early trials to investigate the feasibility of using the echo canceller for full-duplex data transmission. A block diagram of a voice-type echo canceller is shown in Fig. 3.3 (a). As can be seen, the transmitter output is applied simultaneously to the hybrid circuit and the cancellr.

Experimental results showed that this type of echo cancellers is not practical due to several reasons. First, the implementation is quite difficult and costly even in digital form [4]. Second, to achieve cancellation over the full frequency range, taps must be spaced closer than half the reciprocal value of the upper frequency limit of the echo signal. In other words, the tab spacing is not simply equal to the symbol interval T. Due to those reasons besides that the output signal from the transmitter is not in a simple form (due to modulation and filtering occurring in the transmitter), a prohibitive number of multiplications are required. Finally, the achieved bit rate was only 2000 bit/s [5]. Hence, other researchers thought of a new structure where it is possible to overcome some of these problems. The new structure is called the data-driven or data-type echo canceller.

3.3.2 Data-Type Cancellers

This type was first proposed by Mueller in 1976 [4]. Figure 3.3 (b) shows a

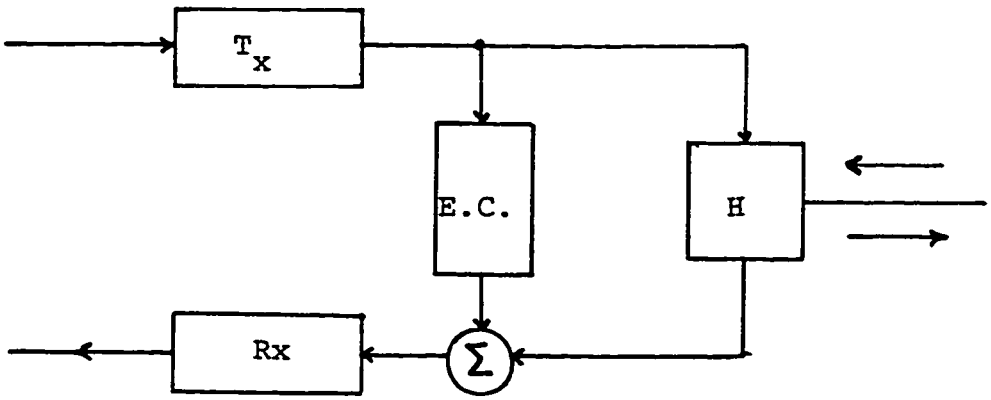

(a) Voice-type echo canceller

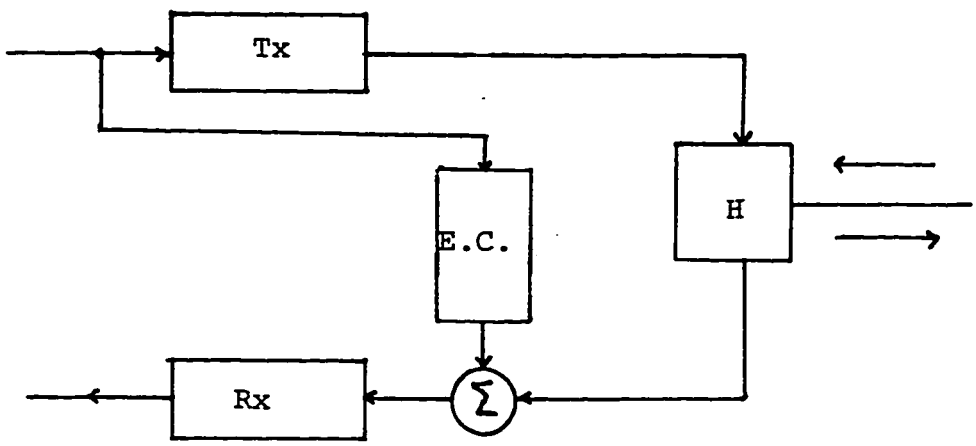

(b) Data-type echo canceller

Figure 3.3 Echo cancellers: classifications based on the input.

schematic structure of a data-type canceller. Now the input of the canceller is the input data directly before the transmitter. Hence, the echo signal is synthesized directly from the data symbols themselves. This type of cancellers is used when the linear modulation schemes (such as various methods of QAM signal constellations, PSK, VSB, and SSB signaling) are used for data transmission. In this case the passband data signal can be expressed as a linear combination of the data symbols. As long as the echo path is linear, the echo signal is such a linear combination. Hence, the cancellation signal can therefore be synthesized directly from the data symbols [5].

The main advantage of the data-type canceller over the voice-type is that the tap signals can now be binary, hence the multiplications can be reduced to simple additions and subtractions. Moreover, due to the exploitation of the various relationships existing between the baud rate, sampling rate and the carrier frequency, the achieved bit-rate of transmission can now be up to 9600 bits/s.

Moreover, cancellation can be achieved in passband or baseband, in digital or analog form, and either on a continuous basis or only at the sampling instants, resulting in a number of possible arrangements of this data-type canceller, see Fig. 3.4. In the continuous case, the canceller generates samples at several times the symbol rate, while for compensation at the sampling instants only, the canceller operates at the symbol rate, in synchronism with the far transmitter clock [4]. Based on that, the data-type canceller is divided into two different and important structures: synchronous cancellers and Nyquist-rate

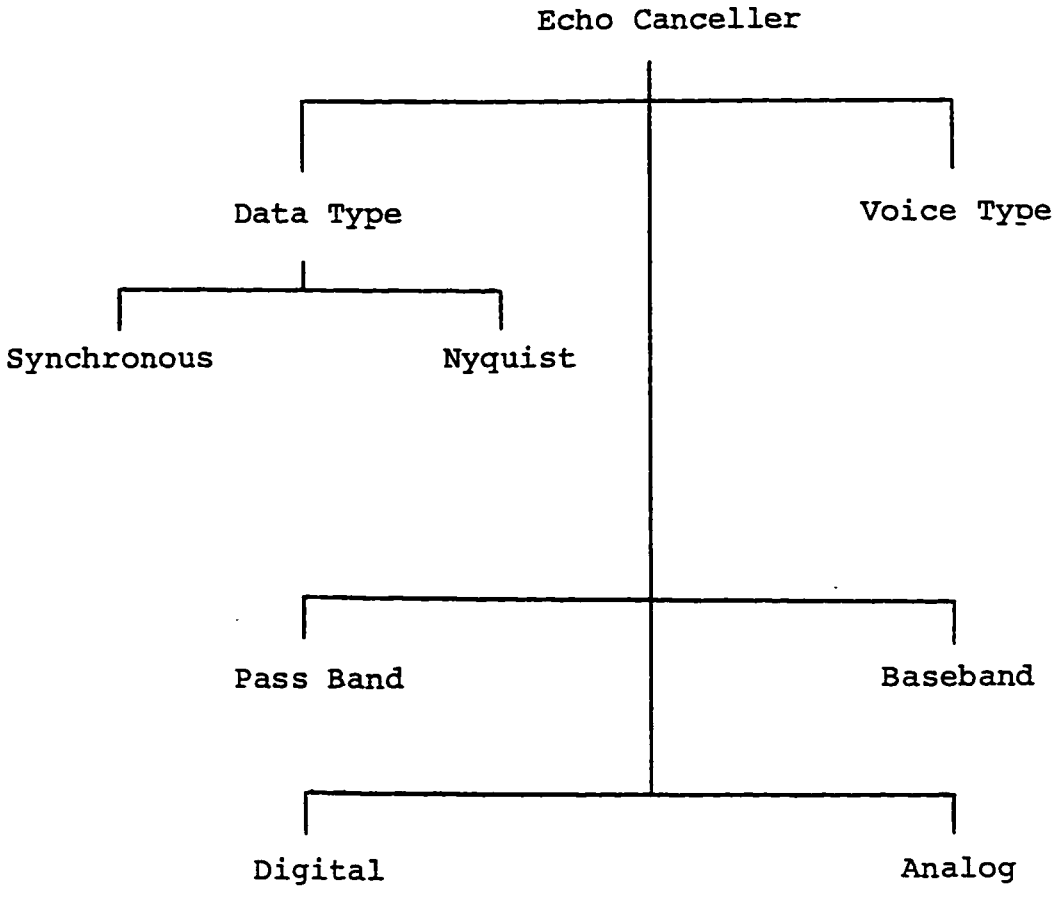

Figure 3.4 Classification of Echo Cancellers.

cancellers.

Synchronous data-type echo cancellers. In fact, the first data-driven echo canceller proposed by Mueller [4] was a synchronous one, shown in Fig. 3.5. It is characterized by the following:

- The canceller's taps are spaced by T, Where T is the data symbol period.
- Adaptation of the canceller coefficients is based on the receiver's output error; the difference between each unquantized output sample and the receiver decision on the discrete-valued data symbol from the far end.
- The canceller operates at the symbol-rate.

the error, e_n , at the receiver output is defined as the difference between the receiver output and the far transmitted symbol at time index n with respect to the symbol period T. To express this error, the following definitions are used,

a_n = near-end data symbols

b_n = far-end data symbols

h_{I_n} = channel impulse response

$g_n = h_{I_n} - \delta_{n0}$ = intersymbol interference

h_n = echo path impulse response

c_n = canceller tab weights

ξ_n = noise samples, mean 0, variance σ^2

N = number of taps to cancel near echo

M = number of taps to cancel far echo

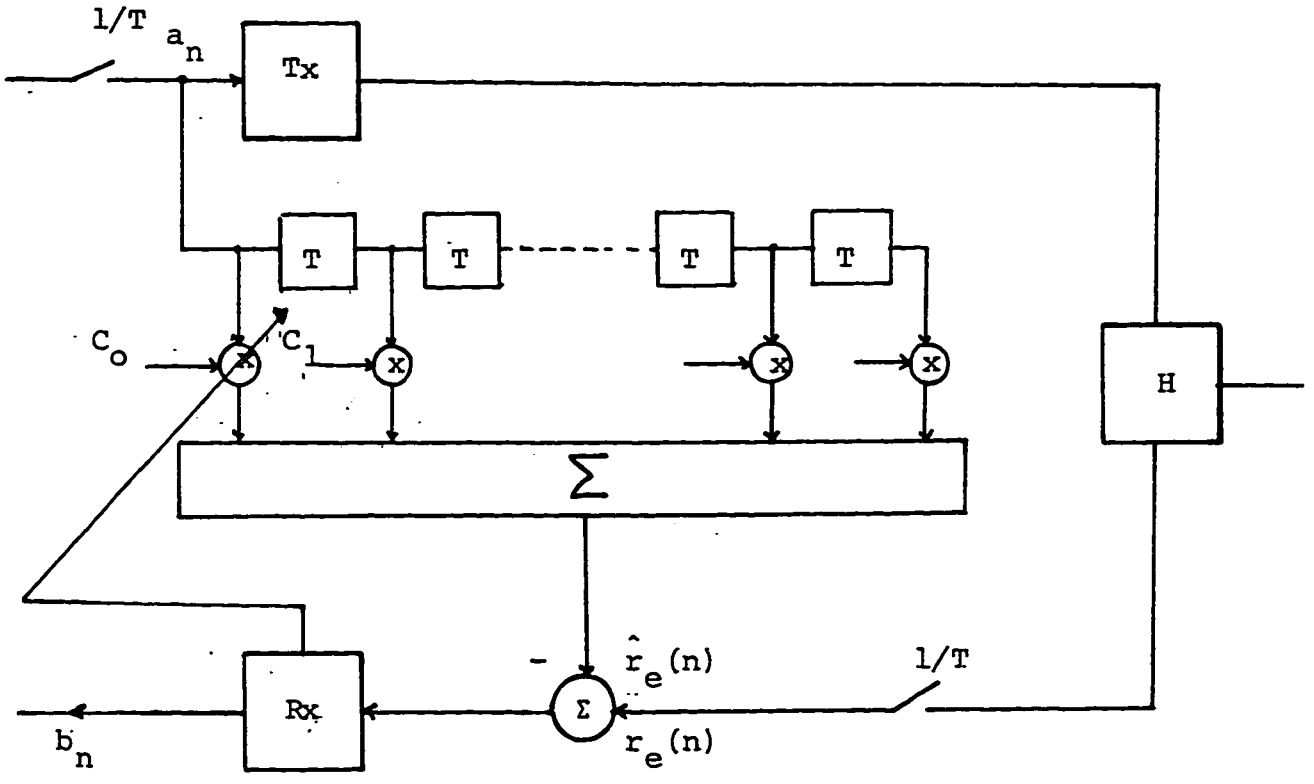

Figure 3.5 Synchronous data-driven echo canceller.

then the error e_n between the output of the receiver and the ideal value b_k is

$$e_n = \sum_{i=-\infty}^{\infty} b_{n-i} h_i + \sum_{i=-N}^{\infty} a_{n-i} h_i - \sum_{i=-N}^{M} a_{n-i} c_i + \xi_n - b_n \qquad (3.30)$$

which can be rewritten as

$$e_n = \sum_{i=-\infty}^{\infty} b_{n-i} g_i + \sum_{i=-N}^{M} a_{n-i}(h_i - c_i) + \sum_{i=M+1}^{\infty} a_{n-i} h_i + \xi_n \qquad (3.31)$$

It is clear that the optimum choice of canceller's coefficients which cancels all echoes within reach of the canceller is

$$c_i = h_i, \qquad -N \le i \le M \qquad (3.32)$$

Introducing the error vector

$$\boldsymbol{\varphi} = \mathbf{h} - \mathbf{c} \qquad (3.33)$$

where $\mathbf{h}$ and $\mathbf{c}$ are vectors with components h_n and c_n respectively, and $\mathbf{h}$ is understood to include only those echo response samples within reach of the canceller. Assuming that a_n and b_n are statistically and mutually independent random variables that take values ± 1 with equal probability then the mean square error is

$$\varepsilon = E[e_n^2] = \boldsymbol{\varphi}^T \boldsymbol{\varphi} + R \qquad (3.34)$$

where the uncncellable mean-squared error is

$$R = \sum_{i=-\infty}^{\infty} g_i^2 + \sum_{i=M+1}^{\infty} h_i^2 + \sigma^2 \tag{3.35}$$

R is composed of intersymbol interference, uncancelled echo noise stemming from samples outside of the reach of the canceller, and channel noise.

A stochastic gradient algorithm, least mean squares (LMS), can be used for adaptive tap adjustment. The gradient of the MS error with respect to tap vector is given by

$$\frac{\partial \varepsilon}{\partial \mathbf{c}} = \frac{\partial}{\partial \mathbf{c}} \boldsymbol{\varphi}^T \boldsymbol{\varphi} = -2E[\mathbf{a}_n \mathbf{e}_n] = -2\boldsymbol{\varphi} \tag{3.36}$$

Then according to the LMS algorithm described before, the recursion equation is

$$\mathbf{c}_{n+1} = \mathbf{c}_n + \alpha \mathbf{a}_n \mathbf{e}_n \tag{3.37}$$

where α is a constant step size.

The main disadvantage here is that good performance of the canceller is dependent on the synchronization of the transmitters in the two stations, which is not usually the case.

Nyquist-rate cancellers. The Nyquist-rate cancellers was first presented by Falconer, Mueller, and Weinstein in late 1976 [4] and was fully described by Weinstein in his paper in July 1977 [12]. Its structure is characterized by the

following:

- The tap spacing is now at $T' = (T/L)$ sec., where L is an integer whose typical value is 3 or 4.
- Adaptation of the canceller coefficients is now based on the error signal taken prior to the receiver shown in Fig 3.5. In this case, the error signal contains the distant signal as an uncorrelated additive 'noise'.
- The canceller operates at (L) times the symbol-rate; i.e. it generates samples at a rate of L/T.

To describe the operation of the Nyquist-rate cancellers the same previous definitions of data symbols and impulse responses are used, besides the assumption that

$$T = LT', \quad L \text{ an integer} \tag{3.38}$$

where T' is the tap delay spacing and T is the symbol interval.

The data symbols, a_n , are sampled at the sampling rate $1/T'$ which is always greater than the symbol rate 1/T. Therefore, canceller's delay lines in Fig. 3.6 will only be sparsely filled. In fact, they will contain L-1 zeroes for each nonzero symbol where L is the number of samples per symbol interval. Hence we observe that not all the canceller's coefficients will be used simultaneously in computing the output of the canceller which is also generated at the sampling rate $1/T'$. However, different subsets of coefficients are used in a cyclic fashion as the input symbols move down the delay line in Fig. 3.6; i.e.,

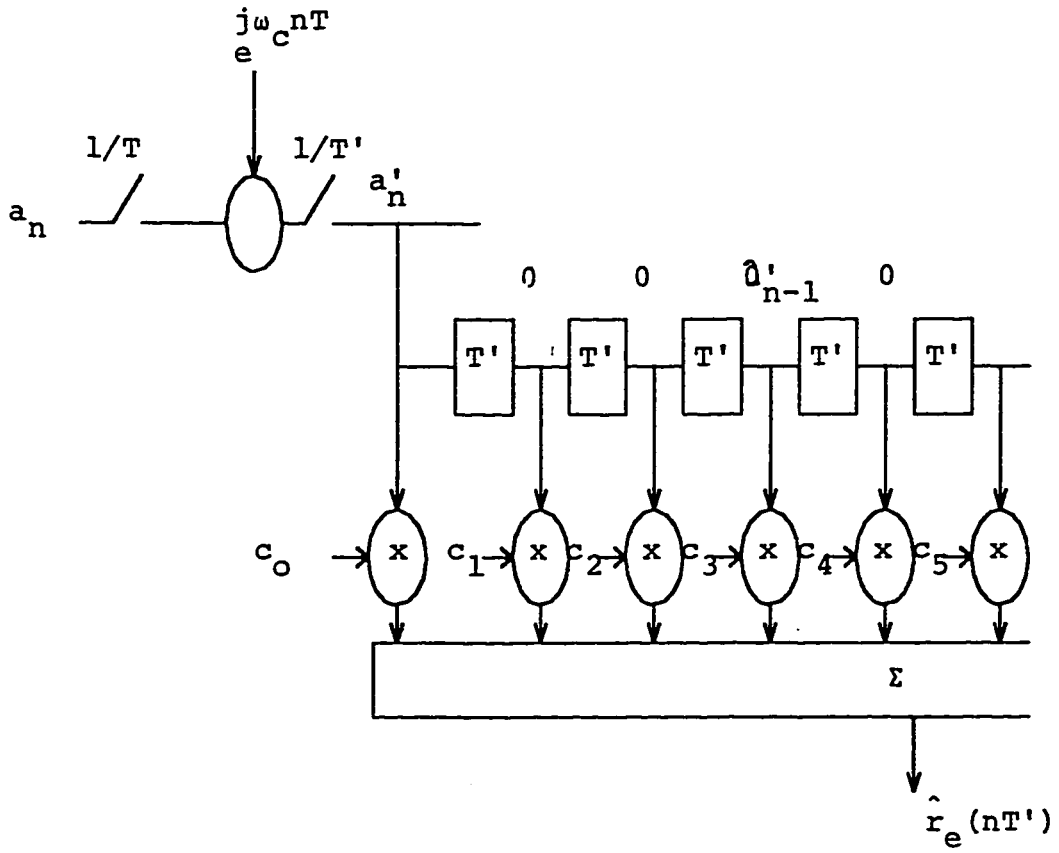

Figure 3.6 Data driven echo canceller of Nyquist type
T = 3T'

$\{c_{-N}, c_{-N+L}, c_{-N+2L},\ldots\}$, $\{c_{-N+1}, c_{-N+1+L}, c_{-N+1+2L},\ldots\}$, $\{c_{-N+2}, c_{-N+2+L}, c_{-N+2+2L},\ldots\}$,.....,
$\{c_{-N+(L-1)}, c_{-N+(L-1)+L}, c_{-N+(L-1)+2L},\ldots\}$. There are L such subsets which are each used once per symbol interval. All the subsets of coefficients are correlated with the same input vector $(a_n, a_{n-1},\ldots)$ in a given symbol period [16].

Therefore, the canceller can be considered as a parallel combinations of L "subcanclIers," all having the same delay line, but different set of coefficients, as shown in Fig. 3.7 (a). One of the subcancellers is shown in Fig. 3.7 (b). The taps of each of the transeversal filters are now spaced at T rather than T', and none of the entries of the delay lines is zero. The ith subcanceller consists of the tap vector $\mathbf{c}_i$ whose elements are $c_{-N+i+kL}$, where i = 0...L-1. The output of the canceller is generated at the sampling rate $1/T'$ by computing, in a cyclic fashion, the outputs of the subcancellers shown in Fig. 3.7 (a). Let kT′ to be measured in symbol interval, T, plus remainder, i.e.,

$$kT' = nT + iT' = (nL + i)T' \tag{3.39}$$

where n is the largest multiple of T contained in kT', and i = k mod(L). Then the output of the canceller, at the sampling instant, can be expressed as

$$\hat{r}_e(kT') = \hat{r}_e[(nL+i)T'] = \sum_{m}^{M+N-i/L} a_{n-m}c_{-N+i+mL}$$

$$= \hat{s}_e[(nL+i)T'] = \mathbf{a}_n^T\mathbf{c}_i, \quad i = 0...L-1 \tag{3.40}$$

where

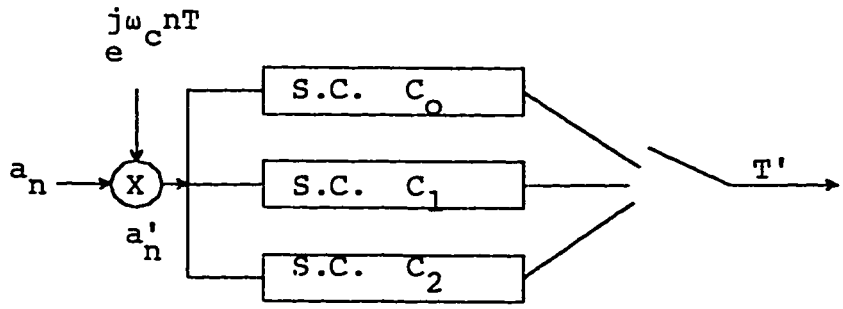

(a) Modified canceller structure

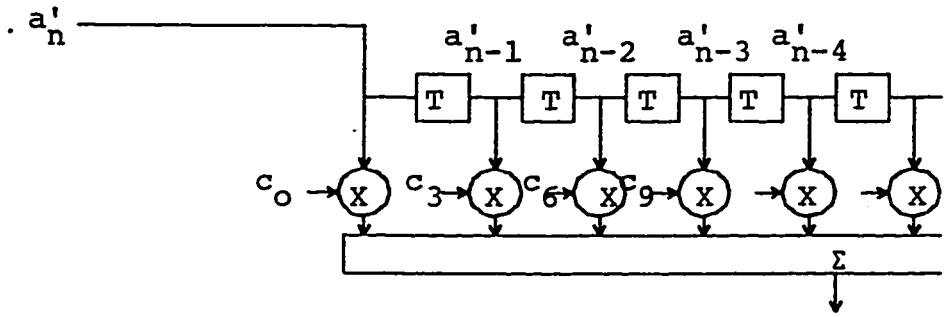

(b) Subcanceller structure

Figure 3.7 Nyquist type canceller : Modified structure.

$\mathbf{a}_n^T = [a_n, a_{n-1}, a_{n-2}, \ldots]$

and

$\mathbf{c}_i^T = [c_{-N+i}, c_{-N+i+L}, c_{-N+i+2L}, \ldots, c_M]$

The received echo signal is

$$r_e(t) = \sum_n a_n h(t-nT) \tag{3.41}$$

It is sampled at rate of $1/T'$, which will be assumed to be at least twice the highest frequency of $r_e(t)$. Then the echo signal at the sampling time is

$$r_e(kT') = \sum_n a_n h(kT'-nT)$$

$$= \sum_n a_n h\,[(k-nL)T'] \tag{3.42}$$

Defining

$$h_k \equiv h(kT') \tag{3.43}$$

the echo signal at the sampling instant, after some manupulations, can be written as

$$r_e(kT') = r_e\,[(nL+i)T'] = \sum_m a_{n-m} h_{i+mL}$$

$$= r_e\,[(nL+i)T'] = \mathbf{a}_n^T \mathbf{h}_i, \quad i = 0 \ldots L-1 \tag{3.44}$$

where

$$\mathbf{a}_n^T = [a_n, a_{n-1}, a_{n-2}, \ldots]$$

and

$$\mathbf{h}_i^T = [r_i, r_{i+L}, r_{i+2L}, \ldots].$$

From Eq. (3.44) we can see that the echo channel can also be considered to consist of a parallel combination of L subchannels. Hence, convergence of the whole canceller can be achieved by having each subcanceller converges to the corresponding subchannel. Therefore, for adaptation of the tap coefficients of the canceller, the MSE between the output of each subcanceller and the corresponding echo subchannel is minimized separately. That is, each subcancellr's output is computed once per symbol interval, an error is derived, and the LME algorithm is used to update the tap coefficients. Nyquist cancellation is obtained by cyclicly repeating these operations at the sampling rate $1/T'$ for all the subcancellers [16].

From Eq. (3.39) and Eq. (3.44) the outputs $\hat{r}_e(nT+iT')$ and $r_e(nT+iT')$ of the ith subcanceller and the ith subchannel at time $nT+iT'$ arc

$$\hat{r}_e(nT+iT') = \mathbf{a}_n^T \mathbf{c}_i \tag{3.45}$$

$$r_e(nT+iT') = \mathbf{a}_n^T \mathbf{h}_i + \xi_{n,i} \tag{3.46}$$

where $\xi_{n,i}$ is an additive interference signal which is uncorrelated with the signal to be cancelled. This interference will generally consists of the distant data signal, contribution for the echo subchannel which are beyond the reach of the canceller, and some additive noise.

The error $e_{n,i}$ between the output of the ith subchannel and the ith subcanceller is

$$e_{n,i} = r_e(nT+iT') - \hat{r}_e(nT+iT')$$

$$= \mathbf{a}_n^T(\mathbf{h}_{n,i} - \mathbf{c}_{n,i}) + \xi_{n,i}, \quad i=0,1,...,L-1 \tag{3.47}$$

where it is again clear that perfect cancellation can be achieved when the N_iM_i tap coefficients of the ith subcanceller are equal to the corresponding subchannel sampled values. The MSE to be minimized is

$$\varepsilon_{n,i} = E[e_{n,i}^2] = E[\{(\mathbf{h}_{n,i} - \mathbf{c}_{n,i}) + \xi_{n,i}\}^2] = \boldsymbol{\varphi}_{n,i}^T\boldsymbol{\varphi}_{n,i} + E[\xi_{n,i}^2] \tag{3.48}$$

where $\boldsymbol{\varphi}_{n,i}$ is defined to be the error vector, between the echo subchannel samples $\mathbf{h}_{n,i}$ and the tap coefficients $\mathbf{c}_{n,i}$, corresponding to the ith subcanceller. Note that $\varepsilon_{n,i}$ cannot be smaller than the irreducible noise $E[\xi_{n,i}^2]$. The minimum MSE is given by

$$\min\varepsilon_{n,i} = A \sum_{n>N_i} h^2(nT+iT') + E[\xi_{n,i}^2] \tag{3.49}$$

where the data-symbol power is given by A. This min. MSE is obviously not

the same for all the subcancellers.

As in the previous analysis, the adjustment algorithms for the updating of the subcanceller tap coefficients are obtained by taking the gradient of the MSE in Eq. (3.48) with respect to the tap vectors $\mathbf{c}_{n,i}$ i.e.;

$$\frac{\partial \varepsilon_{n,i}}{\partial \mathbf{c}_{n,i}} = \frac{\partial}{\partial \mathbf{c}_{n,i}} \boldsymbol{\varphi}_{n,i}^{T} \boldsymbol{\varphi}_{n,i} = -2E[\mathbf{a}_n e_{n,i}] = -2\boldsymbol{\varphi}_{n,i} \tag{3.50}$$

The corresponding stochastic tap adjustment algorithm is then

$$\mathbf{c}_{n+1,i} = \mathbf{c}_{n,i} + \alpha \mathbf{a}_n e_{n,i}, \quad i=0,1,...,L-1 \tag{3.51}$$

which is very similar to Eq. (3.37), however the error is now taken before the receiver.

The advantage of this structure is that it operates independently of the local receiver and do not require synchronization of the two data stations provided that the error is sampled at the local transmitter timing. Consequently, it is completely independent on symbol rate or modulation format of the remote transmitter as opposed to the synchronous cancellers [12].

The price paid for this freedom of synchronization of the two transmitters in the two stations is the following:

- The difficulty associated with the adaptation in the presence of the distant signal.
- The need to sample the received signal and to update the canceller tap

coefficients at intervals that are typically three or four times shorter than symbol intervals.

- Number of calculations (simple additions when the data are binary) will increase by an order of L.

Hence, depending on the application, one should make a compromise between the advantages and disadvantages of those two structures. In other words, if the two data stations are not very far so that an acceptable synchronization between the two remote transmitters can be easily achieved, it is better to use the symbol-interval canceller to have less complex structure and less number of computations.

3.3.3 Baseband and Passband Cancellers

Whether the input data to the canceller is in the baseband or in the passband (i.e. the data taken before or after the modulator) the data-driven cancellers is classified as passband or baseband cancellers. Notice that the voice-type cancellers is always of a passband type. The passband echo canceller is preferable over the baseband type. This is a passband signal. Therefor, no further modulation (for the output of the canceller) or demodulation is needed for the reflected echo signal.

3.3.4 Digital and Analog Cancellers

The output of the canceller is in a digital form. while the incoming echo signal is in an analog form. Therefor, before compensation, we need either a D/A converter, to convert the canceller's output to an analog form, or an A/D converter, to convert the incoming echo signal to a digital form. However, the input of the receiver should be in analog form because it has its own sampler for the synchronization with the clock of the far transmitter. Based on the compensation, if it is performed in analog form or digital form, echo cancellers are classified as digital and analog types. To avoid further D/A conversion for the output of the compensator, analog compensation is preferrable for less complexity structure.

3.4 PROBLEMS ENCOUNTERED IN ECHO CANCELLATION

It has been mentioned earlier that we usually have to deal with two kinds of echo; the near echo and the far echo. The near echo propagates through a channel that is essentially linear and time invariant, and thus it can be perfectly compensated by an echo canceller if its memory span and the digital precision are large enough. On the other hand, the far echo channel is generally plagued by impairments that can seriously degrade the performance of a standard echo canceller. Such impairments include nonlinearity, additive noise, phase jitter and frequency offset. Worst-case nonlinearities in the echo channel do not degrade substantially the performance of the echo canceller. The additive noise

affects the adaptation operation. However, its effect can be neglected at full-duplex operation since the far transmitted signal, that has larger power, exists. The degradation performance due to phase jitter can only be significant under simultaneous worst-case conditions of phase jitter and signal power levels, and these cases might not be statistically significant. The most damaging of all the channel impairments commonly encountered in far echos is the frequency offset, even in small amounts [7]. We deal with this particular impairment in the following sections.

3.4.1 Effect of Frequency Offset

Frequency offset is generated in the far echo due to the modulation and demodulation that take place when the signal passes through an analog carrier system if it does exist. For example, consider the signal sent by the transmitter Tx of the modem on the left of Fig 3.8. In the carrier system, this signal is first shifted up in frequency by a modulator M having a modulation frequency f_m. At the end of the carrier system, the signal is shifted down to baseband by a demodulator D′ having a demodulation frequency f_d'. In many cases, the modulator M and the demodulator D′, which can be thousands of miles apart, are not synchronized in frequency, so that $f_m - f_d' \neq 0$. As a result, the demodulated baseband signal will have frequency components which will be offset by $\Delta f = f_m - f_d'$ with respect to the original baseband signal. This 'Δf' effect is called frequency offset and is, indeed, commonly encountered in point-

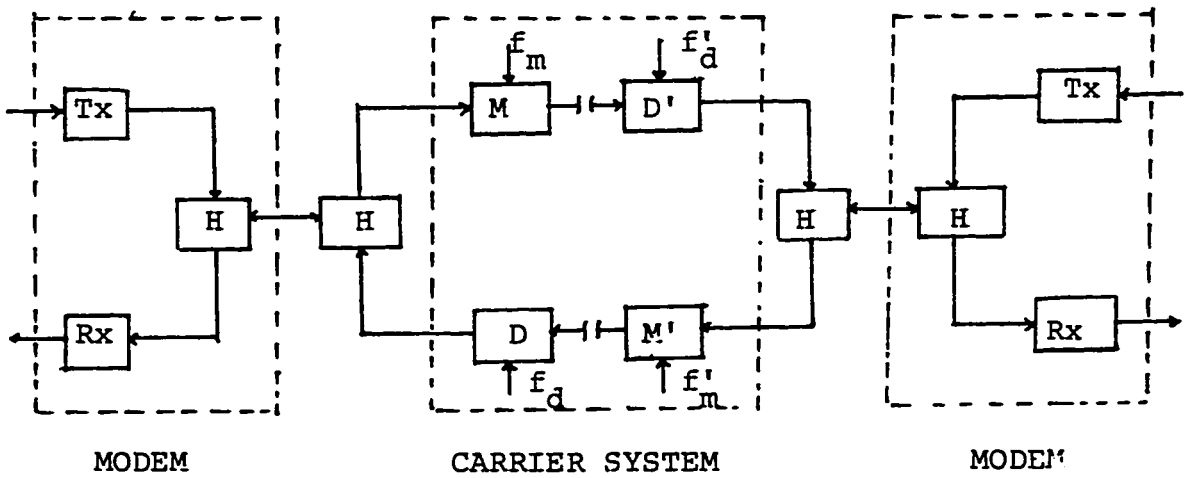

Figure 3.8 Frequency offset generation in a direct distance dialing connection.

to-point telephone connection. The far echo seen by the modem to the left is the signal that leaks through the hybrid H after demodulator D′ and loops back to the modem through the carrier system. Hence, it is again modulated up and demodulated down with frequencies f_m' & f_d , respectively. The overall 'Δf' effect for the far echo is

$$\Delta f = (f_m' - f_d) + (f_m - f_d') \tag{3.52}$$

If $\Delta f \neq 0$, we have frequency offset in the far echo. Although the amount of frequency reported in [19] were quite small (< 1 Hz in U.S.A.), these amounts would still not be compensated for by a standard echo canceller, as reported in [7].

Effect of frequency offset can be understood if we refer to Fig. 3.9. E_F represents the received far echo signal and $\hat{E}_F$ is its estimate obtained as the output of the far canceller. The phase error or the phase jitter is γ. Frequency offset, " Δf ",is the rate of change of the angle γ. The interpretation of this frequency offset is that we can consider that the sampled far echo channel's impulse response are rotate by increments Δf. More detailed analysis of frequency offset effect is given in Chapter 4. For proper cancellation the coefficients of the far end section of the canceller should be rotated by the same amount. Then, we should have a mean to estimate this frequency offset.

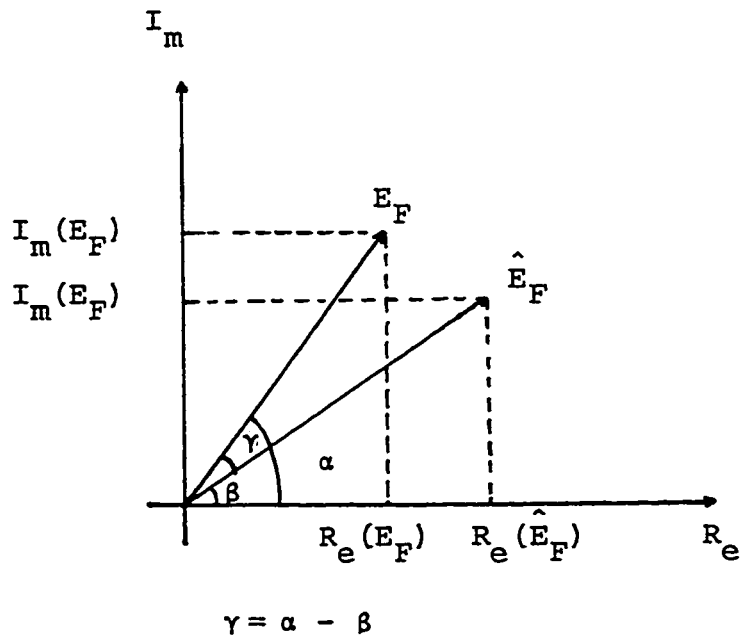

Figure 3.9 Frequency offset in the far echo.

3.4.2 Frequency Offset Compensation

To compensate for the frequency offset in the far echo, the far canceller should be able to estimate this frequency offset. This can be obtained by an adaptive gradient algorithm, which is similar to 1st order PLL, to track continuously the change in the angle γ. Then a solution of the frequency offset problem is to perform joint adaptation of the coefficients of the far canceller and the PLL [8], [12]. Such an algorithm, as proposed by Wang and Werner in March 1988 [8], is as follows:

$$\mathbf{C}_{n+1} = \mathbf{C}_n + \alpha A_n^* e^{-j\hat{\theta}_n} E_{e_n} \tag{3.53}$$

where $\mathbf{C}_n$ is the complex tap coefficients, $\hat{\theta}_n$ is the angle by which the estimated far echo component ($\hat{E}_F$) should be rotated, and E_{e_n} is the complex error defined by

$$E_{e_n} = E_{F_n} - \hat{E}_{F_n} \tag{3.54}$$

The phase adjustment algorithm for the PLL is

$$\hat{\theta}_{n+1} = \hat{\theta}_n - \mu \mathrm{Im}[\hat{E}_{F_n} e^{j\hat{\theta}_n} E_{e_n}^*] \tag{3.55}$$

Equations (3.53) and (3.55) constitutes the joint adjustment algorithm.

3.5 SUMMARY

From the treatment in this chapter, we have seen that the echo canceller structure can be mainly devided into two catagories : voice-type cancellers and data-type cancellers. The latter is preferrable for two main reasons. Firstly, its implementation is easier. Secondly, computation complexity is greatly reduced. Furthermore, there are two types of data-type cancellers : synchronous cancellers and Nyquist rate cancellers. The tap spacing in synchronous cancellers is T where T is the symbol period. Nevertheless, the tap spacing in the Nyquist rate canceller is T′, where T′ is the sampling interval. Other classifications of echo cancellers (Passband/Baseband, Digital/Analog) are also mentioned. In the next chapter, the canceller type selected to be studied, is designed and presented in details.

CHAPTER 4

THE SYSTEM DESIGN

In this chapter, the system design to study the echo cancellation problem is presented in detail. Three main tasks have been carried out in this system. The first is studying the effect of different impairments (noise, frequency offset, phase hits,...) on the performance of the echo cancellers. The second is investigating the existing technique for echo cancellation. The third is verifying and studying the performance of the new proposed technique for echo cancellation.

The system is properly designed to match the practical requirements and the CCITT specifications. The block diagram of the overall system design is shown in Fig. 4.1. Various blocks seen in the diagram are explained in the subsequent sections.

4.1 P/N GENERATOR AND THE SIGNAL-SPACE ENCODER

The input to the system shown in Fig. 4.1 is a stream of binary bits of 0's and 1's at 4800 bps which is the output of a pseudo noise (P/N) generator to

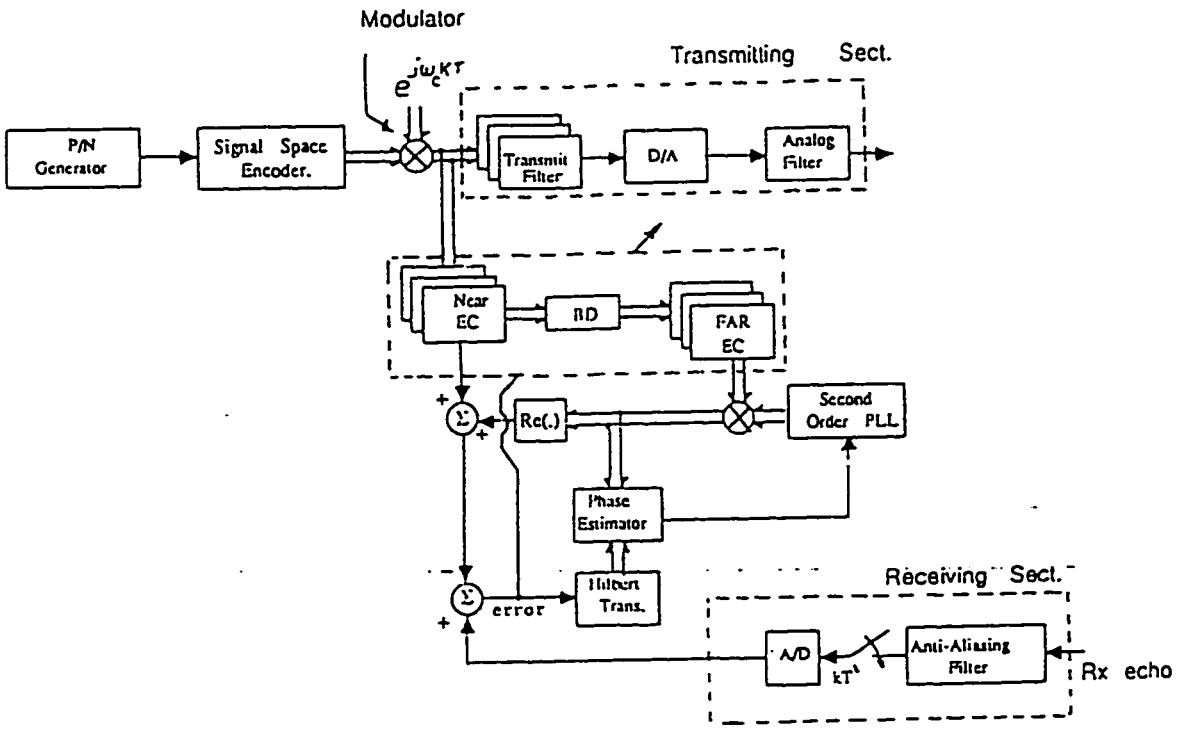

Figure 4.1 The system design.

ensure flat spectrum over the band 600 - 3000 Hz. The P/N generator is a shift register sequence generator, see Fig. 4.2. According to the V.32 scrambler of the CCITT [17] (call modem), the length of the shift register is of 23 delay elements. Each delay element is 1/4800 seconds. The generating polynomial of the output is

$$GP = 1 + x^{-18} + x^{-23} \tag{4.1}$$

where the summation sign (+) indicates the module 2 addition. The output given by Eq.(4.1) is of maximal length* [20], i.e. the sequence will repeat itself every $2^{23}-1$.

The signal space encoder encodes the output of the P/N generator into QPSK scheme. In this scheme, we have four symbols located at differents points in the signal constellation as shown in Fig. 4.3. Every two binary bits will be represented by one point. Accordingly, the output of the encoder consists of two components, the in-phase and the quadrature, denoted as a and b, respectively. These components have values of ± 1 at 2400 Bauds, which represents the symbol (Baud) rate of the register.

---

* Maximal code is the longest code that can be generated by a given shift register of a given length.

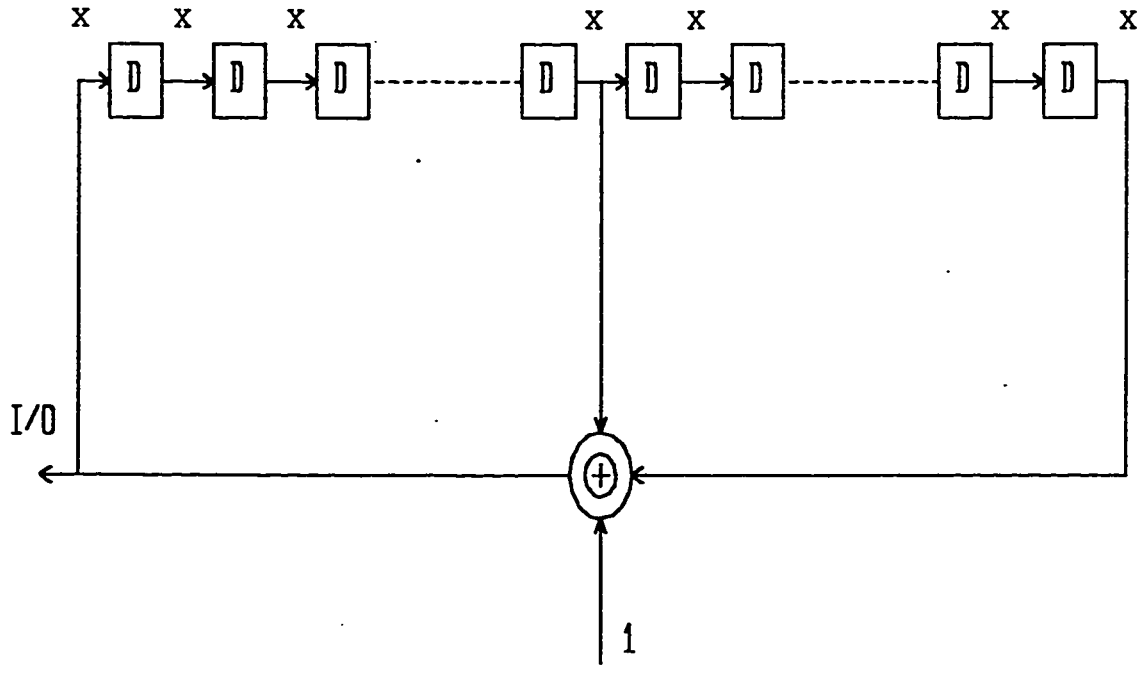

Figure 4.2 A Shift register sequence generator.

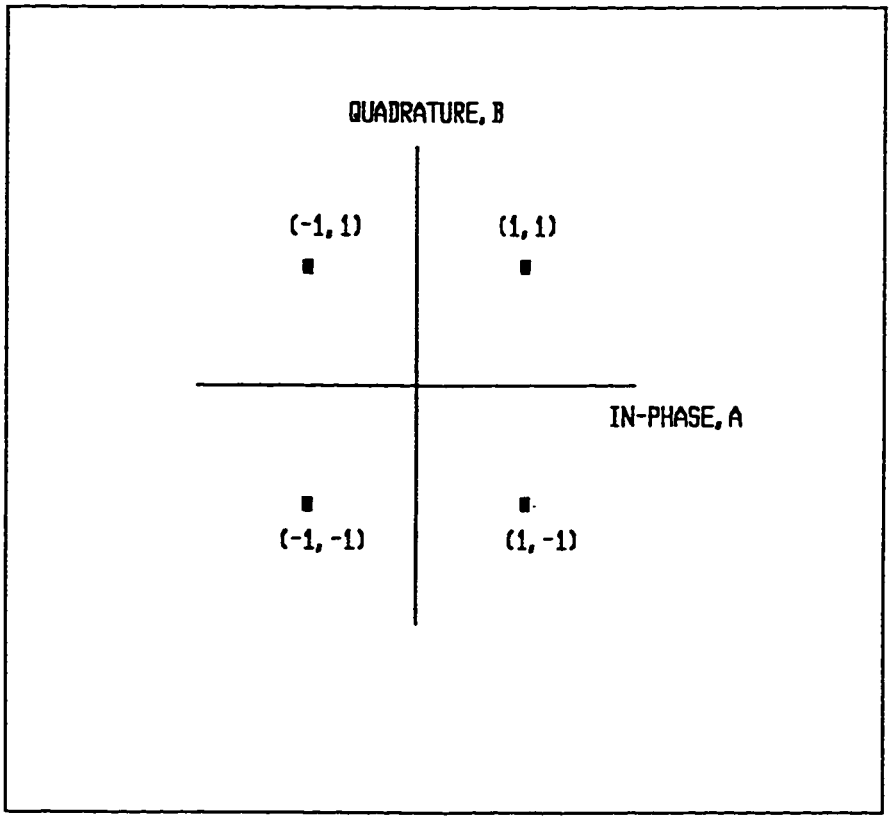

Figure 4.3 Signal space diagram (QPSK)

4.2 THE MODULATOR

A carrier frequency of 1800 Hz is used to modulate the in-phase and the quadrature components. Because of the convenient relation between the carrier frequency and the Baud rate, the modulation simply becomes a process of rotating the symbols (a+jb) in the signal space as explained below.

Let $a_n + jb_n$ denotes a point in the signal space at time nT where T is symbol period 1/2400 s. The output of the modulator denoted by $a'_n + jb'_n$, is

$$\begin{aligned} a'_n + jb'_n &= [\, a_n + jb_n \,][\, e^{(j2\pi f_c nT)} \,] \\ &= [\, a_n + jb_n \,][\, \cos(2\pi n f_c T) + j\sin(2\pi n f_c T) \,] \end{aligned} \tag{4.2}$$

Now, T = 1/2400 s., and f_c = 1800 Hz then

$$2\pi f_c T = 3(\frac{\pi}{2}) \tag{4.3}$$

Substituting Eq. (4.3) into Eq. (4.2) we get

$$a'_n + jb'_n = [\, a_n + jb_n \,][\, \cos(\frac{3n\pi}{2}) + j\sin(\frac{3n\pi}{2}) \,] \tag{4.4}$$

from which we get

$$a'_n = a_n\cos(\frac{3n\pi}{2}) - b_n\sin(\frac{3n\pi}{2}) \tag{4.5}$$

$$b'_n = a_n \sin(\frac{3n\pi}{2}) + b_n \cos(\frac{3n\pi}{2}) \qquad (4.6)$$

The rotated symbol $a'_n + j\,b'_n$ is tabulated in Table 4.1 for time index, n, of 0 to 7. Notice that the pattern repeats itself every four Bauds. Figure 4.4 illustrates this modulation process. Notice that the rotated symbol again has components of ± 1. This will be the input of the transmitting filter as well as the echo canceller.

4.3 TRANSMITTING AND RECEIVING SECTIONS

The first block in the transmitting section is the transmit filter. Notice that it consists of three subfilters. Then, for each input symbol we have three output values within the symbol period T. The justification of this process is very similar to the subcancellers concept explained in chapter 3. This is equivalent to saying that the modulated symbols are sampled at a rate of 7200 Hz (three times the Baud rate of 2400 Hz). The real output of the transmitting filter is converted to analog using a D/A converter and then applied to an analog filter to smooth the transmitted signal through the telephone line.

The received echo signal is first input to an anti-aliasing filter. The output of the filter is sampled the same rate of 7200 Hz and should be synchronized with the sampling rate of the near transmitter. The signal is then converted to digital using an A/D converter.

TABLE 4.1 The rotated symbols (a′ + jb′) at time index n from 0 to 7.

n	$\cos(\frac{3n\pi}{2})$	$\sin(\frac{3n\pi}{2})$	a′ + jb′
0	+1	0	a + jb
1	0	-1	b - ja
2	-1	0	-a - jb
3	0	+1	-b + ja
4	+1	0	a + jb
5	0	-1	b - ja
6	-1	0	-a - jb
7	0	+1	-b + ja

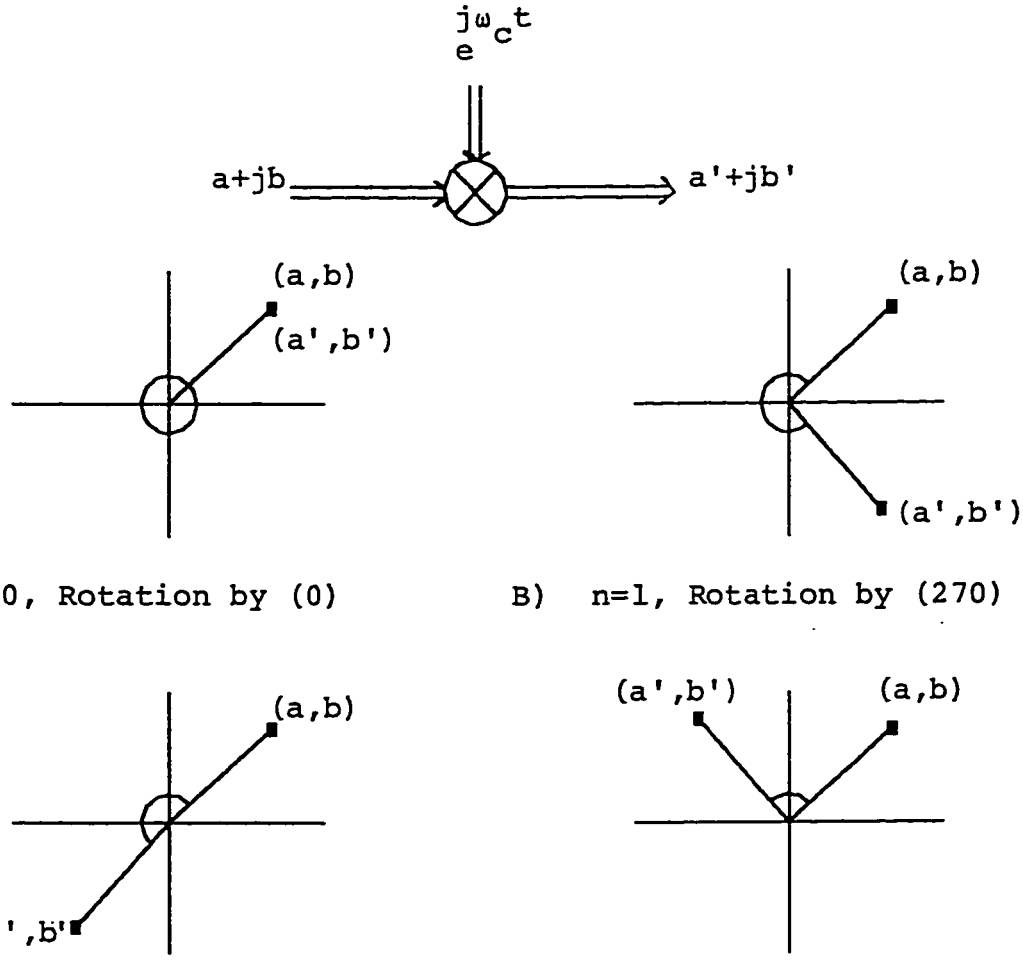

A) n=0, Rotation by (0)

B) n=1, Rotation by (270)

B) n=2, Rotation by (180)

D) n=3, Rotation by (90)

Figure 4.4 Modulation process

However, it should be pointed out that during full-duplex transmission the timing of the receiver should be synchronized with the far transmitter not the near one.

4.4 THE ECHO CANCELLER

It has been seen in chapter 2, Eq. (2.1), that the echo signal can be represented as the following

$$s(t) = \mathrm{Re}\left[\sum_n A_n g(t-nT) e^{j\omega_c t}\right] \tag{4.7}$$

where $A_n = a_n + jb_n$ is the discrete-valued multilevel complex symbol to be transmitted. It is also the output of the signal space encoder. g(t) is the baseband pulse shape, 1/T is the symbol rate and $\omega_c/2\pi$ is the carrier frequency.

The complex signal in brackets in Eq. (4.7) is an analytic signal X(t) where

$$X(t) = s(t) + j\tilde{s}(t) = \sum_n A_n g(t-nT) e^{j\omega_c t} \tag{4.8}$$

where $\tilde{s}(t)$ is the Hilbert transform of s(t). Equation (4.8) can be rewritten as

$$\begin{aligned} X(t) &= \sum_n A_n e^{j\omega_c nT} g(t-nT) e^{j\omega_c (t-nT)} \\ &= \sum_n A'_n R(t-nT) \end{aligned} \tag{4.9}$$

where

$$A'_n = A_n e^{j\omega_c nT} = a'_n + jb'_n \tag{4.10}$$

which is the rotated symbol mentioned in Sect. 4.3, and

$$R(t) = g(t)\, e^{j\omega_c t} \tag{4.11}$$

Still R(t) in Eq. (4.11) is an analytic signal and it has a band-pass characteristic. After passing through the echo channel with impulse response $h_e(t)$, the analytic signal of the echo becomes

$$X_1(t) = X(t)*h_e(t) = \sum_n A'_n H(t-nT) \tag{4.12}$$

in which '*' denotes the convolution operation and H(t) is defined as

$$H(t) = R(t)*h_e(t) \tag{4.13}$$

The echo signal defined in Eq. (2.2) is the real part of $X_1(t)$ in Eq. (4.12).

Based on Eq. (4.12), a complex filter (echo canceller) with impulse response

$$C(t) = c(t) + jd(t) \tag{4.14}$$

is used. The complex output of the canceller is given by

$$\begin{aligned} E(t) &= \sum_n A'_n C(t-nT) \\ &= \sum_n [\, a'_n c(t-nT) - b'_n d(t-nT)\,] \\ &\quad + j \sum_n [\, b'_n c(t-nT) + a'_n d(t-nT)\,] \end{aligned} \tag{4.15}$$

The real and imaginary parts of E(t) are obtained by using real tapped-delay line filters c(t) and d(t) twice, but with different inputs as shown in Fig. 4.5. This structure of a complex filter is called "cross-coupled structure" [8].

Digital implementation is assumed for this structure. The complex filter is implemented with two transversal filters having adjustable tap coefficients vectors **c** and **d**. Tap spacing T' will be T/3, where T is the symbol period of 1/2400 s. That is to say that the sampling rate $1/T'$, which is 7200 Hz will be 3 times the symbol rate 1/T, which is 2400 Hz. Then as described previously in chapter 3, the canceller will consist of three parallel complex "subcancellers" all having the same delay line, but different sets of tap coefficients, as shown in Fig. 3.6.

The i'th subcanceller consists of the complex tap vector $\mathbf{C}_i = \mathbf{c}_i + j\mathbf{d}_i$ whose elements are c_{i+3k} and d_{i+3k} , i=0,1,2 and k is the time index corresponding to the sampling period T'. The output of the canceller is generated at the sampling rate 7200 Hz by computing, in a cyclic fashion, the outputs of the three subcancellers. Each subcanceller will operate at the symbol rate and have the cross coupled structure shown in Fig. 4.5. Since each suncanceller behaves independently of the others [8], The behavior of the echo canceller will be determined by the design parameters of a subcanceller, and not by the total number of subcancellers.

Hence, our canceller is a pass-band data driven canceller that will operates at Nyquist rate. It consists of two sections; a near and a far section. The two

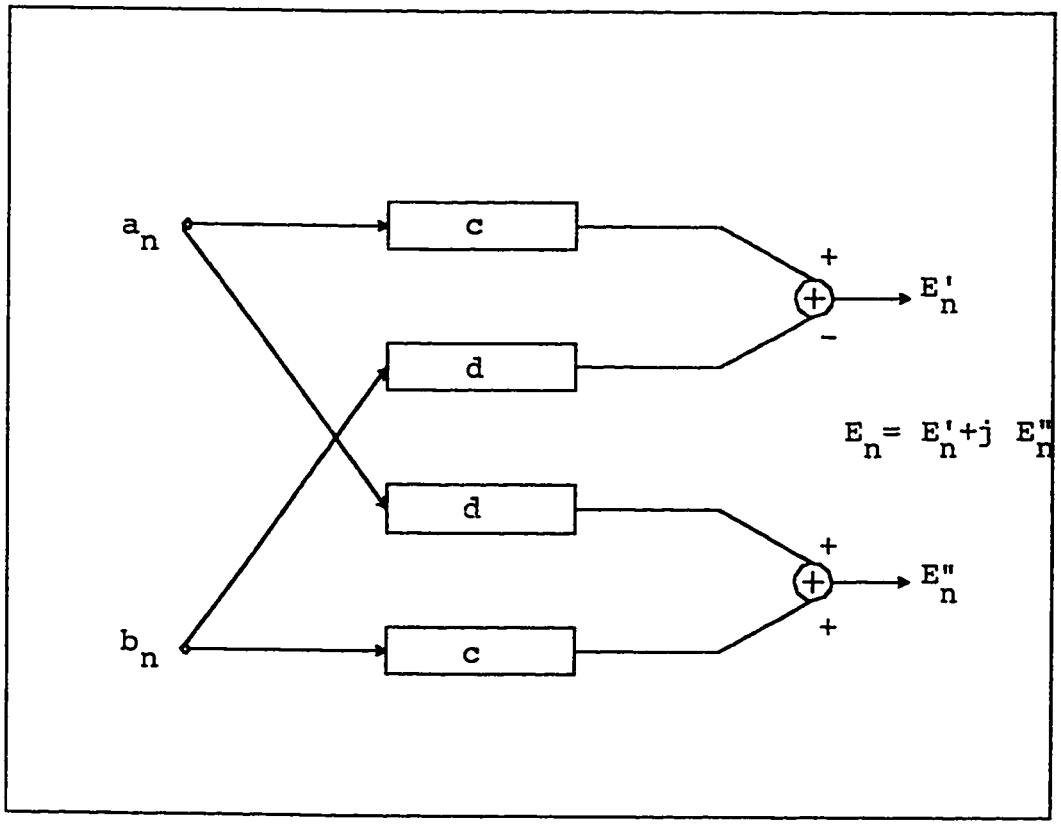

Figure 4.5 Cross-coupled structure.

sections are separated by a bulk delay. As shown in Fig. 4.1, The real output of the near section is only computed while the complex output is computed for the far canceller. This is because, as will be seen in Section 4.5.1, the complex form is needed to compensate for the frequency offset by which the far echo component is corrupted.

Note that the echo canceller represents the echo channel in addition to the transmitting section. Both the output of the echo canceller which represents the estimated echo and the output of the A/D converter are applied to a subtractor. The output of the near canceller is

$$\mathrm{Re}[\hat{\mathbf{E}}_{N_{n,i}}] = \mathrm{Re}[\mathbf{C}^{T}_{N_{n,i}}\mathbf{A}_{n}] , \quad i=0,1,2 \tag{4.16}$$

where n,i denote $nT+iT'$ defined in Eq. (3.39) and i denotes the ith subcanceller. $\mathbf{C}_{N_n} = [\mathbf{c}_{N_n} + j\mathbf{d}_{N_n}]$ is the complex vector coefficients of the near canceller, $\mathbf{A}_n$ stands for the rotated symbols and $\mathbf{C}^{T}_{N_n}$ denotes transpose of $\mathbf{C}_{N_n}$. From now, the i index will be removed and it will be understood that any subsequent equation related to the canceller is in terms of each subcanceller. The output of the far canceller, however, is

$$[\hat{\mathbf{E}}_{F_n}] = [\mathbf{C}^{T}_{F_n}\mathbf{A}_{n}] \tag{4.17}$$

where $\mathbf{C}_{F_n} = [\mathbf{c}_{F_n} + j\mathbf{d}_{F_n}]$ is the complex vector coefficients of the far canceller. As seen in Fig. 4.1, the far complex output will be rotated by an increment angle due to the frequency offset estimated by the PLL. Let's forget about the

frequency offset for the time being assuming that there is no frequency offset, then the output of the whole canceller is

$$\mathrm{Re}[\,\mathbf{C}_n^T\mathbf{A}_n\,] = \mathrm{Re}[\,\mathbf{C}_{N_n}^T\mathbf{A}_n\,] + \mathrm{Re}[\,\mathbf{C}_{F_n}^T\mathbf{A}_n\,] \tag{4.18}$$

Also, from Eq. (4.12), the sampled analytic signal of the incoming echo can be written as

$$X_{1,n} = \mathbf{H}_n^T\mathbf{A}_n \tag{4.19}$$

where $\mathbf{H} = [\,\mathbf{h}_1 + j\mathbf{h}_2\,]$ is the complex vector of the sampled impulse response of the echo channel. Hence, the error signal can be represented as

$$e_n = \mathrm{Re}[\mathbf{H}_n^T\mathbf{A}_n] - \mathrm{Re}[\,\mathbf{C}_{N_n}^T\mathbf{A}_n] - \mathrm{Re}[\,\mathbf{C}_{F_n}^T\mathbf{A}_n\,] + \xi_n \tag{4.20}$$

where ξ_n is an additive interference signal which is uncorrelated with the signal to be cancelled. This error, defined in Eq. (4.20) is used to update the coefficients of the echo canceller according to the LMS algorithm with adjustable step size. The LMS algorithm is already described in Section 3.2.3. The updating equation is

$$\mathbf{C}_{n+1} = \mathbf{C}_n + \alpha e_n\mathbf{A}_n^* \tag{4.21}$$

which leads to

$$\mathbf{c}_{n+1} = \mathbf{c}_n + \alpha e_n\mathbf{a}_n \tag{4.22}$$

$$\mathbf{d}_{n+1} = \mathbf{d}_n - \alpha e_n \mathbf{b}_n \tag{4.23}$$

4.5 FREQUENCY OFFSET MEASUREMENT

Let f_l be the amount of frequency offset introduced by the carrier system. The analytic signal of the far incoming echo becomes

$$\mathbf{E}_{F_n} = \mathbf{H}_{F_n} \mathbf{A}_n e^{j2\pi f_l nT} \tag{4.24}$$

Denoting $(2\pi f_l nT)$ by θ_n the real part of $\mathbf{E}_F$ can be written as

$$2\mathrm{Re}[\mathbf{E}_{F_n}] = (e^{j\theta_n}\mathbf{A}_n^T)\mathbf{H}_{F_n}^* + \mathbf{H}_{F_n}^T(e^{j\theta_n}\mathbf{A}_n)^*$$

$$= \mathbf{A}_n^T(e^{j-\theta_n}\mathbf{H}_{F_n})^* + (e^{j-\theta_n}\mathbf{H}_{F_n}^T)\mathbf{A}_n^T \tag{4.25}$$

From Eq.(4.25), we can look at the effect of the frequency offset in two ways. First, we can consider that the symbols vector are rotated by small angles θ_n at the input of the channel. Alternatively, we can assume that the vectors $\mathbf{A}_n$ are the channel's inputs and that the sampled channel's impulse response $\mathbf{H}_{F_n}$ are rotated by angles θ_n [7]. For this reason, the locally estimated far echo should be rotated by increments equal to θ_n. This leads to include a frequency offset estimator in the system.

It has been mentioned earlier in chapter 3 that the frequency offset can be

measured using a second order phase locked loop (PLL). The implementation of the PLL is established by including a phase comparator where the instantaneous phase error between the received far echo and the locally generated far echo is estimated as seen below .

4.5.1 The Phase Estimator and the Hilbert Transformer

The phase estimation process is explained with reference to Fig. 3.9. E_F and $\hat{E}_F$ denote the complex form of the far incoming echo and the locally estimated far echo, respectively. If we represent these two components as vectors in a complex plane, as shown in Fig. 4.6, then the phase difference can be approximated as the following

$$\begin{aligned} \hat{\gamma} \approx \sin(\hat{\gamma}) &= \sin(\alpha - \beta) \\ &= \sin(\alpha)\cos(\beta) - \sin(\beta)\cos(\alpha) \\ &= \frac{\mathrm{Im}(E_F)\mathrm{Re}(\hat{E}_F) - \mathrm{Re}(E_F)\mathrm{Im}(\hat{E}_F)}{|E_F||\hat{E}_F|} \end{aligned} \tag{4.26}$$

which can be written as

$$\hat{\gamma} \approx \sin(\hat{\gamma}) = \frac{\mathrm{Im}(E_F - \hat{E}_F)\mathrm{Re}(\hat{E}_F) - \mathrm{Re}(E_F - \hat{E}_F)\mathrm{Im}(\hat{E}_F)}{|E_F||\hat{E}_F|} \tag{4.27}$$

From Eq. (4.20), the error can be written in terms of E_F ,E_N ,$\hat{E}_F$ and $\hat{E}_N$ as the following

$$e_n = \mathrm{Re}[\, E_{F_n} - \hat{E}_{F_n} \,] + \mathrm{Re}[\, E_{N_n} - \hat{E}_{N_n} \,] + \xi_n \qquad (4.28)$$

Where E_N and $\hat{E}_N$ are also the complex form of the near incoming echo and the locally estimated near echo. ξ_n is an additive interference signal which is uncorrelated with the echo signal to be cancelled.

Since the far echo component is not separately available for the estimator, the complex error denoted by E_{e_n} can replace the quantity $(E_F - \hat{E}_F)$ term in Eq. (4.27) and then take the average to estimate $\hat{\gamma}$. Notice also that $| E_F | \approx | \hat{E}_F |$, then we have

$$\hat{\gamma} \approx E\left[\frac{\mathrm{Im}[E_{e_n}]\,\mathrm{Re}[\hat{E}_{F_n}] - \mathrm{Re}[E_{e_n}]\,\mathrm{Im}[\hat{E}_{F_n}]}{| \hat{E}_{F_n} |^2} \right] \qquad (4.29)$$

or simply we can use

$$\hat{\gamma}_n \approx \frac{\mathrm{Im}[E_{e_n}]\,\mathrm{Re}[\hat{E}_{F_n}] - \mathrm{Re}[E_{e_n}]\,\mathrm{Im}[\hat{E}_{F_n}]}{E[\, | \hat{E}_{n_F} |^2 \,]} \qquad (4.30)$$

as an estimate of $\hat{\gamma}_n$. E_{e_n} is a the complex error whose real part is e_n defined in Eq. (4.20).

If the factor $1/E[\, | \hat{E}_{F_n} |^2 \,]$ is ignored, the performance of the PLL will change while the power of the far echo changes. In the simulation this term has been ignored since our echo channel is not varying.

The Hilbert transformer shown in the overall system block diagram of Fig. 4.1 is used to obtain the imaginary part of the error signal from its real part as the following

$$\tilde{e}_n \approx e_{n-1} - e_{n+1} \tag{4.31}$$

where $\tilde{e}_n$ denotes The Hilbert transform of e_n. Equation (4.31) is justified as follows. Taking the Z-transform of Eq. (4.31), we get

$$\begin{aligned} E(z) &\approx E(z)(z^{-1} - z^{+1}) \\ &\approx E(z)H(z) \end{aligned} \tag{4.32}$$

where E(z) is the Z-transform of e_n and H(z) is defined as

$$H(z) = z^{-1} - z^{+1} \tag{4.33}$$

which approximates the transfer function of the Hilbert transformer. More details about discrete Hilbert transformer properties can be found in [21]. It should be pointed out that the noise introduced due to the Hilbert transformer does not have much effect. This is because in data mode, the far transmitted signal, which is a strong source of noise to the canceller, does exist.

4.5.2 The Second Order Phase Locked Loop

Details of the 2nd order digital PLL shown in Fig. 4.1 are depicted in Fig. 4.6. It consists of a first order loop filter followed by a Numerically Control

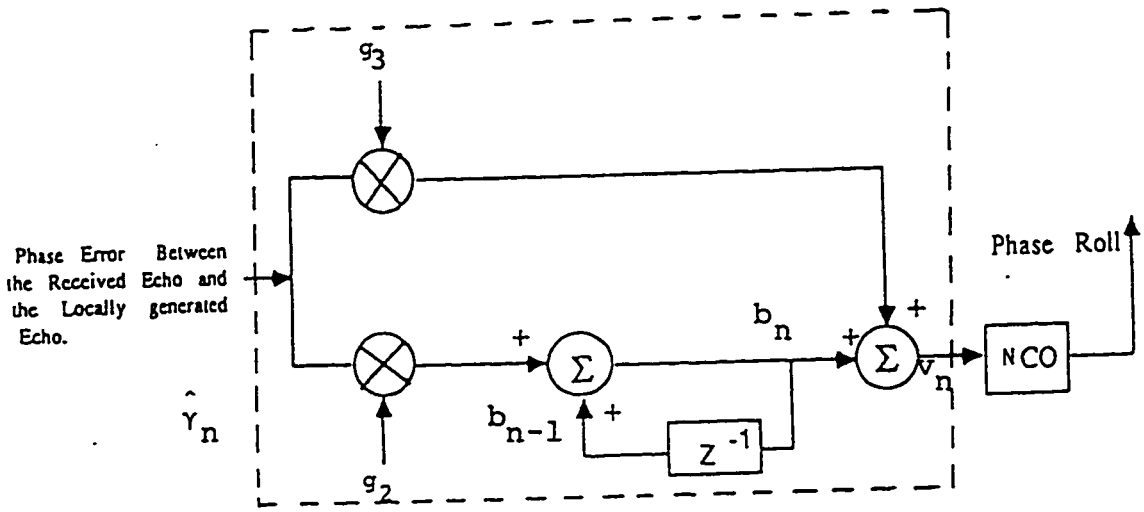

Figure 4.6 Digital second order PL

Oscillator (NCO). The NCO is a simple integrater. The equations describing the 1st order loop filter are

$$b_{n+1} = b_n + g_2\hat{\gamma}_n \tag{4.34}$$

$$v_n = b_n + g_3\hat{\gamma}_n \tag{4.35}$$

Where g_1 and g_3 are constants representing the gain values of the filter. As the phase difference $\hat{\gamma}_n$, estimated by the phase estimator goes to 0, then $v_n = b_n$ which is the quantity related to the frequency offset.

The output of the NCO, which is also the output of the PLL is the angle by which the locally generated far echo signal should be rotated. This angle is the integration of the frequency offset captured by the loop filter. The NCO is described by the following equation

$$\hat{\theta}_{n+1} = \hat{\theta}_n + gv_n \tag{4.36}$$

where g is also a constant. Substituting Eq. (4.35) into Eq. (4.36) we get

$$\hat{\theta}_{n+1} = \hat{\theta}_n + gb_n + g\,g_3\hat{\gamma}_n \tag{4.37}$$

Let $g\,g_3$ be denoted by g_1, then Eq. (4.37) becomes

$$\hat{\theta}_{n+1} = \hat{\theta}_n + gb_n + g_1\hat{\gamma}_n \tag{4.38}$$

Equations (4.34) and (4.38) completely describe the operation of the PLL. They

are the two equations used in the simulation. The term gb_n in Eq. (4.38) is the increment angle due to frequency offset. The actual estimated frequency offset, then, is

$$\Delta f_n = \frac{gb_n}{2\pi T} \tag{4.39}$$

where T is the symbol period.

As seen in Fig.4.1, the estimated far echo component $\hat{E}_F$ is rotated by the estimated angle $\hat{\theta}$, given in Eq.(4.38). Then, the real part of $\hat{E}_F$ is obtained and added to the real part of the estimated near echo $Re[\hat{E}_N]$.

In this case, the time updating equation for the far canceller should be changed as seen below. Since the data vector is still A_n , the estimated far echo component becomes

$$Re[\hat{E}_{F_n}] = Re[\, e^{\hat{\theta}_n} C_{F_n}^T A_n \,] \tag{4.40}$$

Now, we can look at the coefficient vector, $C_{F_n}^T$ of the far subcanceller as $e^{j\hat{\theta}_n} C_{F_n}^T$. Hence, the update equation of the far canceller becomes

$$e^{i\hat{\theta}_n} C_{n+1} = e^{j\hat{\theta}_n} C_n + \alpha e_n A_n^* \tag{4.41}$$

or

$$C_{n+1} = C_n + \alpha e_n e^{-j\hat{\theta}_n} A_n^* \tag{4.42}$$

From Eq.(4.42), we notice that the updating equation (4.24) can be used however the complex form of the error, E_{e_n} should be rotated by $-\hat{\theta}_n$ before using it in the updating as proposed by Wang and Werner in [8].

4.6 SUMMARY

In this chapter, the echo canceller structure selected for our system is presented and analysed. The structure is a data-type canceller that operates at Nyquist rate. Various blocks assembling the system are explained. All necessary mathematical derivations for the simulation have been derived. In the next chapter, the design is completed by choosing the proper values of the parameters and the constants associated with the system.

CHAPTER 5

SIMULATION RESULTS

In this chapter, results of study performed on the designed system explained in chapter 4 are presented. Our aim is to study the effects of several impairments (e.g. noise and frequency offset) on the performance of the echo canceller. This will help for compensation for these impairments. Moreover, the existing techniques for echo cancellation and frequency offset compensation are investigated. The new proposed methods for further improvements over the existing designs are explained with simulation and evaluation in the following Chapter.

5.1 ECHO CHANNEL CHARACTERISTICS

The echo channel used in our simulation is taken from actual measurements using a channel simulator [22]. The channel has near and far sections. The near echo channel has duration of 11.7 ms and gives an attenuation of -3 dB While the far one has duration of 13.3 ms and gives an attenuation of -18 dB. In general, The attenuation level of the echo channel is under program control in the simulation process. The echo channel is shown in Fig. 5.1. With the taps spaced by the sampling time $T' = 1/ 7200$ s, the length of the corresponding echo

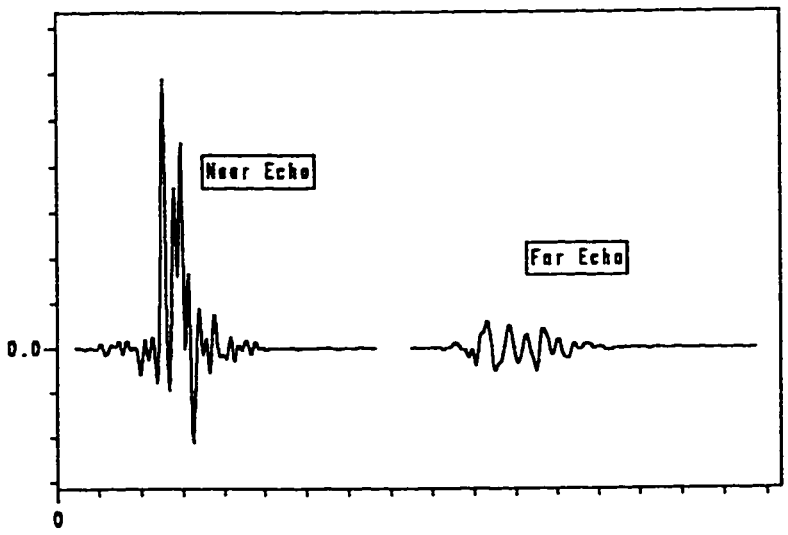

(a) Real.

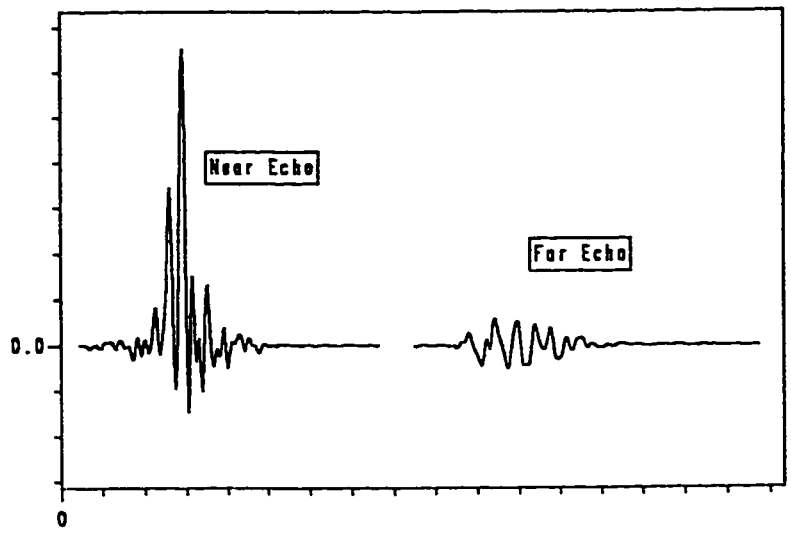

(b) Imaginary.

Figure 5.1 The echo channel.

canceller's (near & far) sections are M = 84, N = 90 taps, respectively.

5.2 ADAPTATION PROCESS AND THE OPTIMUM STEP SIZE

To begin with, the adaptation process is made according to the LMS algorithm explained in Chapter 3 and restated in Section 4.6 in Eqs. (4.20) and (4.21). These two equations (representing the LMS algorithm) are reproduced here for convenience:

$$\mathbf{C}_{n+1} = \mathbf{C}_n + \alpha e_n \mathbf{A}_n^* \tag{5.1}$$

$$e_n = \mathrm{Re}\,[\mathbf{A}_n^T(\mathbf{H}_n - \mathbf{C}_n)] + \xi_n \tag{5.2}$$

where n is a time index with respect to the symbol time, 1/2400 s, **H** is the complex vector for sampled values of the echo channel, $\mathbf{C}_n$ is the coefficient vector of the canceller at time index n, $\mathbf{A}_n$ is the symbol input vector, e_n is the error signal and α is the step size.

With noise free, the optimum step size which is seen to provide the minimum MSE is found to be 1/2L = 0.0083, which agrees with the theoretical value given in [8]. This is shown in Fig. 5.2 where the MSE is plotted versus the step size. Convergence of the canceller with this step size is shown in Fig. 5.3(a), where the squared error is plotted versus time. We notice the existence of large ripples. However, to look closely at the behavior of the error we plot the mean-squared error (MSE) versus time. This is shown in part (b) of the

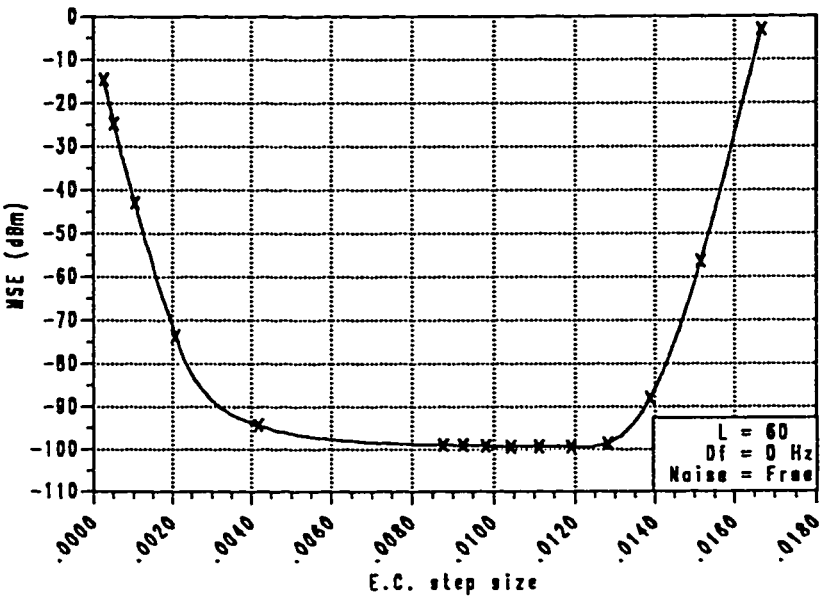

Figure 5.2 Achievable MSE as a function of frequency offset.

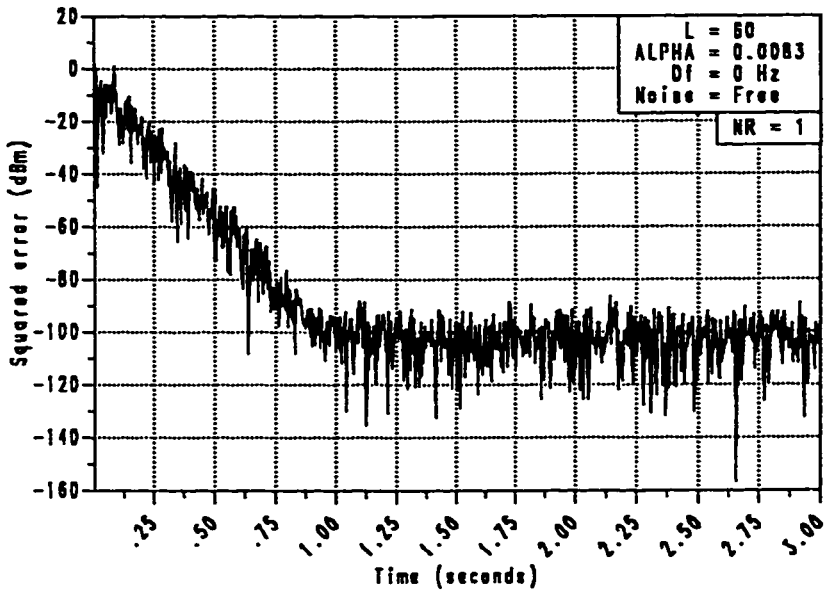

(a) No averaging (NR = number of runs).

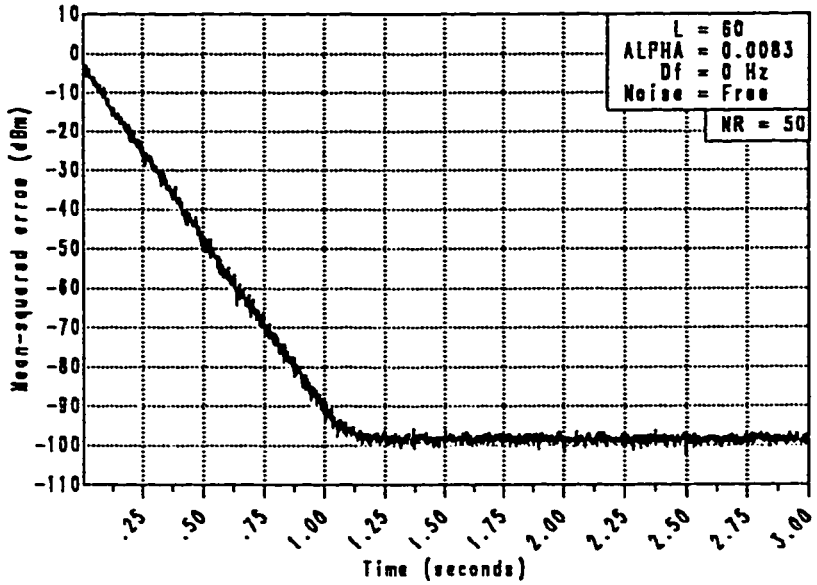

(b) With averaging (NR = 50).

Figure 5.3 Convergence of the canceller with the optimum step size.

same graph. The mean-squared error is obtained by sending 50 sequences of transmitted symbols, calculating the squared error for each sequence, then taking the average of these squared errors. It should be pointed out that in practice, only one shot is used. Therefore, smaller step size may be used at later stages of training.

5.3 EFFECT OF NOISE

To examine the effect of noise on the performance of the echo canceller, an additive Gaussian noise is added to the received echo signal at a selected level of power according to the following definition.

5.3.1 Power of the Noise

In telephone networks, the signal transmitted from the other end is typically received at -30 dBm assuming that it is transmitted at 0 dBm. The signal-to-noise ratio (SNR) is defined as

$$\text{SNR} = 10 \log \frac{P_s}{\sigma_n^2} \text{ dB} \tag{5.3}$$

where P_s is the power of far transmitted signal and σ_n^2 is the power of the noise.

On this basis, if the desired signal-to-noise ratio is SNR_o, then

$$SNR_o = (P_s)_{dBm} - (\sigma_n^2)_{dBm} \tag{5.4}$$

If $(P_s)_{dBm} = -30$ then

$$\sigma_n^2 = -30 - SNR_o \quad dBm \tag{5.5}$$

That is to say the -30 dB in Eq. (5.5) accounts for the typical attenuation in the telephone channel.

5.3.2 Performance of the Canceller in the Presence of Noise

It has been stated earlier in chapter 3 that the achieved MSE can not be less than the power of the irreducible noise $E[\xi_n^2]$ in Eq.(3.49). Therefore, we expect that the presence of noise will increase the achieved MSE which is desired to be as small as possible. Hence, the ERLE is expected to decrease. Figure 5.4 shows the performance of the canceller with SNR = 20 dB. This means that the power of the noise is -50 dBm. However, the achieved MSE is -47 dBm. The MSE is not as small as the power of the uncancelled noise (-50 dBm). This is because the presence of the noise in the error affects the updating process of the canceller taps, i.e. there taps exhibit some variation in their estimation.

Figure 5.4 shows also that the speed of convergence is not affected by the noise. We notice that the convergence time of the canceller's taps is the same for values signal-to-noise ratio of 20 and 30 dB. This is because we are using the same step size. Note that an increase of 10 dB in SNR, reduces the

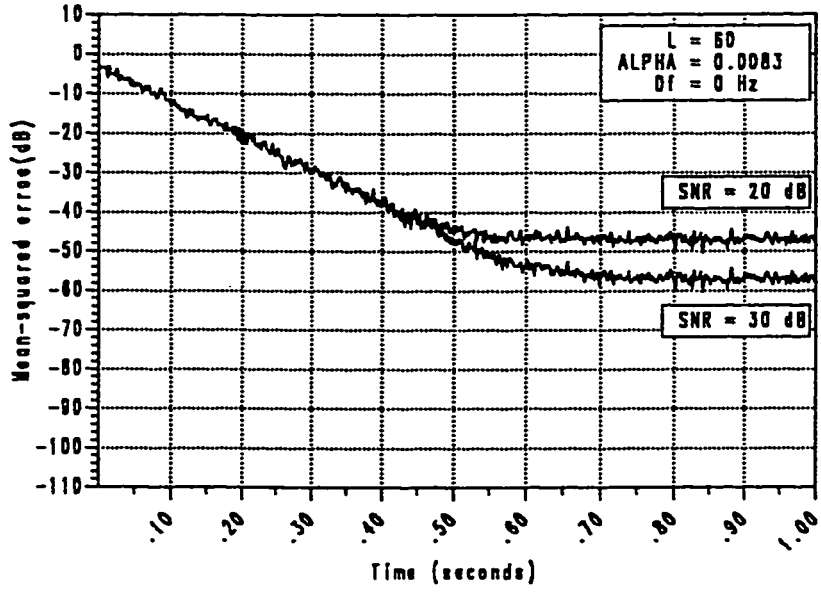

Figure 5.4 Effect of noise: MSE as a function of time.

achieved MSE by 10 dB, i.e. the MSE is -47 dBm for SNR= 20 dB, while the MSE is -57 dBm for SNR= 30 dB.

At the same level of noise (SNR = 20 dB), Fig. 5.5 shows that the achieved ERLE is about 44 dBm. Keeping in mind that the ERLE is the ratio of the received echo to the residual echo, we can fairly say that our simulation results agree with the echo level we have as follows:

$$\text{Received echo} = -3 \text{ dBm}$$

$$\text{Residual echo} = -47 \text{ dBm}$$

then the ERLE is

$$\text{ERLE} = -3 - (-47) = 44 \text{ dBm}.$$

Finally, it is expected that noise has larger effect on the far canceller rather than the near one. This is due to the fact that in our case the level of the far echo is less than the near echo by 15 dB. To see this effect, we define the taps relative MSE ($<\varepsilon^2>$) as follows

$$<\varepsilon^2> = \frac{\sum_{n=0}^{N+M} (\mathbf{H}_n - \mathbf{C}_n)^2}{\sum_{n=0}^{M+N} (\mathbf{H}_n)^2} \tag{5.6}$$

where **H** is the complex vector of sampled values of the echo channel and **C** is the complex coefficient vector of the canceller. The taps relative MSE is shown in Fig. 5.6 for both the near and the far cancellers. Note the -15 dB difference between them (i.e. $<\varepsilon_N^2> = -53$ dB , $<\varepsilon_F^2> = -38$ dB).

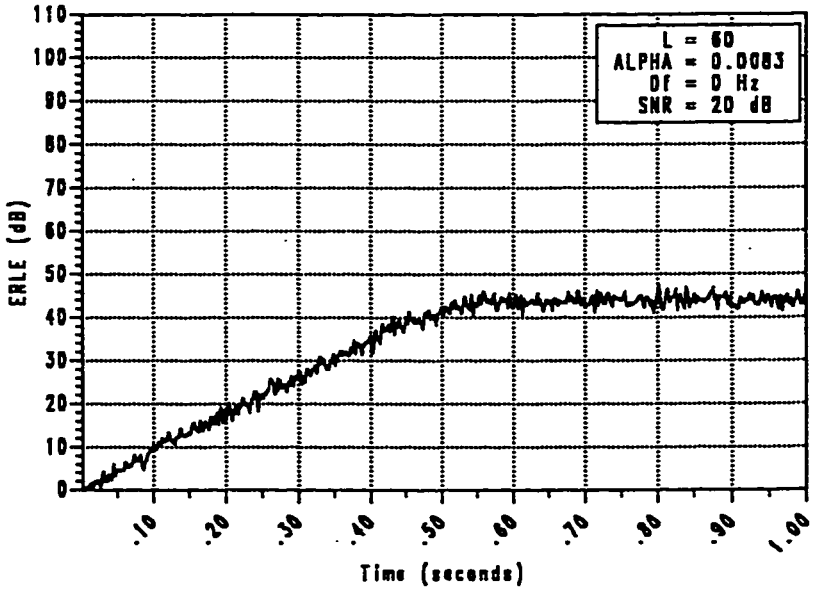

Figure 5.5 Achievable ERLE in presence of noise.

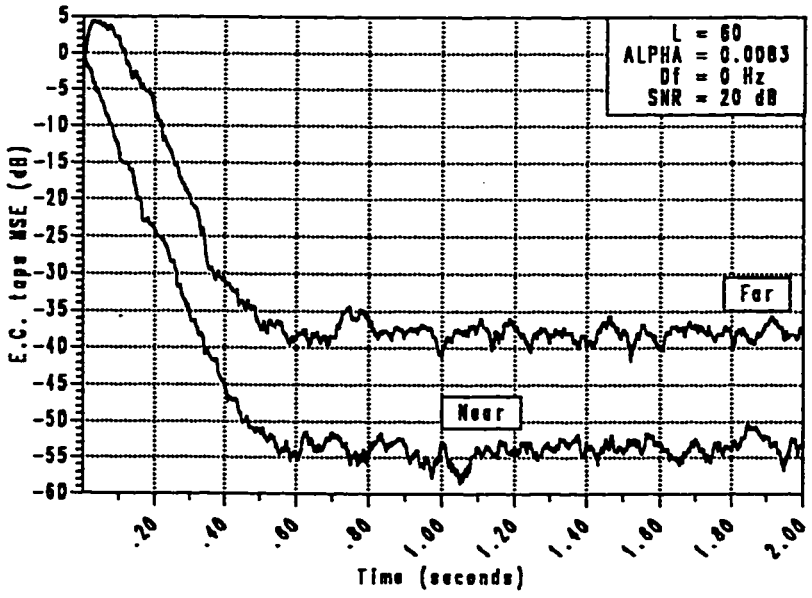

Figure 5.6 Convergence of the canceller's taps in presence of noise.

5.4 EFFECT OF FREQUENCY OFFSET (PHASE ROLL)

As stated in chapter 3, the most damaging of all the impairments commonly incountered in far echo is the frequency offset. In this section, this effect is studied by investigating the performance of the canceller in the presence of the frequency offset.

To get feeling of this effect, Fig. 5.7 is obtained by conducting the following simulated experiment. The echo canceller is first converged when no frequency offset presents in the echo channel. The canceller's taps are then frozen and a frequency offset of 2 Hz is introduced in the channel. Notice the periodic evolution of the MSE. As previously stated, the effect of frequency offset can be modeled by a periodic rotation of the sampled values of the complex output of the far echo channel. Thus, the MSE will pass through a minimum when these sampled values are in phase with the complex output of the far echo canceller. It will pass through a maximum when these complex values are out of phase by 180 degrees.

Performance degradation due to frequency offset. To examine the performance of the canceller in presence of frequency offset, in contrary with previous experiment, a frequency offset is introduced in the channel at the start of the adaptation process of the canceller taps. The PLL is switched off all the time. Degradation of the performance in this case is shown in Fig. 5.8. It is shown how the achieved ERLE is decreased drastically with the increase of the frequency offset. This degradation is also shown in Fig. 5.9 where the MSE (a)

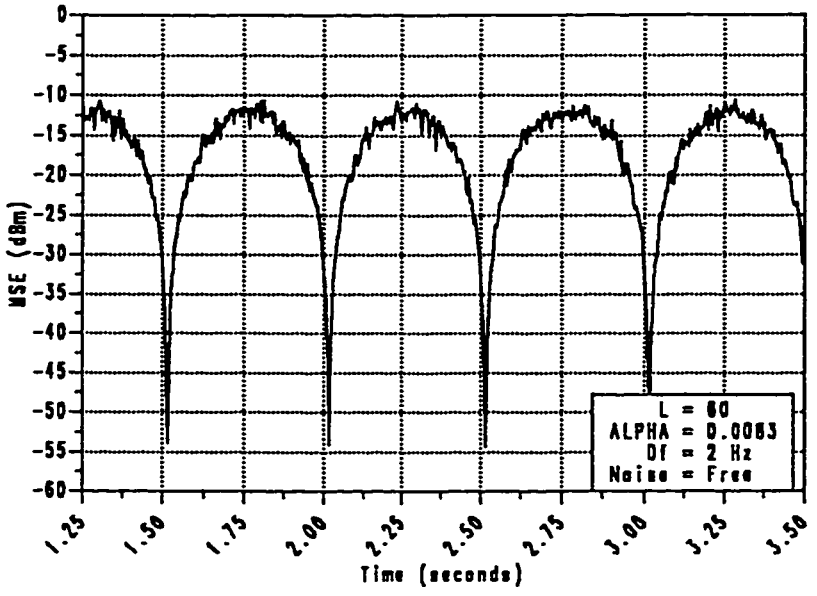

Figure 5.7 Evolution of the MSE in presence of frequency offset and with frozen taps.

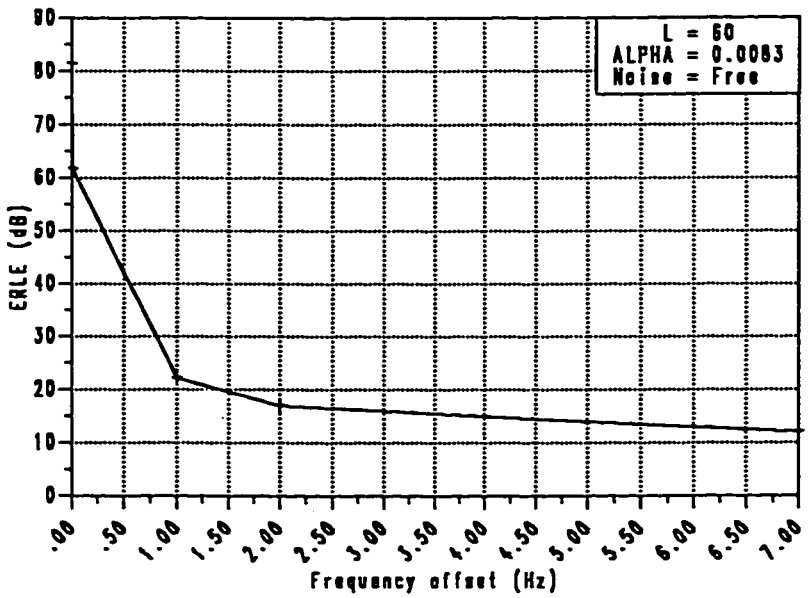

Figure 5.8 Achievable ERLE as a function of frequency offset.

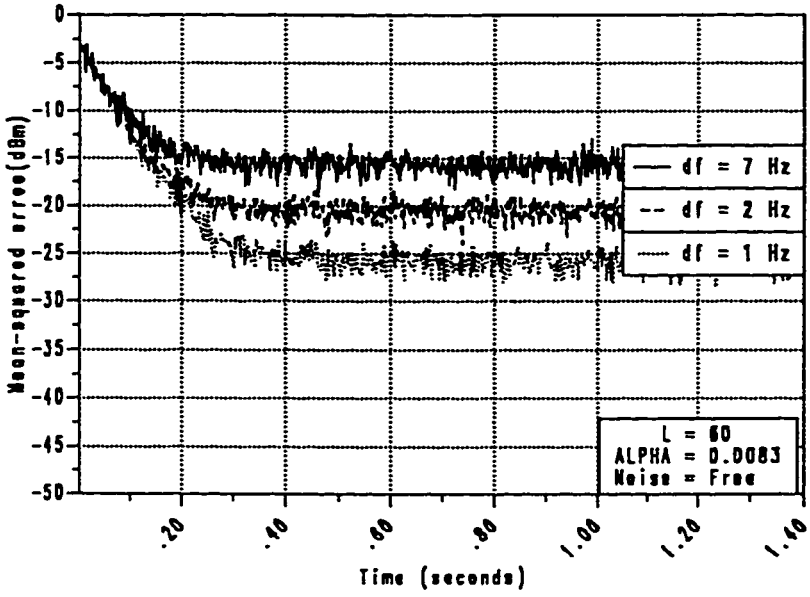

(a) MSE.

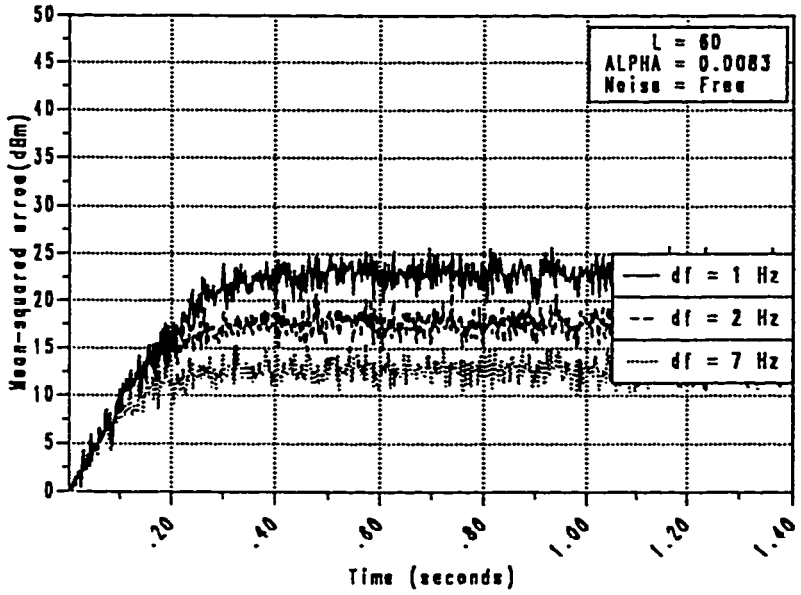

(b) ERLE.

Figure 5.9 Performance of the canceller in presence of frequency offset.

and the ERLE (b) are plotted versus time for frequency offset values of 1,2 and 7 Hz. Note how the MSE increases as frequency offset increases while the ERLE decreases.

The achieved MSE and consequently the achieved ERLE can be compared with the case when no frequency offset presents. This is shown in Fig. 5.3. Table 5.1 shows some values of the MSE for different frequency offsets. Note how much lost in dB when the introduced frequency offset is 1 Hz, for example. In this case, a lost of about 24 dB is the effect.,

Effect of the step size. Effect of step size in the tracking capability of the canceller the presence of frequency offset is also studied and is shown in Fig. 5.10 for frequency offsets of $\Delta f = 0.1$ Hz and $\Delta f = 1$ Hz. We notice that the ERLE increases even beyond the optimum step size ($\alpha = 0.0083$). This is because the canceller converges faster with larger step size, hence it is more likely to follow the rotation of the echo channel's sampled impulse response [7],[8].

The near and the far cancellers. As it is expected, since the far echo is only corrupted by frequency offset, the far canceller is affected more by the frequency offset as shown in Fig. 5.11. In part (a) of the figure, the relative MSE of the canceller taps defined in Eq.(5.6) is shown for both the near and the far canceller in the absence of frequency offset. In part (b), this shown for frequency offset of 1 Hz. Statistical data related to part (b) are shown in Table 5.2.

TABLE 5.1 Degradation due to frquency offset.

Freq. offset (Hz)	MSE (dBm)
0	- 50
1	- 26
2	- 21
7	- 16

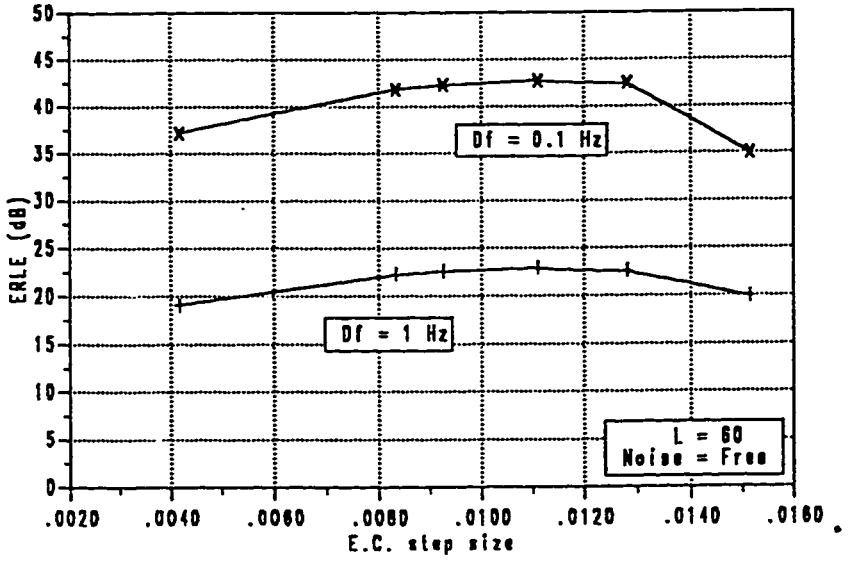

Figure 5.10 Effect of step size on the tracking capability of the E.C. in presence of frequency offset.

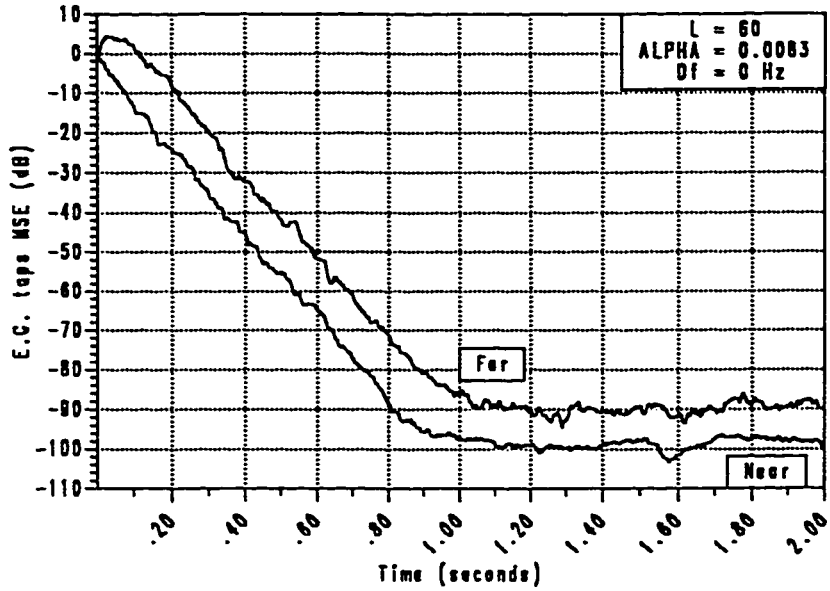

(a) No frequency offset.

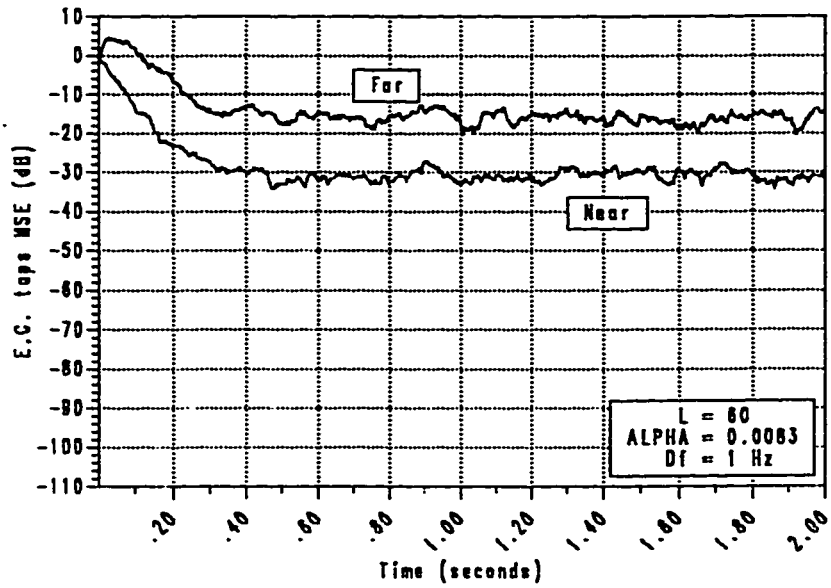

(b) Frequency offset of 1 Hz.

Figure 5.11 Effect of frequency offset on the canceller's taps.

TABLE 5.2 Effect of frequency offset on canceller's taps (statistical data).

	MSE	Mean	Variance
Δf = 1Hz	ε_N	-30.8 dB	-19.0 dB
	ε_F	-16.2 dB	- 4.4 dB
Δf = 0Hz	ε_N	0.13E-9	-86.1 dB
	ε_F	0.11E-8	-76.2 dB

5.5 COMPENSATION FOR FREQUENCY OFFSET

It has been shown in Chapter 4 that the solution of the frequency offset problem is to use a second order PLL to estimate the frequency offset, hence tracking continuously the change in the angle between the the actual and the estimated far echo components. Joint adaptation is performed for both the canceller taps and the frequency offset estimated by the second order PLL. This means that the PLL is switched on at the beginning of the training period and it is kept on all the time. The updating equations of the PLL has been derived in Chapter 4 in Eqs. (4.34) and (4.38). They are reproduced here for convenience :

$$b_{n+1} = b_n + g_2\hat{\gamma}_n \tag{5.7}$$

$$\hat{\theta}_{n+1} = \hat{\theta}_n + gb_n + g_1\hat{\gamma}_n \tag{5.8}$$

where b_n is the quantity related to the frequency offset, $\hat{\gamma}_n$ is the instantaneous estimate of the angle between the actual and the estimated far echo components. $\hat{\gamma}_n$ is the input of the PLL and is obtained from the phase estimater. $\hat{\theta}_n$ is the angle by which the estimated far echo component should be rotated to coincide with the actual component.

For a frequency offset of 1 Hz, convergence of the PLL is shown in Fig. 5.12. Five different sets of the first order loop gains (g_1 and g_2) are used. These loop gains affect the speed and the smoothness of the convergence of the PLL.

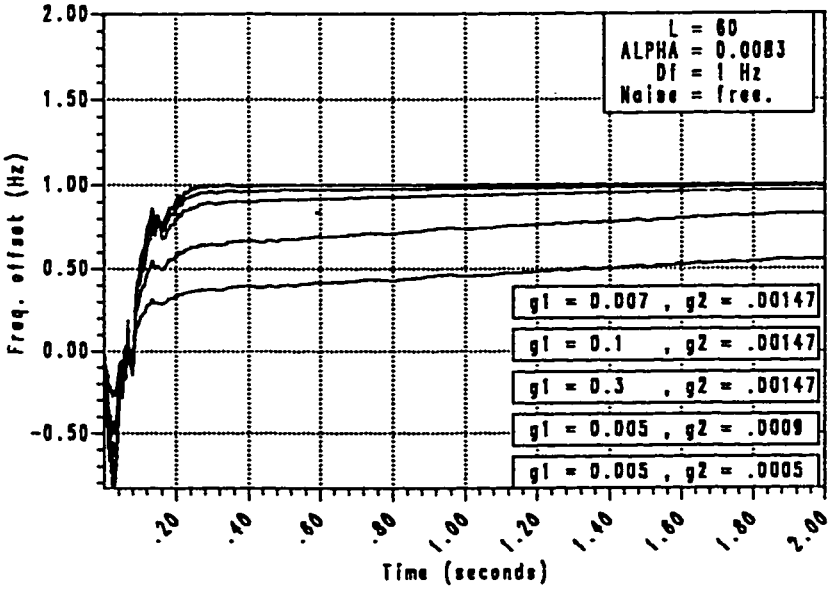

Figure 5.12 Joint adaptation: convergence of the PLL.

In practice, these gains should be properly engineered because they are highly dependent on the power of the far echo. A proposed solution, given by Macchi & Park in [24], is to get an estimate of the incoming echo and use this estimate as a multiplication factor in the phase estimator. Performance of the canceller at the same level of frequency offset is shown in Fig. 5.13. As shown in the figure the achieved MSE with PLL is almost identical to that given in Fig. 5.3 when no frequency offset exists. In other words, the 24 dB lost due to frequency offset of 1 Hz is retained with the PLL.

Although the performance of the joint adaptation technique described above is good enough, we have two main problems associated with it. First, computation complexity increases. More computations are now required due to the following devices: The phase estimator, the Hilbert transformer, and the PLL. This is besides that the new updating equation of the far canceller, (Eq. (4.40)) involves more computations now than it would with no frequency offset. These computations can be handled during the training period, where all the processor time is available for the canceller. However, the situation is different in the data mode where the receiver shares the processor time with the canceller. Moreover all these computations, for both the canceller and the receiver, should be executed within the symbol interval $T = .42$ms. Hence, a very fast processor is needed for this task.

The second problem associated with joint adaptation technique is the phase hit effect. In telephone switching circuit, it is quite possible that a step change (click) in phase to be introduced to the far echo. This has a serious effect on the

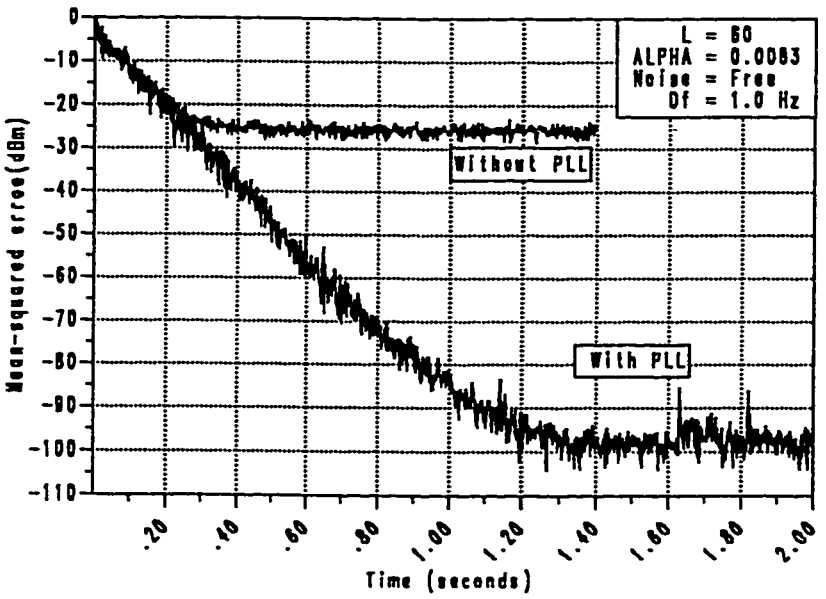

Figure 5.13 Joint adaptation: performance of the canceller.

canceller performance as seen in Fig. 5.14, which is obtained by conducting the following simulated experiment. The canceller is first converged in presence of frequency offset of 1 HZ. Then, after convergence and at time 1 s, a phase click of 180 degree was introduced to the far echo. As shown in Fig. 5.14(a) the canceller's taps are heavily affected. They have to converge again to the already converged value before the phase hit. Of course, this is considered to be a serious problem in the data mode operation where a very good performance of the canceller, to ensure no interference, is required. Figure 5.14(b) shows the phase difference between the actual and the estimated far echo through the experiment.

5.6 SUMMARY

The system design given in chapter 4 is completed in this chapter by determining the proper values of the canceller parameters, and the digital PLL constant gains. Simulation results can be summerized as follow. The optimum step size is found to be 0.0083 which is the reciprocal of twice the length of each subcanceller (60). The noise degrades the performance of the canceller because it appears as a large error in the updating equations. The canceller performance is mostly degraded in presence of frequency offset. The joint adaptation technique to compensate for frequency offset is verified. In the next chapter, the new proposed techniques for further improvements over the existing one are explained with simulation and evaluation.

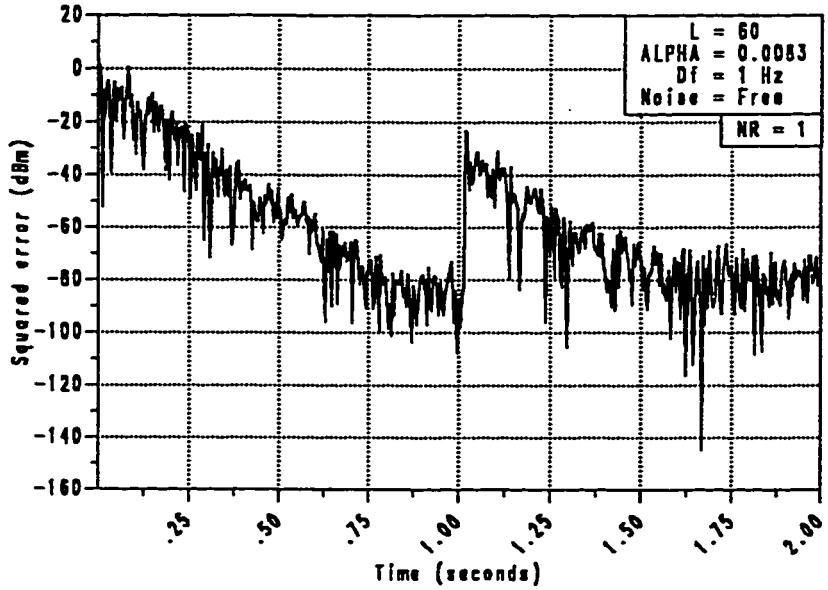

(a) Convergence of the canceller.

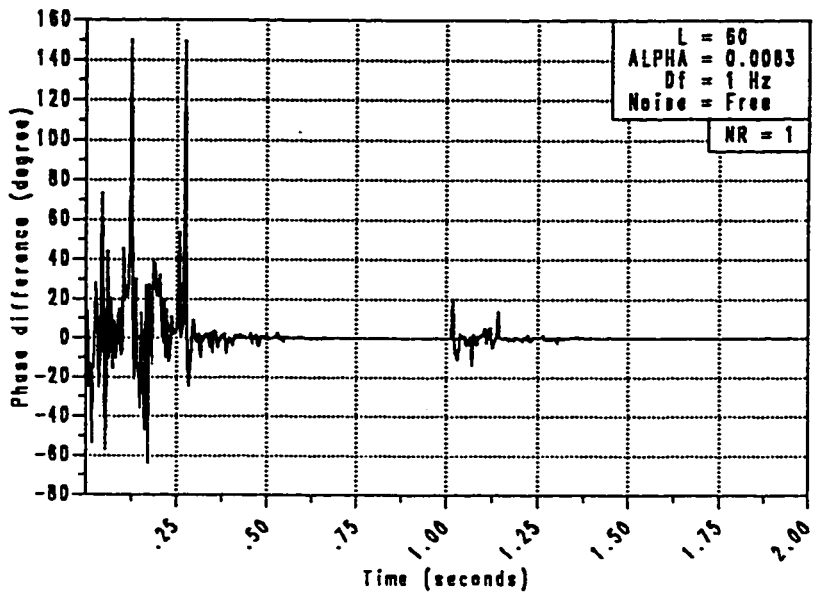

(b) Phase difference.

Figure 5.14 Joint adaptation: effet of phase hit.

CHAPTER 6

NEW TECHNIQUES FOR FREQUENCY OFFSET COMPENSATION AND FOR PHASE ROLL ESTIMATION DURING DATA MODE

As stated in the previous chapter, the computation complexity and the phase hit effect are two main problems associated with the joint adaptation technique. This motivates the research to look for further improvement. Two new techniques are proposed in this chapter. The new techniques contribute in the direction of reducing the computation complexity. Simulation results and evaluation of the new techniques are presented here.

6.1 SEQUENTIAL ADAPTATION (NEW PROPOSED TECHNIQUE)

In this section a new technique is proposed to reduce the computation complexity and to overcome the phase hit effect. This technique is called **Sequential Adaptation.** In this technique separate adaptation for canceller's taps and the PLL is performed. First, at the beginning of the training period with the PLL switched off, canceller's taps are only updated with a step size somewhat greater than the optimum one. Then, after convergence of the taps,

they are frozen and the PLL is switched on all the time to compensate for frequency offset.

The new technique is justified as follows. In the training period, the far transmitted signal is absent. Hence larger step size can be used for fast convergence of canceller's taps, refer to Fig. 5.10. With fast convergence, the canceller taps can accommodate for frequency offset, specially, if the amount of frequency offset is less than 0.5 HZ to achieve a good ERLE. When the taps are frozen, the steady state values of the taps represent the channel impulse response besides the frequency offset effect. After freezing the taps, switching on the PLL is necessary to keep tracking of the frequency offset.

Testing. There is no problem with freezing the taps. All what we have to do is to put the step size equal to zero. However what should be shown is the convergence of the PLL after freezing the taps. Now, the taps do not represent the actual channel. To test the new technique the following simulated experiment is conducted with a frequency offset of 0.5 Hz introduced to the system. The PLL is switched off. The canceller's taps are updated with a step size α equal to 0.011 (α_{opt} = 0.0083 with no frequency offset) for one second. By that time the canceller converged to a MSE value of -32.5 dBm as shown in Fig. 6.1(a). The PLL converged to 0.5 Hz within 1.5 s. Fig. 6.1(b). Note that the MSE dropped to -34 dBm. The same experiment is conducted with frequency offset of 1 Hz. Convergence of the canceller and the PLL as shown in Fig. 6.2(a) and (b), respectively.

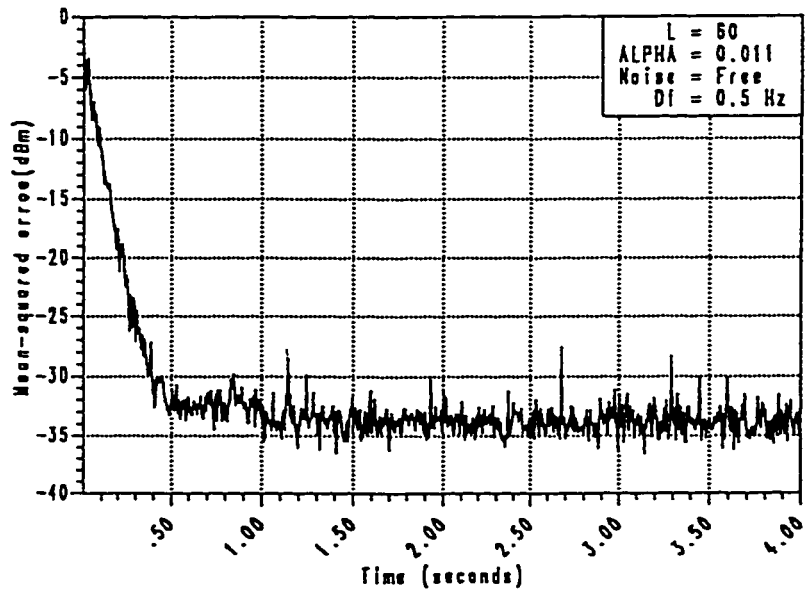

(a) Convergence of the canceller

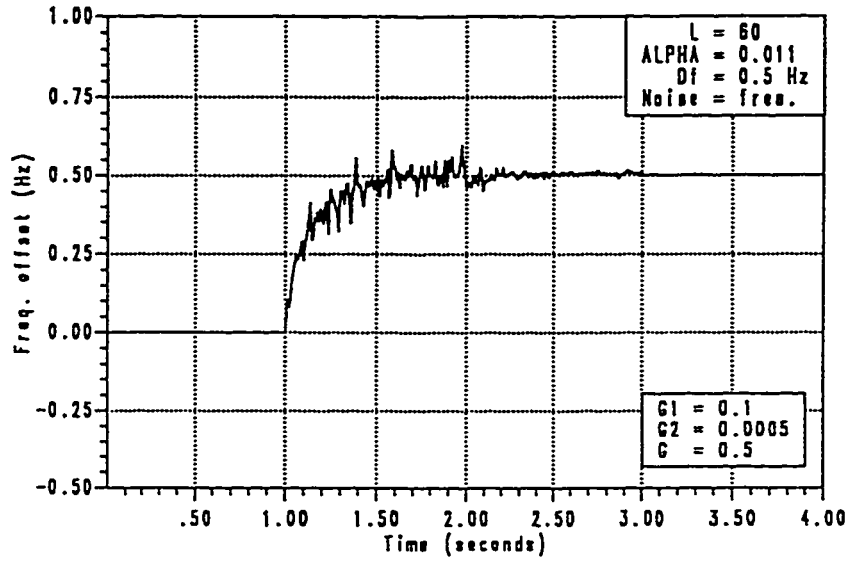

(b) Convergence of the PLL.

Figure 6.1 Sequential adaption: Δf = 0.5 Hz.

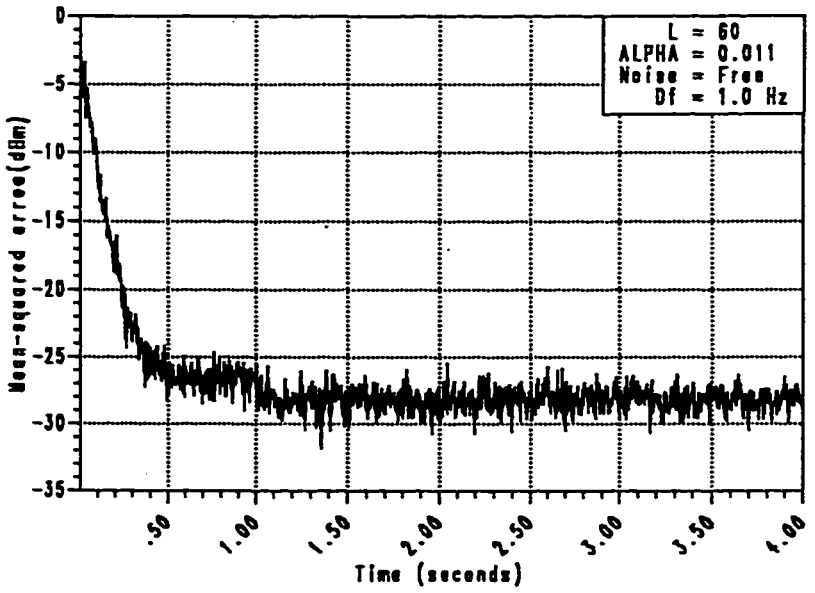

(a) Conergence of the canceller.

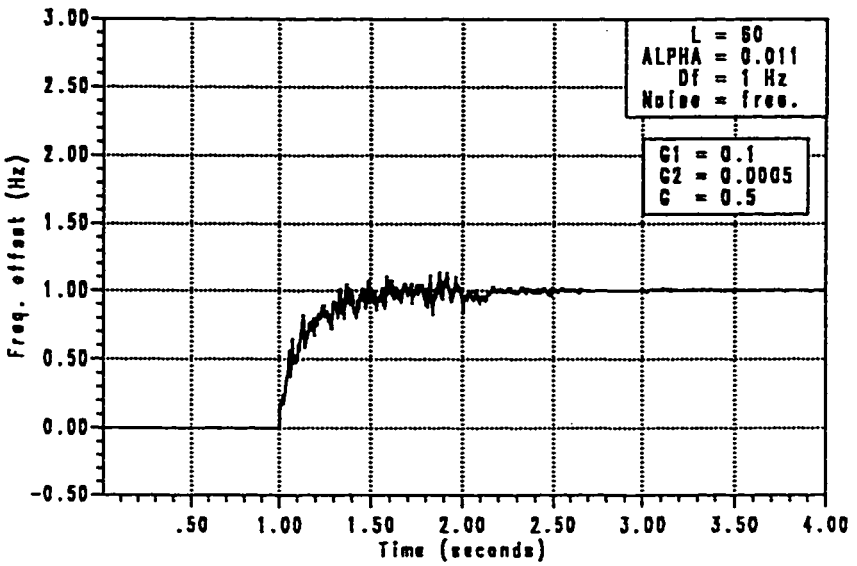

(b) Convergence of the PLL.

Figure 6.2 Sequential Adaptation :

Δf = 1.0Hz

Performance of the new technique with a phase hit. Since the taps are now frozen. It is expected that any sudden occurrence of a phase hit will have less effect on the canceller's performance. To see this effect, the same previous simulated experiment, shown in Fig. 5.14, i conducted with a frequency offset of 0.5 HZ. A phase hit of 180 degree is introduced to the system at t = 3 s. This is shown in Fig. 6.3. Notice that the convergence of the canceller is not affected heavily as the case was in Fig. 5.14.

6.2 EVALUATION AND COMPARISON BETWEEN SEQUENTIAL ADAPTATION AND JOINT ADAPTATION

In this section quantitative and qualitative analysis regarding the proposed new technique of echo cancellation (Sequential Adaptation) and the existing technique (Joint Adaptation), is discussed. At the end of the section, recommendations for practical applications are given.

6.2.1 Computation Complexity (Cost)

It has been seen in Section 5.6 that in joint adaptation tremendous amount of calculations are required within the symbol time, T = 0.42 ms. In particular, in the data mode operation where the processor time is divided between the canceller and the receiver.

In the new technique (Sequential Adaptation), the taps are frozen in data

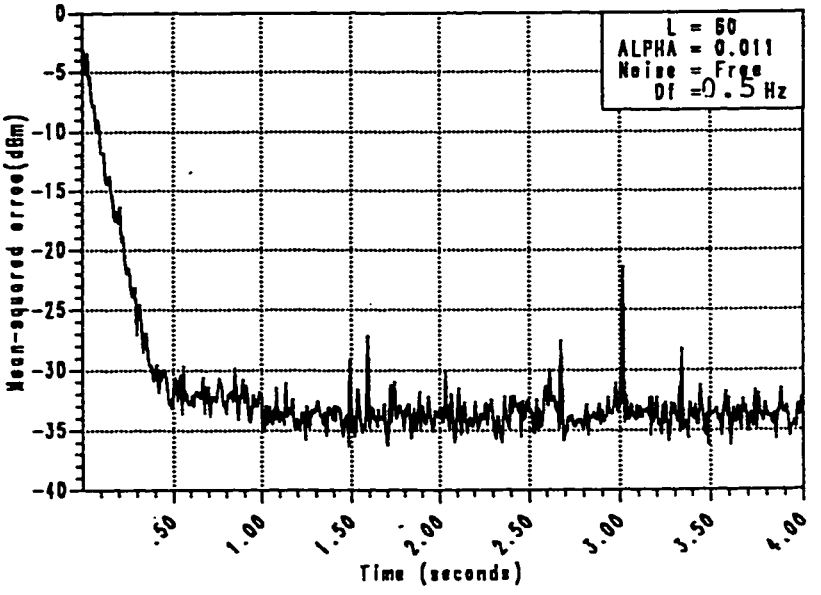

Figure 6.3 Secucntial adatation : effect of phase hit.

mode operation and the PLL only is switched on. Hence the processor time is divided only by the receiver and the PLL. Keeping in mind that the amount of computations related to the PLL is within 1/150 per symbol interval of the taps computation, we can fairly say that computation complexity related to the canceller is reduced by 50% in the data mode operation.

In sequential adaptation, the training period is divided into two intervals: the first interval is the time by which the canceller's taps converges while the second one is the time by which the PLL converges. Average number of additions and multiplications, per symbol interval, is calculated and shown in Table 6.1 for the two techniques. Again, the new technique beats the existing one: the number of additions is reduced by almost 54% and the number of multiplications is reduced by almost 35%. 'N' and 'M', shown in the table denote the length of the near and the far sections of the canceller, respectively.

6.2.2 Performance

Table 6.1 shows the achieved ERLE for both techniques at frequency offset of 0.5 Hz. For joint adaptation the achieved ERLE is +50 dB while it is +32 dB in Sequential adaptation. Although, the ERLE decrease by 18 dB in the sequential adaptation, it is good enough for practical applications.

Moreover, we notice from Table 6.1 that the convergence time is almost doubled in the new technique. Finally, It should be noted that the new technique has better performance under any sudden phase hit that may be

TABLE 6.1 Quantitative comparison between the 'Sequential technique' and the 'Joint technique' $\Delta f = 0.5Hz$.

	Computaion complexity		Performance	
	+	x	ERLE	Con. Time
Joint	4(N+2M)+4 1108	6(N+2M)+11 1667	50 dB	0.55 s.
Seq. (1) (2)	4(N+2M)-2 2(N+2M)+4 602	6(N+M) 1080	32 dB	1.0 s.

N : Lenght of the near canceller.

M : Lenght of the far canceller.

(1) : indicates the first interval of the sequential technique.

(2) : indicates the second interval of the sequential technique.

introduced to the system, as shown in Fig. 5.14 & 6.3. As stated earlier, this is because the taps are frozen.

6.2.3 Recommendations for Practical Applications

The achieved reduction of computation complexity in the new technique, means reduction of cost. This is because, a very fast processor is not needed now. However, this is basically at the expense that the training period is longer in the new technique. Besides, the achieved ERLE is less, especially if the frequency offset is greater than 0.5 Hz. Therefore, this technique is recommended to be used at frequency offset within 0.5 Hz. A compromise should be made between the cost and the training period time. An alternative technique is proposed for those applications where the cost is a main factor.

If the frequency offset is greater than 0.5 Hz, the achieved ERLE will definitly be less than 30 dB, (see Fig. 5.8). Then, it is recommended to use joint adaptation in the training period only and freeze the taps in the data mode. In this case, the computation complexity is as it is in joint adaptation in the training period only. However, it is decreased in the data mode as the case in sequential adaptation. As has been stated in section 5.6, joint adaptation can be accommodated in the training period because all the time of the processor is available for the canceller.

Performance of the canceller is the same as in Fig. 5.12 and 5.13. Neverless, performance of the canceller is better with a sudden phase hit as shown in Fig.

6.4. Figure 6.4 was obtained by conducting the same simulated experiment of Fig. 5.14.

6.3 A NEW APPROACH TO PHASE ROLL ESTIMATION DURING DATA MODE

It has been explained earlier in Chapter 4, that the first step in compensation for frequency offset, introduced to the far echo, is to include a phase estimator (comparator). The phase estimator gives an estimate of the instantaneous phase error between the received far echo and the locally generated far echo. This is accomplished by obtaining the imaginary part of the the error from its real part, using a H.T., (Eq. (4.31)). Then the phase is estimated using the formula given in Eq. (4.30) and reproduced here for convenience:

$$\hat{\gamma} \approx \frac{\mathrm{Im}[E_{e_n}]\,\mathrm{Re}[\hat{E}_{F_n}] - \mathrm{Re}[E_{e_n}]\,\mathrm{Im}[\hat{E}_{F_n}]}{E[\,|\hat{E}_{F_n}|^2\,]} \tag{6.1}$$

Based on this estimate, the PLL updates the estimated frequency and consequently updates the angle $\hat{\theta}$, by which the locally generated far echo should be rotated.

As we have seen, in either technique: joint or sequential, the PLL should be kept operating in the data mode. The PLL has already converged in the training period to the frequency offset introduced to the system. In data mode,

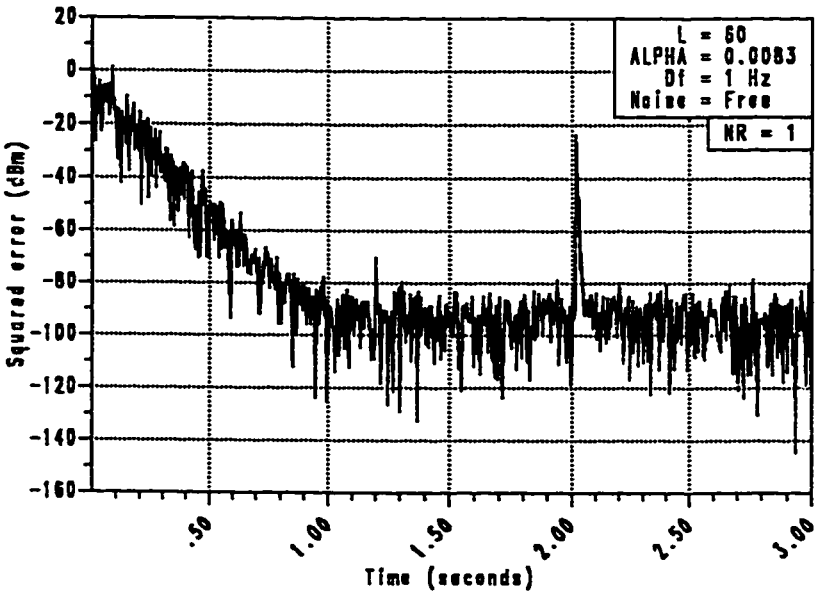

Figure 6-4 Joint in trianing only: effect of phase hit.

the PLL should only keep tracking the frequency offset.

As mentioned in Section 1.3, one of the difficulties associated with data-type cancellers is the timing problem. The echo canceller should be synchronized with the near transmitter while the receiver is synchronized with the far transmitter. This means that two separate D/A converters should be available during double talking. This adds complexity to the system.

Now, we propose **a new approach** utilizing the the sign algorithm to keep the PLL capable to track the frequency offset with one bit only. In this technique, there is no need to the Hilbert transformer and the phase estimator defined in Eq. (6.1). The new approach (technique) is described with reference to Fig. 6.5 as follow. Let the complex form of the far incoming echo, $\mathbf{E}_F$, and the estimated far echo, $\hat{\mathbf{E}}_F$, be represented as two vectors in the complex plane. We assume that at any instant, the phase difference, $\hat{\gamma}$, between the vector $\mathbf{E}_F$ and the vector $\hat{\mathbf{E}}_F$ is so small that both of them are in the same quadrant in the complex plane.

Take any of the cases shown in Fig. 6.5. We always notice that the sign of the estimated angle, $\hat{\gamma}$, is related to signs of the error signal, e_n, and the imaginary part of the estimated far echo by the following relation

$$\mathbf{Sgn}[\hat{\gamma}_n] = -\mathbf{Sgn}[\, e_n \mathrm{Im}(\hat{\mathbf{E}}_{F_n}) \,] \tag{6.2}$$

where **Sgn** [x] means the sign of x. Equation (6.2) implies that the sign of the estimated angle, $\hat{\gamma}$, can be determined from the sign bits of the error signal, e_n,

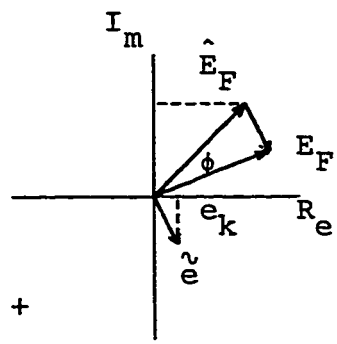

Sgn (E_n) = +

Sgn $(I_m(\hat{E}_F)$ = +

Sgn (ϕ) = -

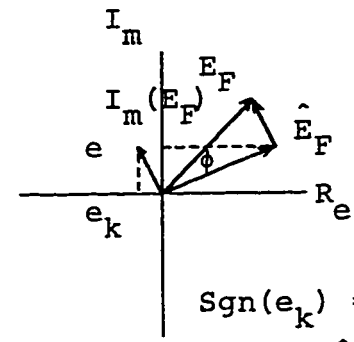

Sgn(e_k) = -

Sgn$(I_m(\hat{E}_F)$ = +

Sgn(ϕ) = +

(a) First Quadrant

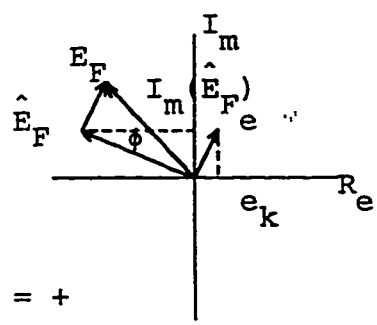

Sgn (e_k) = +

Sgn $(I_m(\hat{E}_F))$ = +

Sgn (ϕ) = -

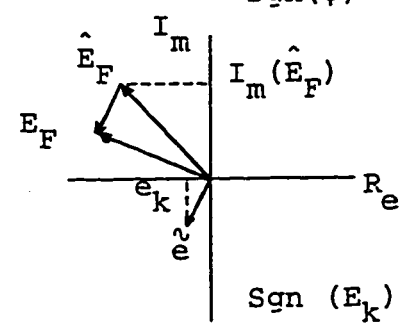

Sgn (E_k) = -

Sgn $(I_m\hat{E}_F)$ = +

Sgn (ϕ) = +

(b) Second quadrant

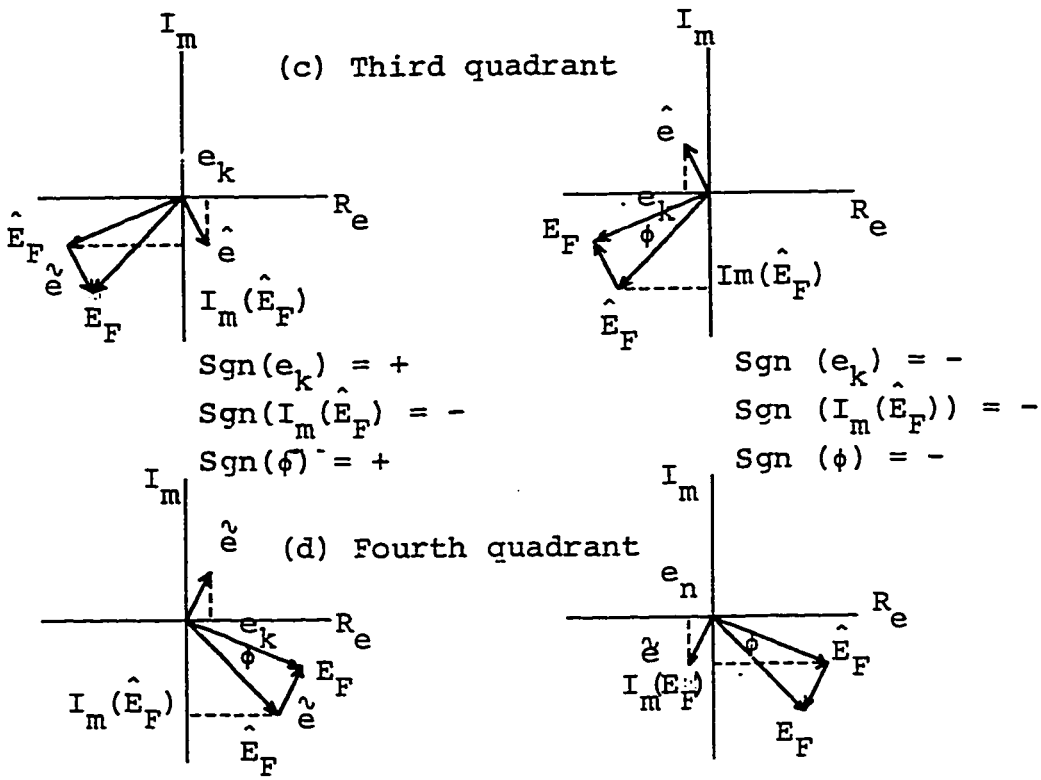

Figure 6.5 The sign algorith.

and the imaginary part of the estimated far echo, $\mathrm{Im}[\mathbf{E}_{F_n}]$.

The technique goes as follows. Take a constant value of the angle $\hat{\gamma}$ and call it γ_o Determine what the sign of the angle $\hat{\gamma}$ should be from Eq. (6.2). Hence the new equation for the new phase estimator is

$$\hat{\gamma}_n = -\mathbf{Sgn}[\, e_n \mathrm{Im}(\hat{\mathbf{E}}_{F_n}) \,]\gamma_o \tag{6.3}$$

Equation (6.3) completely describes the new 'Sign Algorithm'.

Since the angle $\hat{\gamma}$ has a constant absolute value, $\hat{\gamma}_o$, the technique is similar to an up-down counter that has a fixed up or down step to go through. Therefor, the value of γ_o will affect the accuracy of the estimated frequency offset. Moreover, it will affect the speed of convergence of the PLL of any step change occurs to the frequency offset.

Testing. The new approach to phase estimation was tested by conducting the following experiment. A frequency offset of 1 Hz was introduced to the system. The PLL was allowed to converge, by joint adaptation, for 1.5 Sec. Then, an additional frequency offset of 0.01 Hz was introduced to the system in parallel to switching the new phase estimator (new technique) on. The constant γ_o was taken to be 0.05 degree. Convergence of PLL is shown in Fig. 6.6, which shows the phase difference between $\mathbf{E}_F$ and $\hat{\mathbf{E}}_F$. Note that it goes to zero within 1 Sec.

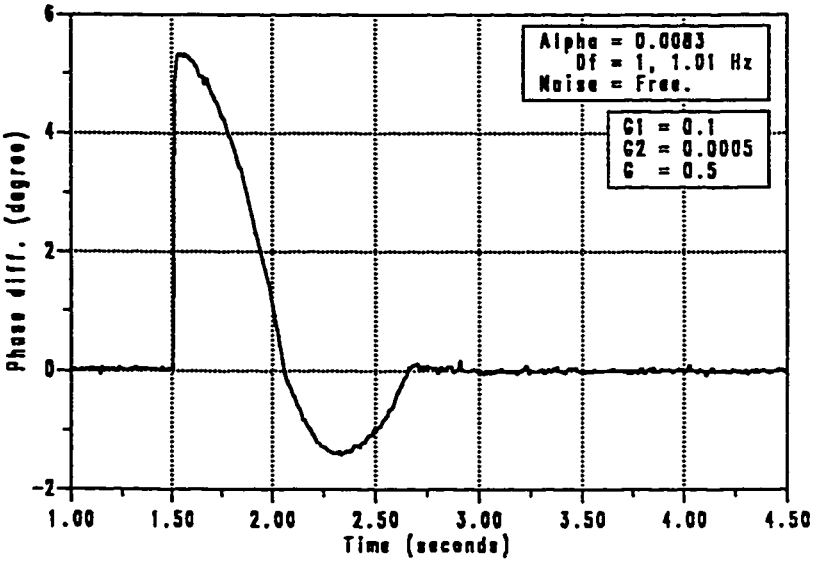

Figure 6.6 Sign algorithm approach:

$\gamma_o = 0.05°$

To see the affect of the value of γ_0 on the speed of convergence, the same previous experiment was conducted at $\gamma_0 = 0.01$ degree. The phase difference takes longer time to converge to zero as shown in Fig. 6.7.

6.4 SUMMARY

In this chapter, two new techniques namely 'sequential adaptation' and 'sign technique', are proposed. Results of the simulation and the analysis show that the first new technique (Sequential Adaptation) is effective in terms of reducing the computation complexity. Moreover, it has a better performance compared with the joint adaptation under any sudden phase hit. In the second new technique (sign technique), it has been verified by analysis and simulation that it is possible to compensate for frequency offset with one bit only. The A/D converter, shown in the overall block diagram of Fig. 4.1, can be replaced by a D/A converter to be located after the output of the canceller and before the subtractor. Compensation is performed in analog form now. This reduces the complexity of the system since the D/A converter is less complex than the A/D converter. What we need, only, is a 1 bit A/D converter to be used for the 'sign technique'.

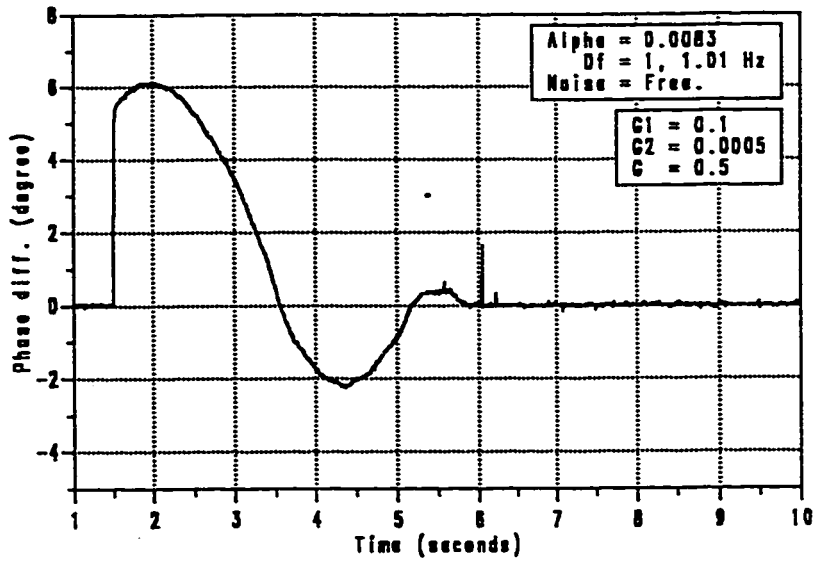

Figure 6.7 Sign algorithm approach:

$\gamma_o = 0.01°$

CHAPTER 7

CONCLUSIONS AND SUGGESTIONS FOR FURTHER RESEARCH

7.1 CONCLUSIONS

A digital voiceband echo canceller is designed. The canceller is of data-type structure and operates at Nyquist rate. The structure is divided into two sections: a near section and a far section. The designed canceller is tested through simulation under various impairments. An echo channel, taken from actual measurements using a channel simulator, is used in the simulation. The echo channel has durations of 11.7 ms and 13.3 ms for the near and far channels, respectively. The attenuation level of the echo channel is under program control in the simulation process.

A complete study on the echo cancellation problem is accomplished using the simulation. The study includes the following: the optimum step size of the canceller, the effect of noise, the effect of frequency offset, the performance of the PLL as a solution for the frequency offset problem, and the effect of phase hit. Results of the simulation agree with the theoretical basis given in papers as follow.

The optimum step size to achieve the MMSE is found to be 1/2(M+N), where M and N are the lengths of the near and far sections, respectively. In our case it is found to be 0.0083. The noise affects the achievable MSE because it appears as a residual echo. That is to say that the achievable MSE increases as the power of the noise increases. The frequency offset has the most damaging effect on the performance of the canceller. As shown in [7], it is verified by simulation that the effect of the frequency offset can be modeled by a periodic rotation of the sampled values of the complex output of the far echo channel. This effect can be compensated using a 2nd order PLL and performing joint adaptation for the canceller's taps and the frequency offset estimated by the PLL. Finally, the phase hit disturbs strongly the convergence of the canceller's taps.

A new technique for echo cancellation in the presence of frequency offset is proposed. This technique is called " **Sequential Adaptation** ". In this technique, separate adaptation for canceller's taps and the PLL is performed. The new technique stands on the fact that a large step size can be used to update the taps of the canceller at the beginning of the training period. This is because the far signal does not exist during the training period of the canceller. Hence, the fast convergence of the canceller's taps can accommodate the effect of frequency offset, specially for frequency offsets less than 0.5 Hz. In this case, there is no need to switch the PLL on from the beginning of the of training. The PLL is switched on after canceller's taps convergence and freezing the taps of the canceller. The PLL takes its time to converge to the required frequency offset

before operating in data mode. The canceller taps are kept frozen in data mode operation. The new technique is seen to be very efficient in terms of computation complexity which means a reduction of cost. In the training period, the average number of additions per symbol interval is reduced almost by 54%. The average number of multiplications is reduced by 35%. Moreover, the computation complexity related to the canceller is reduced by 50% in the data mode operation.

The new technique is recommended to be used when the frequency offset is less than 0.5 Hz. This is because the canceller taps, without the PLL, can not compensate for frequency offsets beyond 0.5 Hz even if we increase the step size. In the areas where the introduced frequency offset is greater than 0.5 Hz, it is recommended to use joint adaptation in the training period. However, the canceller taps are frozen in the data mode.

Freezing the taps in data mode is seen to be a good solution for the phase hit problem. However, doing that has the danger that the canceller will not be capable to track any possible change in the echo channel. On the other hand, this is rarely happens in telephone channel. If it happens, a re-training can be initiated by either modem.

A new approach, utilizing the idea of the sign algorithm, for phase estimation is also proposed. A nice relation between the direction of the necessary rotation for the estimated far echo and the signs of both the error signal and the imaginary part of the estimated far echo is derived. Based on the

derived formula, a simple phase estimator which works with only one bit is proposed. This new estimator is used in the data mode operation.

7.2 SUGGESTIONS FOR FURTHER RESEARCH

The following can be good points for further research:

1. Implementation of the proposed new techniques in the real time environment.
2. Derivation of closed forms for the values of the loop filter.
3. Extension to non-linear cancellers for non-linear echo channels.
4. Study the effect of using higher order PLLs.
5. Extension of the proposed techniques in conjunction with a fast start up of training period.

APPENDIX

```
-------------------------------------------------
C  IMPULSE RESPONSE OF TRANSMITTING FILTER (LOW PASS) :
C        H(0) H(1) H(2) ..... H(L-1)
C
C  DELAY LINES :  REAL  RDL
C               IMAG  IDL
C
C  TRANSMITTED SAMPLE ( OUTPUT OF TRANSM. FILTER ) :
C        REAL : S(N)
C        IMAG : SH(N)
C
C     OUTPUT OF TRANSM. SUB-FILTERS ARE DENOTED BY
C        REAL : S1(K)     IMAG. : SH1(K)
C             S2(K)             SH2(K)
C             S3(K)             SH3(K)
C
C  SC : SCRAMPLER REGISTER
C
C-------------------------------------------------
C
C-------------------------------------------------
C
C  ECHO SUBCHANNEL IMPULSE RESPONSE :
C
C   NEAR :   REAL  RCN1  RCN2  RCN3
C            IMAG  ICN1  ICN2  ICN3
C
C   FAR  :   REAL  RCF1  RCF2  RCF3
C            IMAG  ICF1  ICF2  ICF3
C
C
C   REAL NEAR : RCN1(0) RCN1(1) ..... RCN1(G1-1)
C   IMAG NEAR : ICN1(0) ICN1(1) ..... ICN1(G1-1)
C
C   REAL FAR  : RCF1(0) RCF1(1) ..... RCF1(G1-1)
C   IMAG FAR  : ICF1(0) ICF1(1) ..... ICF1(G1-1)
C
C-------------------------------------------------
C
C-------------------------------------------------
```

```
C
C SUBCANCELLER IMPULSE RESPONSE :
C
C   NEAR :   REAL RNE1 RNE2 RNE3
C          IMAG INE1 INE2 INE3
C
C   FAR :   REAL RFE1 RFE2 RFE3
C          IMAG IFE1 IFE2 IFE3
C     .
C
C   REAL NEAR : RNE1(0) RNE1(1) ..... RNE1(L2-1)
C   IMAG NEAR : INE1(0) INE1(1) ..... INE1(L2-1)
C
C   REAL FAR  : RFE1(0) RFE1(1) ..... RFE1(L2-1)
C   IMAG FAR  : IFE1(0) IFE1(1) ..... IFE1(L2-1)
C
C-------------------------------------------------
      REAL RN(48000),EM1(0:2)
      REAL AE(48000),AER(1),ABK1(48000),APHIE(48000)
      REAL TEF(4800),TEN(4800)
      COMPLEX CN1(0:27),CN2(0:27),CN3(0:27)
      COMPLEX CF1(0:31),CF2(0:31),CF3(0:31)
      COMPLEX CNE1(0:27),CNE2(0:27),CNE3(0:27)
      COMPLEX CFE1(0:31),CFE2(0:31),CFE3(0:31)
      REAL RCN1(0:27),RCN2(0:27),RCN3(0:27)
      REAL ICN1(0:27),ICN2(0:27),ICN3(0:27)
      REAL RCF1(0:31),RCF2(0:31),RCF3(0:31)
      REAL ICF1(0:31),ICF2(0:31),ICF3(0:31)
      REAL RCFF1(0:31),RCFF2(0:31),RCFF3(0:31)
      REAL ICFF1(0:31),ICFF2(0:31),ICFF3(0:31)
      REAL RNE1(0:27),RNE2(0:27),RNE3(0:27)
      REAL INE1(0:27),INE2(0:27),INE3(0:27)
      REAL RFE1(0:31),RFE2(0:31),RFE3(0:31)
      REAL IFE1(0:31),IFE2(0:31),IFE3(0:31)
      REAL ARNE1(0:27),ARNE2(0:27),ARNE3(0:27)
      REAL AINE1(0:27),AINE2(0:27),AINE3(0:27)
      REAL ARFE1(0:31),ARFE2(0:31),ARFE3(0:31)
      REAL AIFE1(0:31),AIFE2(0:31),AIFE3(0:31)
      REAL RDL(0:64),IDL(0:64)
      REAL RCL(0:64),ICL(0:64)
      REAL SC(23),NK,NK1,NK2
      INTEGER BD,FS,FC
      COMPLEX Y1,YE1
C
C-----READ IMPULSE RESP. OF  ECHO CHANNEL------
C        L1 : LENGTH OF NEAR ECHO SUBCHANNEL
C        L2 : LENGTH OF FAR  ECHO SUBCHANNEL
```

```
C       BD : BULK DELAY
C       FB : BAUD RATE
C       FS : SAMPLING RATE
C       FC : CARRIER FREQ.
C
      READ (20,*) L1,L2,BD,FB,FS,FC
      WRITE(6,8) L1,L2,BD
      WRITE(6,9) FB,FS,FC
8   FORMAT(' ','L1 = ',I2,3X,'L2 = ',I2,3X,'BD = ',I2)
9   FORMAT(' ','FB = ',F6.1,3X,'FS = ',I5,3X,'FC = ',I5)

      DO 10 I=0,L1-1
         READ (20,*) RCN1(I),RCN2(I),RCN3(I)
10  CONTINUE
11  FORMAT (2X,I7,5X,3(E15.4,3X))
12  FORMAT (2X,F9.6,5X,3(E15.4,3X))

      READ (20,*) TEMP

      DO 15 I=0,L1-1
         READ (20,*)   ICN1(I),ICN2(I),ICN3(I)
15  CONTINUE

      READ (20,*) TEMP

      DO 20 I=0,L2-1
         READ (20,*)   RCF1(I),RCF2(I),RCF3(I)
         RCFF1(I)=RCF1(I)
20  CONTINUE

      READ (20,*) TEMP

      DO 25 I=0,L2-1
         READ (20,*)   ICF1(I),ICF2(I),ICF3(I)
         ICFF1(I)=ICF1(I)
25  CONTINUE

C-------------------------------------------------------
C CHANNEL VARIANCE : NEAR AND FAR
C-------------------------------------------------------
      CALL VARNCE(RCN1,ICN1,CN1,L1,SN1)
      CALL VARNCE(RCF1,ICF1,CF1,L2,SF1)
      CALL VARNCE(RCN2,ICN2,CN2,L1,SN2)
      CALL VARNCE(RCF2,ICF2,CF2,L2,SF2)
      CALL VARNCE(RCN3,ICN3,CN3,L1,SN3)
      CALL VARNCE(RCF3,ICF3,CF3,L2,SF3)
```

```
      RATIO1 = 10*ALOG10(SN1/SF1)
      RATIO2 = 10*ALOG10(SN2/SF2)
      RATIO3 = 10*ALOG10(SN3/SF3)

      WRITE(6,*) SN1,SF1,RATIO1
      WRITE(6,*) SN2,SF2,RATIO2
      WRITE(6,*) SN3,SF3,RATIO3

      CALL NORMAL(RCN1,ICN1,CN1,L1,SN1)
      CALL NORMAL(RCF1,ICF1,CF1,L2,SF1)
      CALL NORMAL(RCN2,ICN2,CN2,L1,SN2)
      CALL NORMAL(RCF2,ICF2,CF2,L2,SF2)
      CALL NORMAL(RCN3,ICN3,CN3,L1,SN3)
      CALL NORMAL(RCF3,ICF3,CF3,L2,SF3)

C     CALL VARNCE(RCN1,ICN1,CN1,L1,SN1)
C     CALL VARNCE(RCF1,ICF1,CF1,L2,SF1)
C     CALL VARNCE(RCN2,ICN2,CN2,L1,SN2)
C     CALL VARNCE(RCF2,ICF2,CF2,L2,SF2)
C     CALL VARNCE(RCN3,ICN3,CN3,L1,SN3)
C     CALL VARNCE(RCF3,ICF3,CF3,L2,SF3)

C     WRITE(6,*) SN1,SF1
C     WRITE(6,*) SN2,SF2
C     WRITE(6,*) SN3,SF3

      C1 = SN1
      C2 = SF1
C     WRITE(6,*) 'C1 = ? , C2 = ?'
C     READ (6,*) C1,C2
C     C1 = -10.
C     C2 = -30.
C     C1 = 10**(C1/10.)
C     C2 = 10**(C2/10.)

C-------------------------------------------------------
C CONSTANTS SETTING
C-------------------------------------------------------
      PI = 22./7.
      SNR = 90.
      F = 2.00
      DF = 1.
      NR = 1
      NK = 2.
      WRITE(6,*) 'SNR = ?  ','DF = ?'
      READ (6,*) SNR,DF
```

```
C------TRAINNING PERIOD-----------------------------

      WRITE(6,*) '-----TRAINNING  PERIOD  CONSTANTS -----'
      WRITE(6,*) 'PLL : ON  OR OFF ?   (ON=1 , OFF=0)'
      READ(6,*) PLLF
      WRITE(6,*) 'FACTOR (F) = ?  '
      WRITE(6,*) 'NUMER OF ITERATIONS (NK1) = ?'
      WRITE(6,*) 'NUMER OF RUNS (NR) = ?'
      READ (6,*) F,NK1,NR

      G1=.005
      G2=.00147
      G =.5
      IF (PLLF .EQ. 1) THEN
      WRITE(6,*) 'LOOP FILTER GAIN : G1 = ?,  G2 = ?'
      WRITE(6,*) 'VCO GAIN (G) = ?'
      READ (6,*) G1,G2,G
      WRITE(6,*) 'G1 = ',G1,'  G2 = ',G2,'  G = ',G
      ENDIF
C-------------------------------------------------

C------DATA  MODE  PERIOD-----------------------------

      WRITE(6,*) 'DO YOU WANT TO OPERATE IN DATA MODE ?
     *(Y=1 , N=0)'
      READ(6,*) DMF

      IF (DMF .EQ. 1) THEN

      WRITE(6,*) 'DO YOU WANT TO FREEZE THE TAPS ?
     *(Y=1 , N=0)'
      READ(6,*) TAPF

      IF (TAPF .NE. 1) THEN
      WRITE(6,*) 'F1 = ?'
      READ(6,*) F1
      ENDIF

      WRITE(6,*) 'PLL : ON  OR OFF ?   (ON=1 , OFF=0)'
      READ(6,*) PLLF2

      IF (PLLF2 .EQ. 1) THEN

      WRITE(6,*)'DO YOU WANT TO USE THE SIGN ALGORITHM ?
     *(Y=1 , N=0)'
      READ(6,*) SAF
```

```
      IF (SAF .EQ. 1) THEN
      WRITE(6,*) 'DPHI1 = ? , NAVG = ?'
      READ(6,*) DPHI1,NAVG
      ELSE
      DPHI1=0.
      NAVG=1
      ENDIF

      WRITE(6,*) 'NEW LOOP FILTER GAIN : G11 = ?,  G22 = ?'
      WRITE(6,*) 'VCO GAIN (GG) = ?'
      G11=G1
      G22=G2
      GG =G
      READ (6,*) G11,G22,GG
      WRITE(6,*) 'G11 = ',G11,'  G22 = ',G22,'  GG = ',GG
      ENDIF

      WRITE(6,*) '---------DATA MODE CONSTANTS----------'
      WRITE(6,*) 'NUMER OF ITERATIONS (NK2) = ?'
      READ (6,*) NK2

      ELSE

      TAPF=0
      SAF=0
      NK2=0.
      DPHI1=0.
      NAVG=1
      ENDIF

C-----------------------------------------------------

      NK=(NK1+NK2)*FB
      IFB=FB

C     DO 26 IN=1,8
C     READ (11,*) DF
      ALPHA=1./F/(L1+L2)

100   WRITE(6,27) ALPHA,SNR,DF,NK/FB,NR
27    FORMAT(' ','ALPHA =',F12.9,3X,'SNR =',F4.1,3X,'DF
     *= ', F9.6, 3X,'NK = ',F4.1,2X,'NR = ',I2)

      CT=G*FB/2/PI
      BKR=DF/CT

C---- SNR = SIGNAL TO NOISE RATIO----------
```

```
C    IF .GT. 50 = NOISE = FREE

          BETA=10**(-30-SNR/20)

C-------------------------------------------------
C INTIALIZATION
C-------------------------------------------------
        CALL DLL(ARNE1,AINE1,L1)
        CALL DLL(ARNE2,AINE2,L1)
        CALL DLL(ARNE3,AINE3,L1)
        CALL DLL(ARFE1,AIFE1,L2)
        CALL DLL(ARFE2,AIFE2,L2)
        CALL DLL(ARFE3,AIFE3,L2)
        DO 28 I=1,NK
         AE(I)=0.
C      AER(I)=0.
         TEN(I)=0.
         TEF(I)=0.
         ABK1(I)=0.
         APHIE(I)=0.
28    CONTINUE

C-------START--------------------

        DO 29 I5=1,NR

C     IF (SNR .LT. 50) THEN
C       READ (10,*) (RN(I),I=1,NK)
C     ENDIF

        E1=0.
        BK1=0.
        PHIE=0.
        DTHE=0.
        NCOUNT=0
        MM=0
        DPHI1=DPHI1/180.*PI
        WRITE(6,*)'  DPHI1 =',DPHI1*180/PI,'  NAVG =',NAVG
C-------------------------------------------------
C INITIALIZATION OF THE SCRAMBLER
C-------------------------------------------------
        READ(16,*)(SC(I),I=1,23)
C-------------------------------------------------
C INITIALIZATION OF DELAY LINES
C-------------------------------------------------
        CALL DLL(EM1,EM1,3)
        CALL DLL(RDL,IDL,L1+L2+BD)
```

```
      CALL DLL(RCL,ICL,L1+L2+BD)
      DO 31 I=1,L1+L2+BD
        CALL SYMBOL(SC,A,B)
        CALL MODLTR(I,A,B,A1,B1)
        CALL UPDAT(RDL,IDL,L1+L2+BD,A1,B1)
        CALL UPDAT(RCL,ICL,L1+L2+BD,A1,B1)
31    CONTINUE
C-------------------------------------------------
C INITIALIZATION OF CANCELLER COEFFICENTS
C-------------------------------------------------
      CALL DLL(RNE1,INE1,L1)
      CALL DLL(RNE2,INE2,L1)
      CALL DLL(RNE3,INE3,L1)
      CALL DLL(RFE1,IFE1,L2)
      CALL DLL(RFE2,IFE2,L2)
      CALL DLL(RFE3,IFE3,L2)

      DO 30 K=1,NK

200   CALL SYMBOL(SC,A,B)
      CALL MODLTR (K,A,B,A1,B1)

C-----UPDATING THE DELAY LINE-------

      CALL UPDAT(RDL,IDL,L1+L2+BD,A1,B1)

C-----ROTATION DUE TO FREQ. OFFSET----------
      IF (DF .NE. 0.) THEN
       DTHETA=2*PI*K*DF/FB

C-----STEP CHANGE IN PHASE----------

C     IF (K .EQ. (NK1/2)*IFB) THEN
C     DTHETA=2*PI*K*DF/FB+PI
C     ENDIF

C---------------------------------------------

       CALL ROTAT1(A1,B1,DTHETA,A11,B11)
       CALL UPDAT(RCL,ICL,L1+L2+BD,A11,B11)
      ELSE
       CALL UPDAT(RCL,ICL,L1+L2+BD,A1,B1)
      ENDIF

C-------------------------------------------------
C ECHO CHANNEL :
C-------------------------------------------------
```

```
C
C----CONVOLUTION : NEAR CHANNEL----------
C
C     YN  : REC.  REAL NEAR ECHO SAMPLE
C     YF  : REC.  REAL FAR  ECHO SAMPLE
C     YNE : EST'ED REAL NEAR ECHO SAMPLE
C     YFE : EST'ED REAL FAR  ECHO SAMPLE
C     YFH : EST'ED IMAG FAR  ECHO SAMPLE
C
      SUM1=0.
      SUM2=0.
      SUM3=0.

      SUME1=0.
      SUME2=0.
      SUME3=0.

      DO 40 I=0,L1-1

         YN1 =(RCN1(I)*RDL(I)-ICN1(I)*IDL(I))*SQRT(C1)
         YN2 =(RCN2(I)*RDL(I)-ICN2(I)*IDL(I))*SQRT(SN2)
         YN3 =(RCN3(I)*RDL(I)-ICN3(I)*IDL(I))*SQRT(SN3)

         YNE1=RNE1(I)*RDL(I)-INE1(I)*IDL(I)
         YNE2=RNE2(I)*RDL(I)-INE2(I)*IDL(I)
         YNE3=RNE3(I)*RDL(I)-INE3(I)*IDL(I)

         SUM1=SUM1+YN1
         SUM2=SUM2+YN2
         SUM3=SUM3+YN3

         SUME1=SUME1+YNE1
         SUME2=SUME2+YNE2
         SUME3=SUME3+YNE3

40    CONTINUE

C------REAL PART OF NEAR ECHOC SAMPLE-----
C------RECEIVED--------
         YN1=SUM1
         YN2=SUM2
         YN3=SUM3
C------ESTIMATED-------
         YNE1=SUME1
         YNE2=SUME2
         YNE3=SUME3
```

```
C----CONVOLUTION : FAR CHANNEL----------

      SUM1=0.
      SUM2=0.
      SUM3=0.

      SUMH1=0.
      SUMH2=0.
      SUMH3=0.

      SUMEH1=0.
      SUMEH2=0.
      SUMEH3=0.

      SUME1=0.
      SUME2=0.
      SUME3=0.

      DO 45 I=0,L2-1

         II=I+L1+BD

         YF1=(RCF1(I)*RCL(II)-ICF1(I)*ICL(II))*SQRT(C2)
         YF2=(RCF2(I)*RCL(II)-ICF2(I)*ICL(II))*SQRT(SF2)
         YF3=(RCF3(I)*RCL(II)-ICF3(I)*ICL(II))*SQRT(SF3)

         YFH1=(RCF1(I)*ICL(II)+ICF1(I)*RCL(II))*SQRT(C2)
         YFH2=(RCF2(I)*ICL(II)+ICF2(I)*RCL(II))*SQRT(SF2)
         YFH3=(RCF3(I)*ICL(II)+ICF3(I)*RCL(II))*SQRT(SF3)

         SUMH1=SUMH1+YFH1
         SUMH2=SUMH2+YFH2
         SUMH3=SUMH3+YFH3

         SUM1=SUM1+YF1
         SUM2=SUM2+YF2
         SUM3=SUM3+YF3

         YFEH1=RFE1(I)*IDL(II)+IFE1(I)*RDL(II)
         YFEH2=RFE2(I)*IDL(II)+IFE2(I)*RDL(II)
         YFEH3=RFE3(I)*IDL(II)+IFE3(I)*RDL(II)

         SUMEH1=SUMEH1+YFEH1
         SUMEH2=SUMEH2+YFEH2
         SUMEH3=SUMEH3+YFEH3

         YFE1=RFE1(I)*RDL(II)-IFE1(I)*IDL(II)
```

```
          YFE2=RFE2(I)*RDL(II)-IFE2(I)*IDL(II)
          YFE3=RFE3(I)*RDL(II)-IFE3(I)*IDL(II)

          SUME1=SUME1+YFE1
          SUME2=SUME2+YFE2
          SUME3=SUME3+YFE3

45    CONTINUE

C------REAL PART OF FAR SAMPLE-----
C------RECEIVED REAL----------
          YF1=SUM1
          YF2=SUM2
          YF3=SUM3
C------ESTIMATED REAL---------
          YFE1=SUME1
          YFE2=SUME2
          YFE3=SUME3

C------IMAG PART OF FAR SAMPLE-----
C------RECEIVED IMAG----------
          YFH1=SUMH1
          YFH2=SUMH2
          YFH3=SUMH3
C------ESTIMATED IMAG---------
          YFEH1=SUMEH1
          YFEH2=SUMEH2
          YFEH3=SUMEH3

C-------------------------------------------------
C  COMPENSATION FOR FREQ. OFFSET
C
C  PLLF : PLL FLAG
C
C-------------------------------------------------

       IF (PLLF .EQ. 1.) THEN

       CALL ROTAT1(YFE1,YFEH1,DTHE,YFE1,YFEH1)

C-------------------------------------------------
C     PHASE ESTIMATION
C-------------------------------------------------

       IF (K .LT. NK1*IFB) THEN

C------1. NORMAL TECHNIQUE------
```

```
C     CALL PHEST(YF1,YFH1,YFE1,YFEH1,PHIE)

        IF (K .GT. 3) THEN
         CALL HLBRT(EM1,EH1)
         CALL PHEST1(EM1(1),EH1,YFE1,YFEH1,PHIE)
        ENDIF

        CALL PLL(G1,G2,G,PHIE,BK1,DTHE)

        ABK1(K)=ABK1(K)+BK1

       ENDIF
C-------------------------------------------------
C
C  PLL IN DATA MODE ONLY
C
C-------------------------------------------------

       IF ((SAF .NE. 1.) .AND. (K .GE. NK1*IFB)) THEN

         CALL PHEST(YF1,YFH1,YFE1,YFEH1,PHIE)

C      IF (K .GT. 3) THEN
C       CALL HLBRT(EM1,EH1)
C       CALL PHEST1(EM1(1),EH1,YFE1,YFEH1,PHIE)
C      ENDIF

         IF (K .EQ. 2*IFB)      G2=.2E-3
         IF (K .EQ. 2*IFB+400)  G2=.1E-3
         IF (K .EQ. 2*IFB+800)  G2=.9E-4
         IF (K .EQ. 2*IFB+1200) G2=.7E-4
         IF (K .EQ. 2*IFB+1600) G2=.5E-4
         IF (K .EQ. 3*IFB)      G2=.4E-5
         IF (K .EQ. 3*IFB+400)  G2=.3E-5

         CALL PLL(G1,G2,G,PHIE,BK1,DTHE)
         ABK1(K)=ABK1(K)+BK1

         ENDIF
C-------------------------------------------------

       IF ((SAF .EQ. 1.) .AND. (K .GE. NK1*IFB)) THEN

C------1. SIGN ALGORITHM----------

       DF=1.01
```

```
      PHIE=DPHI1
      SGN=E1*YFEH1

C     NCOUNT=NCOUNT+1
C     IF (SGN .LT. 0) NCOUNT=NCOUNT-2

      IF (SGN .LT. 0.) PHIE=-DPHI1

C     MM=MM+1
C     MM=MOD(MM,NAVG)

C     IF (MM .EQ. NAVG-1) THEN
C       IF (NCOUNT .LE. 0) PHIE=-DPHI1
          CALL PLL(G1,G2,G,PHIE,BK1,DTHE)
C       NCOUNT=0
C     ENDIF
      ABK1(K)=ABK1(K)+BK1

      ENDIF

C------END OF SIGN ALGORITHM----------

      ENDIF

      CALL PHEST(YF1,YFH1,YFE1,YFEH1,PHIE1)
      APHIE(K)=APHIE(K)+PHIE1/PI*180.

C-------------------------------------------------
C     ERROR  CALCULATION
C-------------------------------------------------

      E1=YN1+YF1-YNE1-YFE1
      E2=YN2+YF2-YNE2-YFE2
      E3=YN3+YF3-YNE3-YFE3

      IF (SNR .LT. 50.) THEN
         E1=E1+BETA*RN(K)
         E2=E2+BETA*RN(K)
         E3=E3+BETA*RN(K)
      ENDIF

C------DATA MODE OPERATION-----------

      IF(DMF .EQ. 1.) THEN

        IF ((K .EQ. NK1*IFB) .AND. (PLLF2 .EQ. 1.)) THEN
```

```
            PLLF=1

            G1=G11
            G2=G22
            G=GG
          ENDIF

          IF (K .GE. NK1*IFB) THEN

C         BETA1=10**(-13/20)
C         E1=E1+BETA1*RN(K)
C         E2=E2+BETA1*RN(K)
C         E3=E3+BETA1*RN(K)

          ALPHA=0
          IF (TAPF .NE. 1.) ALPHA=1./F1/(L1+L2)

          ENDIF
        ENDIF

C-----------------------------------

        CALL UPDAT(EM1,EM1,3,E1,E1)

        AE(K)=AE(K)+E1**2
C     AER(K)=AER(K)+(YN1+YF1)**2

C------COEFFICIENTS UPDATING--------
C------NEAR CANCELLER---------


        SUM=0

        DO 50 I=0,L1-1

          RNE1(I)=RNE1(I)+ALPHA*RDL(I)*E1
          RNE2(I)=RNE2(I)+ALPHA*RDL(I)*E2
          RNE3(I)=RNE3(I)+ALPHA*RDL(I)*E3

          INE1(I)=INE1(I)-ALPHA*IDL(I)*E1
          INE2(I)=INE2(I)-ALPHA*IDL(I)*E2
          INE3(I)=INE3(I)-ALPHA*IDL(I)*E3

          CNE1(I)=CMPLX(RNE1(I),INE1(I))

          SUM=SUM+(ABS(SQRT(C1)*CN1(I))-ABS(CNE1(I)))**2
```

```
50   CONTINUE

       IF (I5 .EQ. 1) THEN
         TEN(K) = SUM/C1
       ENDIF

C------FAR CANCELLER----------

       X = COS(DTHE)
       Y = SIN(DTHE)

       SUM = 0

       DO 60 I = 0,L2-1

          II = I + L1 + BD

          RFE1(I) = RFE1(I) + ALPHA*E1*(X*RDL(II)-Y*IDL(II))
          RFE2(I) = RFE2(I) + ALPHA*E2*(X*RDL(II)-Y*IDL(II))
          RFE3(I) = RFE3(I) + ALPHA*E3*(X*RDL(II)-Y*IDL(II))

          IFE1(I) = IFE1(I)-ALPHA*E1*(X*IDL(II) + Y*RDL(II))
          IFE2(I) = IFE2(I)-ALPHA*E2*(X*IDL(II) + Y*RDL(II))
          IFE3(I) = IFE3(I)-ALPHA*E3*(X*IDL(II) + Y*RDL(II))

          CFE1(I) = CMPLX(RFE1(I),IFE1(I))

          SUM = SUM + (ABS(SQRT(C2)*CF1(I))-ABS(CFE1(I)))**2

60   CONTINUE

       IF (I5 .EQ. 1) THEN
         TEF(K) = SUM/C2
       ENDIF

30   CONTINUE

       DO 73 I = 0,L1-1

         ARNE1(I) = ARNE1(I) + RNE1(I)
         ARNE2(I) = ARNE2(I) + RNE2(I)
         ARNE3(I) = ARNE3(I) + RNE3(I)

         AINE1(I) = AINE1(I) + INE1(I)
         AINE2(I) = AINE2(I) + INE2(I)
         AINE3(I) = AINE3(I) + INE3(I)
```

```
73   CONTINUE

       DO 72 I=0,L2-1

         ARFE1(I)=ARFE1(I)+RFE1(I)
         ARFE2(I)=ARFE2(I)+RFE2(I)
         ARFE3(I)=ARFE3(I)+RFE3(I)

         AIFE1(I)=AIFE1(I)+IFE1(I)
         AIFE2(I)=AIFE2(I)+IFE2(I)
         AIFE3(I)=AIFE3(I)+IFE3(I)

72   CONTINUE
29   CONTINUE

C-------END OF THE START----------------------------

       INCR=10
       NUM=NK/INCR

       WRITE(30,*) '0 ',NUM,' 1'
       WRITE(40,*) '0 ',NUM,' 1'
       WRITE(60,*) '0 ',NUM,' 1'
       WRITE(80,*) '0 ',NUM,' 1'
       WRITE(90,*) '0 ',NUM,' 1'

300  DO 85 I=1,NK,INCR

C    WRITE(30,*) I/FB,AE(I)/NR
C    WRITE(30,*) I/FB,ABK1(I)/NR*CT

       IF ((TEN(I) .NE. 0.) .OR. (TEF(I) .NE. 0.)) THEN
       WRITE(40,*) I/FB,10*ALOG10(TEN(I))
       WRITE(60,*) I/FB,10*ALOG10(TEF(I))
       ENDIF

C    IF (AE(I) .NE. 0.) THEN
C    WRITE(80,*) I/FB,10*ALOG10(AE(I)/NR)
C    WRITE(90,*) I/FB,-10*ALOG10(AE(I)/AER(I))
C    ENDIF

C    WRITE(90,*) I/FB,APHIE(I)

85   CONTINUE

       WRITE(30,*) DF,G1,G2,G
```

```
      WRITE(30,*) DPHI1/PI*180,NAVG

      WRITE(30,27) ALPHA,SNR,DF,NK/FB,NR
      WRITE(80,27) ALPHA,SNR,DF,NK/FB,NR
      WRITE(90,27) ALPHA,SNR,DF,NK/FB,NR

C     WRITE(40,*)'0 28 2'
      WRITE(50,*)'0 28 2'

      DO 70 I=0,L1-1

C     WRITE(40,71) I+1,RCN1(I),ARNE1(I)/NR
C     WRITE(50,71) I+1,ICN1(I),AINE1(I)/NR
        WRITE(50,71) I+1,ABS(SQRT(C1)*CN1(I)),ABS(CNE1(I))

        RNE1(I)=ARNE1(I)/NR
        RNE2(I)=ARNE2(I)/NR
        RNE3(I)=ARNE3(I)/NR

        INE1(I)=AINE1(I)/NR
        INE2(I)=AINE2(I)/NR
        INE3(I)=AINE3(I)/NR

70    CONTINUE
71    FORMAT(' ',I4,3X,3(E15.9,2X))

C     WRITE(60,*)'0 32 2'
      WRITE(70,*)'0 32 2'

      DO 80 I=0,L2-1

C     WRITE(60,71) I+1,RCF1(I),ARFE1(I)/NR
C     WRITE(70,71) I+1,ICF1(I),AIFE1(I)/NR
        WRITE(70,71) I+1,ABS(SQRT(C2)*CF1(I)),ABS(CFE1(I))

        RFE1(I)=ARFE1(I)/NR
        RFE2(I)=ARFE2(I)/NR
        RFE3(I)=ARFE3(I)/NR

        IFE1(I)=AIFE1(I)/NR
        IFE2(I)=AIFE2(I)/NR
        IFE3(I)=AIFE3(I)/NR

80    CONTINUE

      WRITE(40,27) ALPHA,SNR,DF,NK/FB,NR
      WRITE(50,27) ALPHA,SNR,DF,NK/FB,NR
```

```
      WRITE(60,27) ALPHA,SNR,DF,NK/FB,NR
      WRITE(70,27) ALPHA,SNR,DF,NK/FB,NR

400   STOP
      END
C-------------------------------------------------
C-----------------------------------------
C DELAY LINE INITIALIZATION SUBROUTINE (REAL)
C   RDL : REAL DL
C   IDL : IMAG DL
C   L   : LENGTH OF DL
C-----------------------------------------
      SUBROUTINE DLL(RDL,IDL,L)
      REAL RDL(0:L-1),IDL(0:L-1)
      DO 10 I=0,L-1
         RDL(I)=0
         IDL(I)=0
10    CONTINUE
      RETURN
      END
C-----------------------------------------
C DELAY LINE UPDATING SUBROUTINE (REAL)
C INPUT:
C   RDL : REAL DL
C   IDL : IMAG DL
C   L   : LENGTH OF DL
C OUTPUT:
C   X+JY: NEW SYMBOL
C-----------------------------------------
      SUBROUTINE UPDAT(RDL,IDL,L,X,Y)
      REAL RDL(0:L-1),IDL(0:L-1),X,Y
      DO 10 I=L-2,0,-1
         RDL(I+1)=RDL(I)
         IDL(I+1)=IDL(I)
10    CONTINUE
      RDL(0)=X
      IDL(0)=Y
      RETURN
      END
C-------------------------------------------------
C MODULATION :
C          A+JB  : BASEBAND DATA SYMBOL
C          A1+JB1: MODULATED DATA SYMBOL
C-------------------------------------------------
      SUBROUTINE MODLTR (K,A,B,A1,B1)
      K1= MOD(K,4)
      IF (K1 .EQ. 0) THEN
```

```
          A1=A
          B1=B
        ENDIF
        IF (K1 .EQ. 1) THEN
          A1=B
          B1=-A
        ENDIF
        IF (K1 .EQ. 2) THEN
          A1=-A
          B1=-B
        ENDIF
        IF (K1 .EQ. 3) THEN
          A1=-B
          B1=A
        ENDIF
        RETURN
        END
C-----------------------------------------
C ROTATING DUE TO FREQ. OFFSET SUBROUTINE
C INPUT:
C  RCL : REAL PART OF CHANNEL
C  ICL : IMAG PART OF CHANNEL
C  L   : LENGTH OF CHANNEL
C  DF  : FREQ. OFFSET
C  TS  : SAMPLING PERIOD
C OUTPUT:
C  RCL : REAL CHANNEL AFTER ROTATION
C  ICL : IMAG CHANNEL AFTER ROTATION
C
C NOTE THAT THE ROTATED CHANNEL WILL BE
C IN THE SAME INPUT VECTOR.
C-----------------------------------------
        SUBROUTINE ROTATE(RCF,ICF,L,DTHETA)
          REAL RCF (0:L-1),ICF (0:L-1)
          COMPLEX A,B,C
          A=CMPLX(COS(DTHETA),SIN(DTHETA))
          DO 10 I=0,L-1
            B=CMPLX(RCF(I),ICF(I))
            C=A*B
            RCF(I)=REAL(C)
            ICF(I)=AIMAG(C)
10      CONTINUE
        RETURN
        END
C-----------------------------------------
        SUBROUTINE ROTAT1(A1,B1,DTHETA,A11,B11)
          COMPLEX AA,BB,CC,ROT
```

```
        AA=CMPLX(COS(DTHETA),SIN(DTHETA))
C       ROT=ROT*AA
        BB=CMPLX(A1,B1)
C       CC=ROT*BB
        CC=AA*BB
        A11=REAL(CC)
        B11=AIMAG(CC)
      RETURN
      END
C-----------------------------------------
C SYMBOL GENERATOR SUBROUTINE :
C          SCRAMBLER + ENCODER
C     K : TIME INDEX
C
C INPUT  : SC(23) ; SCRAMBLER REGISTER
C
C OUTPUT : A,B    ; SYMBOL BITS
C-----------------------------------------
C
      SUBROUTINE SYMBOL(SC,A,B)
      REAL SC(23),D(2),A,B,X
      DO 10 I=1,2
         X=1+SC(18)+SC(23)
         IF (X .EQ. 1 .OR. X.EQ. 3) THEN
            D(I)=1
         ELSE
            D(I)=0
         ENDIF
         DO 20 J=22,1,-1
            SC(J+1)=SC(J)
20     CONTINUE
         SC(1)=D(I)
10   CONTINUE
      A=2*D(1)-1
      B=2*D(2)-1
C     K=K+1
      RETURN
      END
C-----------------------------------------
C VARIANCE CALCULATION SUBROUTINE :
C
C INPUT  : RC  ; REAL CHANNEL
C          IC  ; IMAG. CHANNEL
C          L   ; LENGTH OF CHANNEL
C          M   ; SCALING FACTOR
C
C OUTPUT : VAR ; THE VARIANCE
```

```
C-----------------------------------------
C
      SUBROUTINE VARNCE(RC,IC,C,L,VAR)
      REAL RC(0:L-1),IC(0:L-1)
      COMPLEX C(0:L-1)
      SUM=0
      DO 10 I=0,L-1
         C(I)=CMPLX(RC(I),IC(I))
         CM=CABS(C(I))
         SUM=SUM+CM**2
10    CONTINUE
      VAR=SUM
      RETURN
      END
C
      SUBROUTINE NORMAL(RC,IC,C,L,VAR)
      REAL RC(0:L-1),IC(0:L-1)
      COMPLEX C(0:L-1)
      SUM=0
      DO 10 I=0,L-1
         C(I)=C(I)/SQRT(VAR)
         RC(I)=REAL(C(I))
         IC(I)=AIMAG(C(I))
10    CONTINUE
      RETURN
      END
C-----------------------------------------------------

      SUBROUTINE PHEST(YF,YFH,YFE,YFEH,PHIE)

C-----------------------------------------------------
C  PHASE ESTIMATOR:
C      Y  :  COPLEX FORM OF THE FAR ECHO SAMPLE
C      YE :  COPLEX FORM OF THE ESTIMATED FAR ECHO SAMPLE
C
C      PHIE : ESTMATED PHASE DIFF. BETWEEN Y AND YE.
C
C-----------------------------------------------------

      COMPLEX Y,YE

      Y=CMPLX(YF,YFH)
      YE=CMPLX(YFE,YFEH)
      YY=CABS(YE)*CABS(YE)

      IF (YY .GT. 0) THEN
        PHIE=(YFH*YFE-YF*YFEH)/YY
```

```
      ELSE
        PHIE=0.
      ENDIF

      RETURN
      END
C-------------------------------------------------------

      SUBROUTINE PHEST1(YF,YFH,YFE,YFEH,PHIE)

      COMPLEX Y,YE

      Y=CMPLX(YF,YFH)
      YE=CMPLX(YFE,YFEH)
      YY=CABS(YE)*CABS(YE)

      IF (YY .GT. 0) THEN
        PHIE=(YFH*YFE-YF*YFEH)
      ELSE
        PHIE=0.
      ENDIF

      RETURN
      END
C-------------------------------------------------------
      SUBROUTINE PLL(G1,G2,G,PHIE,BK,DTHE)
C-------------------------------------------------------
C  2ND ORDER PLL:  LOOP FILTER + VCO
C ---------------
C LOOP FILTER(1ST ORDER):
C     G1 & G2  GAIN OF THE LOOP FILTER
C
C     INPUT : DPHI
C     OUTPUT: VK
C
C VCO:
C     INPUT : VK
C     OUTPUT: DTHE (DTHETA ESTIMATE)
C     G : GAIN OF THE VCO
C-------------------------------------------------------

      BK=BK+G2*PHIE

      DTHE=DTHE+G*BK+G1*PHIE

      RETURN
      END
```

```
C-------------------------------------------------------
C-------------------------------------------------------
C  HELBERT TRANSFORMER
C ------------------
C
C     YH(K) = Y(K-1) - Y(K+1)
C
C-------------------------------------------------------
      SUBROUTINE HLBRT(Y,YH)
        REAL Y(0:2)
        YH=Y(2)-Y(0)
      RETURN
      END
```

REFERENCES

[1] Nier A. M. Verhoeckx, Harry C. Van Den Elzen, Fred A. M. Snijders, and Piet J. Van Gerwen, "Digital Echo Cancellation for Baseband Data Transmission", IEEE Trans. on Acoustics, Speech and Signal Processing, Vol. Assp-27, No. 6, pp. 768-781, Dec. 1979.

[2] S. Haykin, ***Communication Systems*** , John Wiley & Son Inc., New York, 1983.

[3] V. G. Koll and S. B. Weinstein, "simultaneous Two-Way Data Transmission over a Two-Wire Circuit", IEEE Trans. om Comm., Vol. com-21, No. 2, pp. 143-147, Feb. 1973.

[4] K. H. Muller, "A New Digital Echo Canceller for Tow-Wire Full-Duplex Data Transmission", IEEE Trans. om Comm., Vol. com-24, No. 9, pp. 956-967, Sept. 1976.

[5] D. D. Falconer, K. H. Mueller and S. B. Weinstein, "Echo Cancellation Techniques for Full-Duplex Data Transmission on Two Wire Lines", Proc. NTC, Dallas, Dec. 1976.

[6] R. D. Gitlin and J. S. Thompson, "A Phase Adaptive Structure for Echo Cancellation", IEEE Trans. on Comm., Vol. Com-26, No. 8,pp. 1211-1220, August 1978.

[7] J. J. Werner, "Effects of Channel Impairments of the Performance of an In-band Data-Driven Echo Canceller", AT&T Tech. J., Vol. 64, pp. 91-113, Jan. 1985.

[8] J. Wang and J. Werner, "Performance Analysis of an Echocancellation Arrangement that Compensate for Frequency Offset in the Far Echo", IEEE Trans. on Comm., Vol. 36, NO. 3, pp. 364-372, March 1988

[9] A. Kanemasa and K. Niwa, "An Adaptive-Step Sign Algorithm for Fast Convergence of a Data Echo Canceller", IEEE Trans. on Comm., Vol.

Com-35, No. 10, pp. 1102-1108, October 1987.

[10] M. Sondhi and D. A. Berkley, "Silencing Echos on the Telephone Network", IEEE Proceedings, Vol. 68, No. 8, pp. 948-963, August 1980.

[11] "Evaluation of Saudi Arabia Telephone Network for Full-Duplex Data Transmission", KACST Project No. AR-10-57, Progress Report NO. 1, May 1989.

[12] S. B. Weinstein, "A Passband Data-Driven Echo Canceler for Full-Duplex Transmission on Two-Wire Circuits", IEEE Trans. on Comm., Vol. Com-25, No. 7, July 1977.

[13] M. L. Honig and D. G. Messerschmitt, ***Adaptive filters*** , Bell Commun. Research, Inc., U.S., 1984.

[14] M. M. Sondhi, "A Self Adaptive Echo Canceller", Bell Syst. Tech. J., Vol. 45, pp. 1851-1854, 1966.

[15] F. K. Becker and H. R. Rudin, "Application of Automatic Transversal Filters to the problem of the Echo Suppression", Bell Syst. Tech J., Vol. 45, pp. 1847-1850, 1966.

[16] J. Werner, "An Echo-Cancellation-Based 4800 bps Full-Duplex DDD Modem",IEEE J. Selected Areas Commun., Vol. SAC-2, No. 5, pp. 722-730, sept. 1984.

[17] CCITT Recommendation V.32, ITU, 1988.

[18] S. Qureshi, "Adaptive Equalization", IEEE Comm. Magazine, pp. 9-16, Mar. 1982.

[19] S. Haykin, ***Introduction to Adaptive Filters*** , Macmillan Publishing Company, Inc., New York, 1984.

[20] R. C. Dixon, ***Spread Spectrum Systems*** , John Wiley & Son Inc., New

York, 1976.

[21] A. V. Oppenheim and R. W. Schafer, ***Digital Signal Processing*** , Prentice/Hall International Inc., Englewood Cliffs, N. J., 1975.

[22] Mr. Les Brown, private communication, ESE LTD., Prampton, Ontario, Canada.

[23] P. H. Wihke, S. R. Penstone, and R. J. Keightley, "Measurements of Echo Parameters Pertinent to High Speed Full-Duplex Data Transmission on Telephone Circuits", IEEE J. Select. Areas Commun., Vol. SAC-2,Sept. 1984,pp. 703-710.

[24] O. Macchi and K. H. Park, "An Echo Canceller with Controlled Power for Frequency Offset Correction", IEEE Trans. on Comm., Vol. Com-34, No. 4, pp. 408-411, April 1986.